PIVOTED HYDROSTATIC BEARING PADS FOR THE CANBERRA HOMOPOLAR GENERATOR

EP-RR 24

P. O. CARDEN

First Published: December, 1964
Re-issued: December, 1969

Department of Engineering Physics
Research School of Physical Sciences
THE AUSTRALIAN NATIONAL UNIVERSITY
Canberra, A.C.T., Australia.

PIVOTED HYDROSTATIC BEARING PADS

FOR THE

CANBERRA HOMO-POLAR GENERATOR

BY

P. O. CARDEN

First Published: December, 1964
Re issued: December, 1969

Publication EP-RR 24

Department of Engineering Physics
Research School of Physical Sciences
THE AUSTRALIAN NATIONAL UNIVERSITY
Canberra, A.C.T. Australia

CONTENTS

LIST OF SYMBOLS

$\mathcal{a}$, a	Pad dimension $\mathcal{x}$ direction. Eccentricity.
A	Dimensionless number equation 8.11.
A_L	Land area of a pad.
B	Average flux density. Effective plenum circumference.
b	Pad dimension $\mathcal{y}$ direction.
C	Distance between the centres of 2 stabilising surfaces measured in the $\mathcal{x}$ direction - Fig. 8.5.
D	Dimension in $\mathcal{x}$ direction between centre lines of two lands of a pad.
F	General symbol for force. Force per unit length of land in $\mathcal{y}$ direction.
$\mathcal{F}$	Dimensionless form factor - equation VIII.3.
g	Gap width between rotors or rotor and pole face. Dimensionless factor.
h	General symbol for pad clearance to shaft.
h_o	Equilibrium clearance (in discussion of film rigidity); clearance for $\beta = 0$.
h'	Mean value of clearance.

J	General symbol for pad torque factor - dimensionless.
k	Concavity offset for a land surface, Fig. 7.8.
L	Land dimension in direction of x, (U)
m	Effective moment arm - equation 7.19.
M	Shaft centre to pivot point distance Fig. 8.15.
N	Concavity factor - dimensionless. Fig. 7.8.
N_o	Value of N for $\beta = 0$.
n	General symbol for a numeral. Relative plenum depth - equation 7.27.
P	Applied pressure.
P_F	Friction power.
P_h	Hydrodynamic pressure - equation 7.17.
p	General symbol for pressure.
Q	General symbol for oil flow. Oil flow per unit length of land in y direction.
q	Oil flow rate per unit area of pad surface.
R	General symbol for radius.
R_{12}	Component rigidity between items 1 and 2.

R_o Overall rigidity.

r Radius of rotor.

r_s Radius of shaft or bearing.

S Half the length of a cylindrical stabilising land, measured in the x direction - Fig. 8.5.

T Torque on rotor about a diameter.

Torque on a pad per unit length in y direction.

U Bearing linear velocity.

U_o Transition velocity defined by equation - Appendix VI.

U' Normalized linear velocity - dimensionless - Appendix VI.

V Average velocity of oil in film.

W Pad load force.

W_o Equilibrium pad load.

W_s Resultant of all six pad loads on one bearing.

x Co-ordinate in direction of U.

X Dimensionless x co-ordinate $X = \frac{x}{L}$.

y Co-ordinate perpendicular to U but parallel to bearing face.

z Co-ordinate perpendicular to x and y in rectangular system.
Co-ordinate in axial direction in cylindrical system.

z_0 Minimum clearance for cylindrical stabilising land.

α Inclination of land surface - Fig. 7.7.

β Pad inclination - dimensionless - Fig. 7.8.

γ Dimensionless factor less than unity.

δ Dimensionless factor less than unity.
Difference between radii of bearing surface and pad surface.

ϵ Dimensionless number - Appendix VIII.

θ Tilt angle of rotor to pole face or between rotors.
General symbol for angle.

μ Viscosity.

ξ Dimensionless co-ordinate in x direction used in relation to cylindrical surfaces - equation 8.2.

ξ_0 Value of ξ at $\beta = 0$. - equation 8.15.

ξ_1 ξ at edge of stabilizing land.

ψ Dimensionless quantity - equation 8.21.
Similarly ψ_1 & ψ_2

VALUES OF CONSTANTS FOR

POLE BEARINGS

Constant	Large Pad	Small Pad
h_o	3.7 mil.	3.4 mil.
L	1.0 in.	.720 in.
D	4.9 in.	3.1 in.
n	25	21
U (max)	900 in/sec.	650 in/sec.
	75 ft/sec.	54.2 ft/sec.
s	0.6 in.	0.43 in.
c	8.1 in.	5.4 in.
N_o	0	0
ξ_o	1.4	1.4
P_h	227 p.s.i.	138 p.s.i.
P	300 p.s.i.	250 p.s.i.
β max	1.2	1.15
A_L	50 in^2	39 in^{2*}
a	4.8 in.	3.2 in**
b	10 in.	12.78 in.
U_o	275 in/sec	235 in/sec
U'	3.27	2.78
bearing radius	9 in.	6.5 in.
Q	10.2 in^3/sec., 5.85 x 10^{-3} ft^3/sec. 2.2 g.p.m.	
μ	5 x 10^{-4} lb force. sec/ft^2. 3.5 x 10^{-6} lb force. sec/in^2 (Reyn); 24.1 centipoises	

*including stabilizing lands.

**between centres of lands.

SECTION 1

INTRODUCTION

This paper describes a type of pivoted "hydrostatic" bearing pad developed by the author for the Homopolar Generator at Canberra.

Sections 2 to 5 describe the particular problem to be solved, while Section 6 describes, in principle, the solution. In Section 7 the solution is studied in detail revealing that hydrodynamic effects will cause unstable behaviour unless precautions are taken. Section 8 describes a method of overcoming this problem and Section 9 describes the mechanical detail of the completed design.

Finally Section 10 discusses the success or otherwise of the bearing pad in practice.

The author wishes to make the following acknowledgements. The rate of torque generation on the rotors produced by the magnetic field was first worked out by Mr. J.W. Blamey. These calculations were tested with a model by Mr. Blamey and on the homopolar generator by Dr. L.U. Hibbard. The calorimetric measurements mentioned in Section 10 were carried out by Dr. Inall.

The servo mechanism, an essential part of the application of this particular design, is not dealt with in detail but is briefly described in Sections 6 and 9 . The whole of the work was carried out under the broad direction of Sir Mark Oliphant.

SECTION 2

DESCRIPTION OF HOMOPOLAR GENERATOR

The Canberra Homopolar Generator has been designed to store energies of the order of 500×10^6 joules and release it in the form of a pulse lasting approximately two seconds and reaching a peak current of 1.6×10^6 amps. The machine is built between the poles of an electro-magnet, the pole-faces of which are horizontal and 5 feet 2 inches apart. Two mild steel rotors are located between the poles and are intended to rotate at speeds up to 900 R.P.M. in either direction. Each rotor consists of two 20 ton, $11'6\frac{3}{4}''$ diameter discs bonded together but insulated from one another. There are therefore four discs which when connected in series and when rotating in a magnetic field strength of 16,000 gauss should give a maximum voltage of 800. Electrical connections are made to the discs by means of jets of liquid sodium-potassium (NaK) which impinge on their surfaces at the outer edge and at a radius of $23\frac{5}{8}''$. For reasons of symmetry and force balance, the rotors are intended to rotate in opposite directions. Because of this and to facilitate the design of the jets between the rotors, each rotor has been supported on a separate shaft extending through a pole-piece and through the yoke of the magnet. Each shaft runs in bearings located within the pole and is terminated at a thrust bearing outside the yoke.

The rotors being necessarily of steel to enable the desired flux densities to be reached, experience large magnetic forces on their surfaces. Every effort has therefore been made to situate them so that these forces balance to as great a degree as possible. Vertical thrusts have been reduced to the same order of magnitude as the rotor weight, the residual thrust varying about zero depending on the rotor flux density, and being mainly due to the fringing fields. The residual thrust does not alter appreciably with

small changes in the vertical positions of the rotors (e.g. $\frac{1}{8}$"). However the thrust bearings have been designed to cope with momentary thrusts up to 400 tons, which forces might occur during a short circuit within the homopolar generator. The design of the thrust bearings is that of a fairly conventional constant oil-flow pressure fed type, the oil being piped via flow equalizer valves and throttle tubes to 4 plenums on each side of a thrust collar.

The bearings within the poles ideally carry no load since with a balanced geometry there should be no side forces nor torques about a horizontal axis. However there is a unique requirement here for angular rigidity about a horizontal axis. This is brought about by the fact that any small rotation about such an axis will cause a redistribution of flux through the faces of a rotor and a consequent offset of the lines of action of the resultants of magnetic forces on either rotor face. The resulting torque is, for small angles, proportional to the angle of rotation from the horizontal. This mechanism should be compared with that of purely vertical displacements. In this case there is practically no change in flux density, since the sum of the air gaps on both sides of a rotor is unchanged, nor any flux redistribution for the rotor faces remain parallel to the pole face. Except for second order effects of the fringing field and certain other minor effects there are no accompanying large forces.

Torques developed in the manner outlined are of the order of 100 foot-tons per milliradian, and are proportional to the square of the rotor flux density up to about 15×10^3 gauss. Above this figure the incremental permeability to flux across a rotor becomes appreciable leading to an eventual peaking at about 17×10^3 gauss. The rate of torque generation (r.t.g.) is also a function of rotor speed being a maximum at zero and decreasing to a small value above 100 R.P.M. This is caused by the development of eddy currents either in the rotors or in the copper sheets attached to the pole faces.

It will be seen therefore that consideration of rigidity was of prime importance in design. The shaft extending from each rotor into a pole piece is short and thick (typically 18" diameter). In each pole there are two bearings situated 24" apart. The separation of the bearings is as much as is allowed by the dimensions of the pole-pieces which were each machined as complete units. However although one might consider that maximizing the separation of the two bearings would be beneficial in so far as it reduces the rigidity required of them, this is offset to a certain extent by the reduced rigidity of the shaft itself unless its diameter be increased. Taking the above figure for bearing separation and r.t.g. and assuming infinite rigidity of shaft, shaft to rotor connection, pole and magnet yoke, a minimum figure of approximately 4 tons per thousandth of an inch is required of each pole bearing.

The remainder of this paper is devoted to the design and testing of the pole bearings and associated factors.

SECTION 3

TORQUES ON ROTOR DEVELOPED BY THE MAGNETIC FIELD

A simple formula for these torques may be developed as follows: -

Consider an air gap in a magnetic circuit where flux crosses between two circular faces of radius r which are at a slight angle θ. If the faces are regarded as unipotential surfaces, and fringing field is neglected, one arrives at the following formula for the torque on either gap boundary:

$T = \frac{B^2 r^4 \theta}{16 g}$ in c.g.s. units where:

B is the average flux density,

g " " " gap length.

This relation is derived in Appendix I.

Applying this formula to both sides of the upper rotor shown in fig. 3.1 and substituting appropriate values for r and g(g = 6 ins.) and a figure of 17×10^3 gauss for B, one arrives at a value for $\frac{T}{\theta}$ of 2×10^9 in. lb/radian which is of the correct order of magnitude.

However this simple model neglects two effects of major importance:

(a) Flux concentration near the outer edges of the rotors tend to increase $\frac{T}{\theta}$.

(b) At higher values of B, the incremental permeability of the rotor material to flux crossing horizontally reduces to a value where the rotor surfaces are no longer equipotential surfaces. This results in values lower than those predicted by the simple model at high

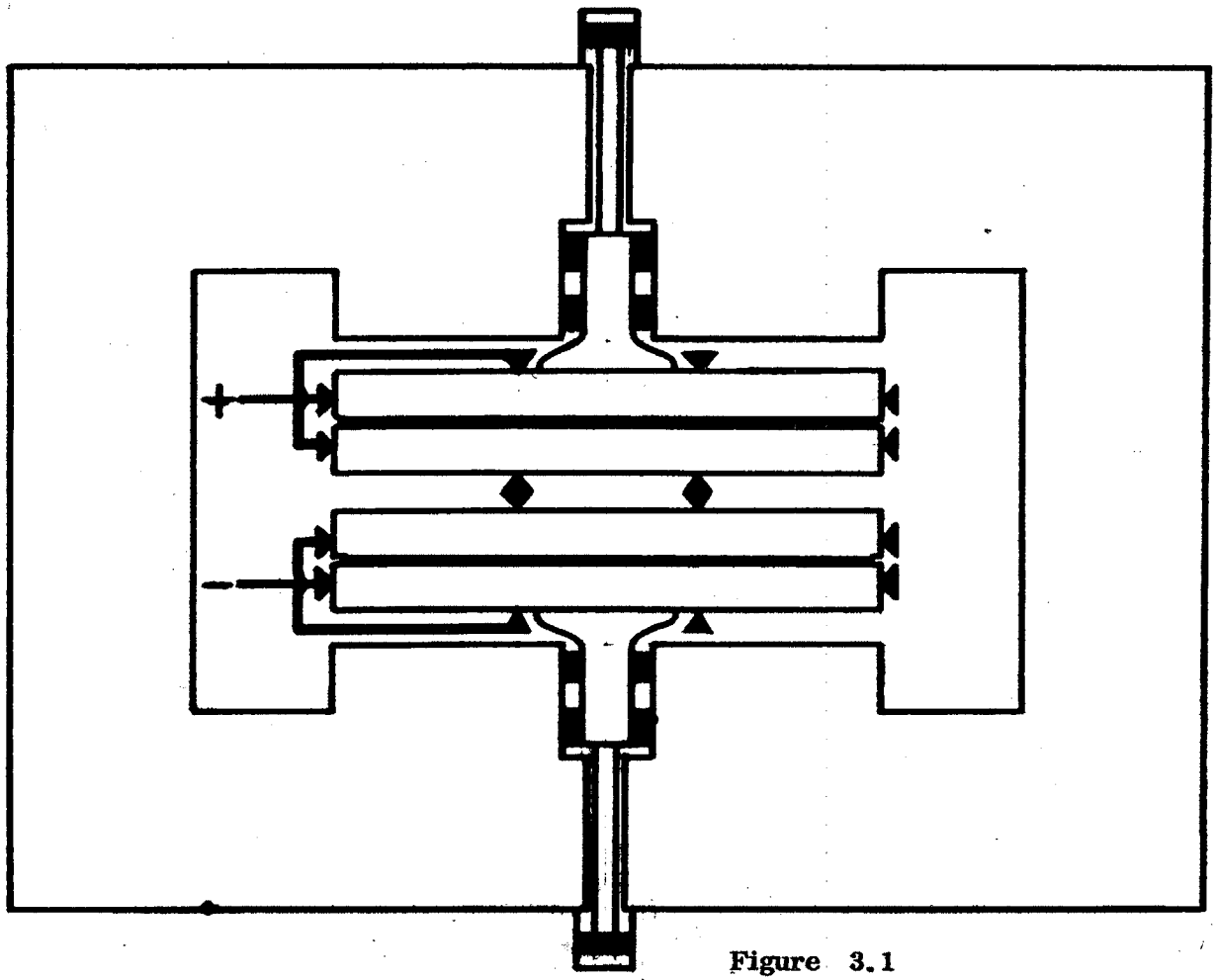

Figure 3.1

B values, and causes a departure from the dependence it predicts, resulting in a peaking at about 17×10^3 gauss.

Both these effects require large corrections. It appears from experimental evidence that the simple model predicts values as much as 30% too high.

Tests carried out to determine the r.t.g.

Two experiments were performed to determine the r.t.g. on the rotors of the finished homopolar generator. The first of these was carried out on a small scale model magnet and rotors (by J.W. Blamey) and from the results was derived a figure of 3×10^9 in.lb/rad. to be used in the design of bearings and associated structures. Later, when one set of bearings of a preliminary design was completed, an assembly consisting of a complete upper rotor, shaft and bearings; and a lower rotor locked parallel to the pole faces were tested to determine both the r.t.g. and the rigidity of the various supporting components. Hydraulic jacks were used on the upper rotor both to control its angular position and to measure the net restraining forces necessary. By taking measurements at various values of field strength and angles of inclination a thorough study was made (by L.U. Hibbard) of this particular arrangement.

The maximum r.t.g. was found to be 1.5×10^9 in.lb/rad. at about 17×10^3 gauss and was substantially proportional to the square of the field strength up to 15×10^3 gauss.

The worst displacement of rotors envisaged is that illustrated in fig. 3.2 where both rotors are inclined at the same angle in opposite directions. Here the contribution to the torque on each rotor by the gap between the rotors is twice what it was in the second experimental arrangement described. The corresponding r.t.g. would therefore be 2.25×10^9 in.lb/rad.

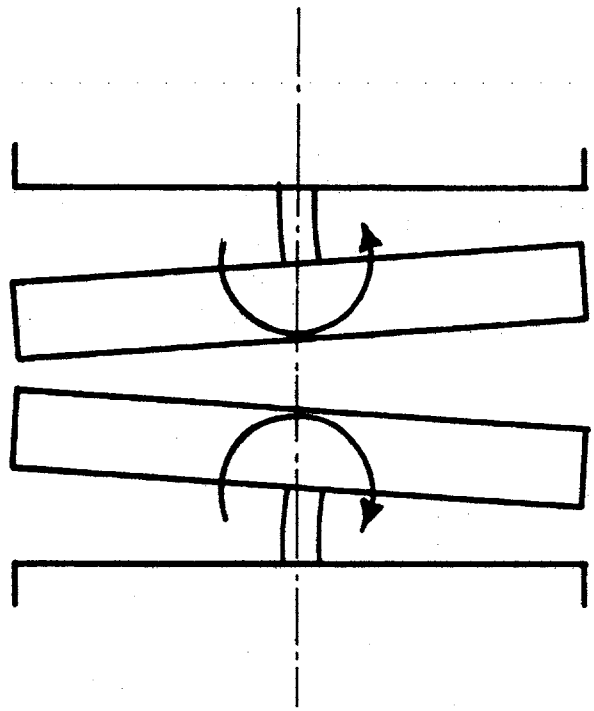

Figure 3.2

A full theoretical treatment of the subject is beyond the scope of this paper. However enough has been said to show that the magnitude and general characteristics of the experimental results are to be theoretically expected.

SECTION 4

GENERAL SPECIFICATION OF POLE BEARINGS

The following specifications of the pole bearings follow from what has already been said regarding the intended duty of the generator, and consideration of the magnetic field environment.

(a) Speed: from zero to 900 r.p.m. (close to 100 radians per second) in either direction with maximum angular accelerations of the order of 100 radians per second.

(b) Magnetic environment: The shaft runs in a strong field. Induced voltage gradients on the surface of the shaft would be of the order of .1 volt/inch. The bearing design must not allow these voltages to create circulating currents large enough to cause damage or appreciable energy loss. (Fig. 4.1).

(c) Voltage: The bearings must provide insulation between each pole piece and adjacent disc to withstand at least 200 volts and preferably 800 volts to allow flexibility in selecting the earthing point of the system.

(d) Accuracy in alignment: The bearing must locate the rotor accurately within the surrounding outer jets, preferably to within 5 mils.*, i.e. 10% of the jet gap. It must also locate the rotor so that its plane surfaces are parallel to the pole faces.

(e) Rigidity: The bearing must provide an overall/rigidity appreciably in excess of 3×10^9 inch pounds/radian at

*thousandth of an inch.

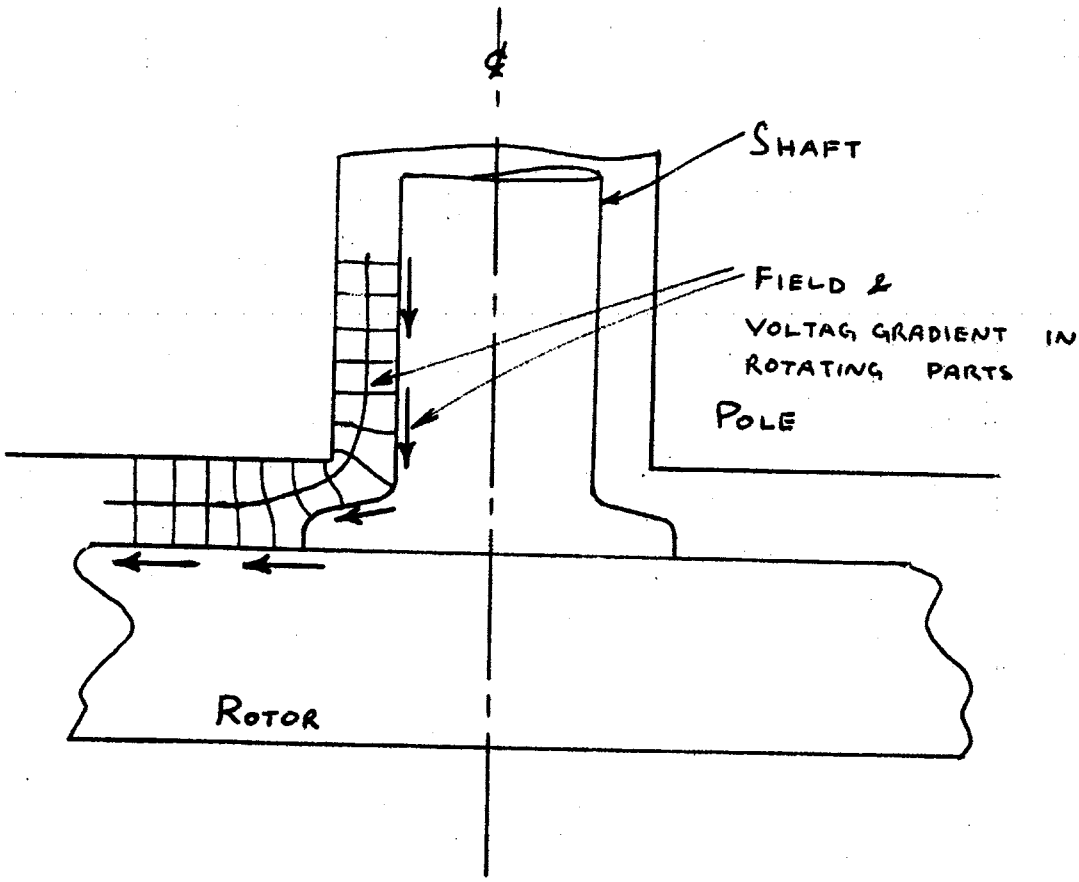

Figure 4.1 The magnetic field crosses a gap between shaft and pole piece where the bearings are situated.
A voltage gradient on the shaft of the order of .1 volt/inch may result.

zero and low speeds (up to about 50 r.p.m.). By overall rigidity is meant the rigidity related to angular displacements of the rotor relative to the poles. This rigidity includes the effects of rotor flexibility, rotor-to-shaft flexibility, shaft bending and bearing housing flexibility, as well as the elastic characteristics of the oil film and pads.

The overall rigidity is related to the component rigidities thus:

$$\frac{1}{R_o} = \frac{1}{R_{12}} + \frac{1}{R_{23}} + \frac{1}{R_{34}} + \cdots \qquad (4.1)$$

where the component rigidities e.g. shaft bending rigidity, are R_{12}, R_{23}, etc. and R_o is the overall rigidity. (Fig. 4.2).

Because of this relation, the rigidity component associated with the bearing element, e.g. oil film, must be considerably greater than 3×10^9 inch pounds/radian. In fact a figure of twice this is called for as a minimum. After application of a further factor of 2 for safety, a requirement of 12×10^9 in. pounds/rad. is arrived at. If bearings are separated by a vertical distance of 2 feet, each must have a linear rigidity of 16 tons/mil.

Further the oil film must have the feature of providing a load whose line of action coincides with the direction of displacement of the shaft i.e. if the shaft moves out of centre in a certain direction, a restoring force should

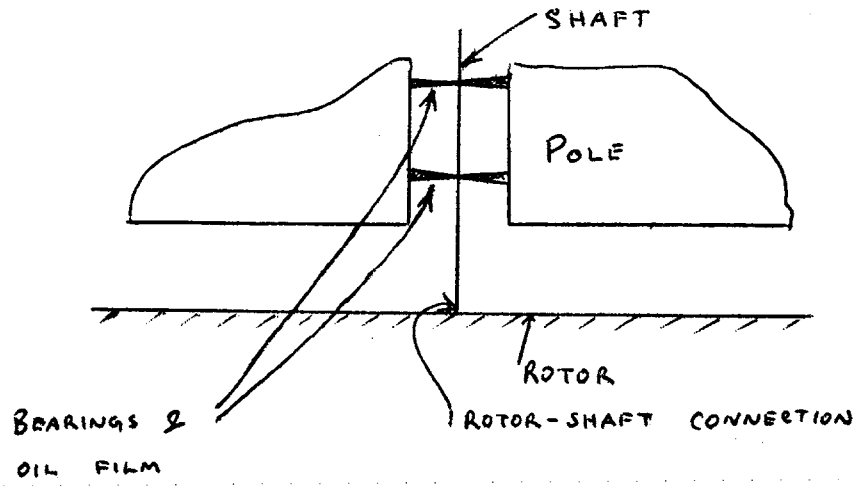

Figure 4.2a Elements whose flexibility must be taken into account when determining overall rigidity of the rotor with respect to the pole.

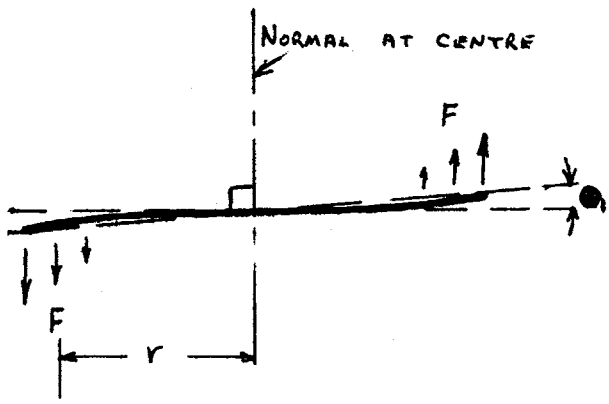

Figure 4.2b

Resultant magnetic torque $2Fr$.

Rotor Rigidity $= \frac{2Fr}{\theta_1}$

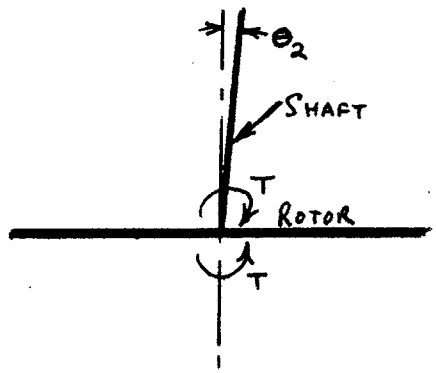

Figure 4.2c

Rotor-shaft connection.

Rigidity $= \frac{T}{\theta_2}$

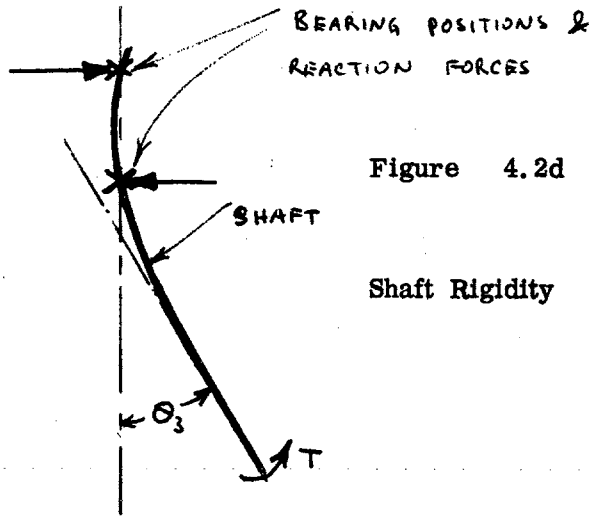

Figure 4.2d

Shaft Rigidity = $\frac{T}{\theta_3}$

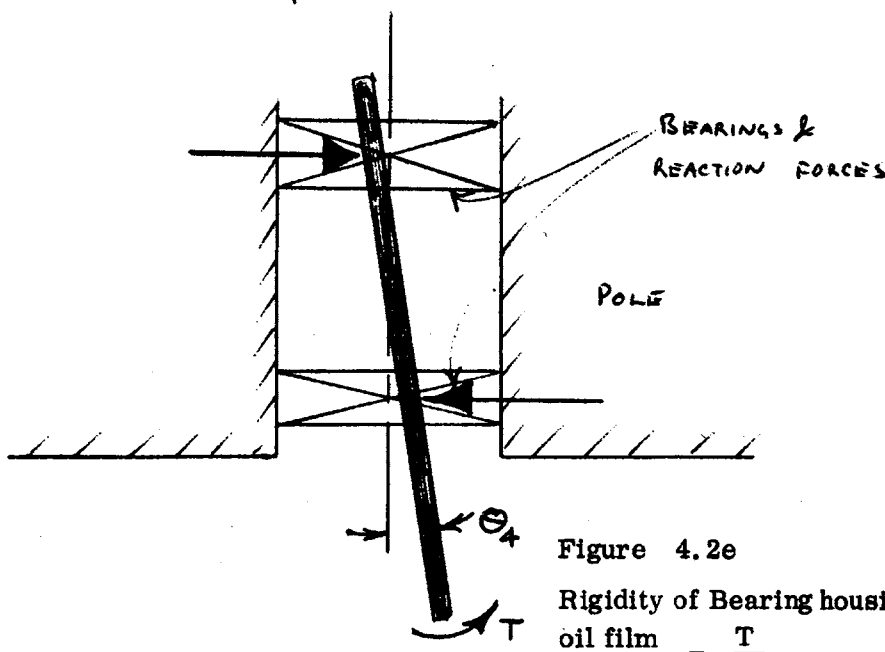

Figure 4.2e

Rigidity of Bearing housings & oil film = $\frac{T}{\theta_4}$

Figure 4.2 Four components of the overall rigidity of the rotor with respect to the pole piece. (The poles are considered infinitely rigid. However even their rigidity and that of the magnet should be included in a complete inventory of components.)

result whose direction is against the direction of the initial movement.

Any angle θ between these two directions not only results in a reduction of the effective restoring force by the factor $\cos\theta$ but the $\sin\theta$ component may cause whirling.

(f) Strength: In normal operation the required bearing strength could only be arrived at by considering the maximum likely displacements of the rotor axis with magnetic field on and the rotor spinning at low speed. For example, a pair of plain journal bearings would operate at zero clearance at zero speed, because the magnetic field would tilt the rotor until solid to solid contact within the bearings limited further movement. The magnetic field would therefore be exerting a torque on the rotor which would have to be resisted by the bearings. This condition would therefore set the required strength under normal circumstances.

Hydrostatically lubricated bearings on the other hand would narrow the possible rotor tilt angle and hence their strength might not need to be so great.

However, the possibility of unexpected displacements or other sources of forces on the bearings make it imperative to build into their design the maximum possible strength.

As an example, it might happen that the NaK escaping from a jet might cause short circuiting of a disc. Almost certainly the short circuit would be unsymmetrical i. e.

mostly on one side of the rotor. The resulting rotor current would therefore cause a horizontal force which would be transmitted to the pole bearings. A short circuit current of 200,000 amps. would, in this case, cause a sideways force of 50 tons.

However, if such currents were to occur, every effort would be made to remove the cause. These accidental forces therefore need not be regarded as part of normal running conditions but should be regarded as occurrences with a very small recurrence rate. A separate bearing element could therefore be considered to resist them specifically. Such an element might have quite poor bearing qualities but must have adequate strength. An example would be a number of skids around the perifery of each rotor which would come into operation should the rotor tilt more than a certain amount.

The maximum rotor tilt would therefore be set by such skids, and so in turn would the required pole bearing strength.

On the basis of skids 1/16 inch from the rotor perifery, and a r.t.g. of 3×10^9 in. pds./rad., it is calculated that the maximum reaction torque required of the bearings is 100 ft. tons. For a separation of 2 feet therefore, the required minimum strength of each bearing is 50 tons. (Fig. 4.3).

(g) Thermal Stability: In the light of the high rigidities required, it might be inferred that, in the case of oil film bearings, clearances will be unusually small; and

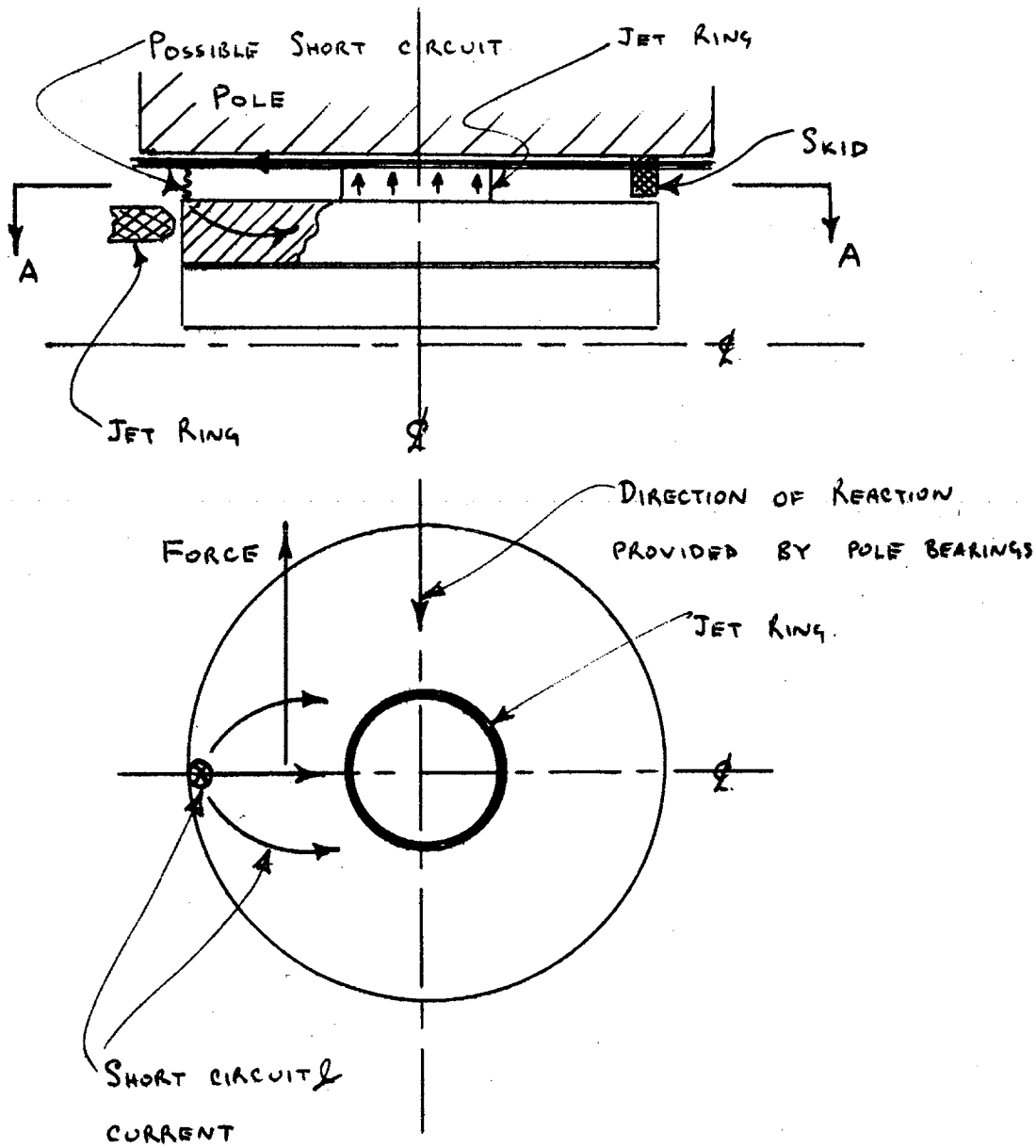

PLAN VIEW SECTION A-A

Figure 4.3 Diagram showing:

(a) Example of short circuit resulting in force on pole bearing.

(b) Position of one of several skids to counter accidental large forces.

in the case of rollers, preloading would have to be resorted to. In both cases therefore, thermal expansion might prove to be a serious problem, leading to a narrowing of clearances and generally increasing friction, eventually ending possibly in seizure. This situation might be expected to be aggravated by the seasonal change in ambient temperature as well as by the various heat sources within the generator. These are windage and electrical heating of the rotors and jets. The most important of these is windage which has been estimated at 50 to 100 K.W. at full speed.

It is essential that each potential design be examined fully in regard to thermal effects.

(h) Economy: The bearing design chosen must be reasonably economical both in constructional costs and running expenses. In this regard the assembly of the bearing in the pole and its alignment with the rest of the machine must not be forgotten.

(j) Size: The design chosen must fit in the holes already provided in the pole pieces. These were previously machined in sections before being welded together and to the magnet.

(k) Reliability: The design chosen must be as reliable as possible because of the inaccessibility of the bearings within the pole pieces. To repair them entails disassembling the whole machine, a lengthy and expensive undertaking.

SECTION 5

UNSUITABILITY OF CONVENTIONAL BEARINGS

The following types of conventional bearings were considered:

(i) Ball and roller type.

(ii) Plain journal bearing.

(iii) Hydrodynamically lubricated pad bearings such as Michell tilting pads and step pads.

(iv) Fixed pad hydrodynamic types-steps etc.

(v) Hydrostatically lubricated types with fixed pads or surfaces. These operated on the principle of supplying a more or less constant oil flow to a number of points on the bearing surface, the pressure at these points varying with the film thickness.

We shall now review these types in the light of the required specification.

(a) Speed: All types apparently can be designed to operate at the full required speed. However, the requirement for low and zero speed operation eliminate all except (i) and (v). Also the requirement for rotation in both directions limits the application of types (iii) and (iv).

(b) Magnetic environment: (i) would require either the balls or faces to be made of plastic or be plastic lined. Other types might require plastic lining unless it is shown that the oil film is a sufficiently good insulator against the voltage gradients.

(c) Voltage: All types could incorporate an insulating barrier some combining the requirement (b). However, this must be considered also in the light of requirement (e).

(d) Accuracy in alignment: All types in principle are satisfactory in this respect at high speed, but only (i) and (v) at low speed.

(e) Rigidity: All types except (v) are unsatisfactory in this respect.

Type (i) being dependent on a few point or line contacts fails to meet these requirements. Especially is this so when one has to consider the effect of plastic balls or rollers because of specification (b).

Type (ii) fails at low speeds unless the oil film completely ruptured leaving solid to solid contact.

Type (iii) also fails because of the requirement of coincidence between the lines of action of displacement and reaction force. There is usually an appreciable angle between these two directions, especially for long bearings where the angle may tend towards 90^{o}.

(f) Strength: In the case of type (i) bearings, "strength" is synonymous with "design load". In the case of the other types it need not be, since it is permissible for the oil film to break down momentarily, provided no permanent damage results. Since the maximum load will only be reached on isolated occasions this appears to be a satisfactory basis of design. Hence, strength refers mainly

to the housings and allied mechanical supports. In principle therefore all types can be rendered adequately strong.

(g) Thermal Stability: This is a serious problem in all types. For example, where a shaft diameter of 18 inches is chosen with a clearance of 3 mils., a temperature differential of $20^{o}C$ will halve the clearance. It should be remembered that the expansion of the bearing is limited by the slow thermal time constant of the massive pole pieces, whereas the shaft may expand relatively rapidly.

(h) Economy: All five types offer reasonable operating efficiency and economy in construction. However, they all require precise manufacturing and assembling techniques to ensure that the rotors will be centred with respect to the jet system and maintained parallel to the pole faces.

(j) Size: All types suffer from the inadequacy of the space allowed. However, balls and rollers suffer most because of the relatively large size of the bearing elements compared to those types which rely on an oil film.

(k) Reliability: No one type is outstanding in the matter of reliability. However one might tend to distrust those designs of a more unorthodox nature. Plastic rollers would fall into this category.

SECTION 6

GENERAL DESCRIPTION OF ADOPTED DESIGN

Of the five bearing types considered, it appeared that type (v) was the most promising. However it still suffered from problems of thermal stability and manufacturing precision (economy).

Preliminary designs showed that clearances in a type (v) bearing would have to be as low as 3 mils., and this with an 18 inch diameter shaft, in order to achieve the required 16 tons/mil. in the oil film alone. If the rigidity of the bearing housings and supports were not an order of magnitude above this, even lower clearances would have to be considered.

Clearly the thermal stability would be a severe problem, not to mention the manufacturing and assembly difficulties.

A way was sought to overcome these remaining problems and if possible to alleviate others.

Consideration of thermal stability gave rise to thoughts of bearing pads where load rather than clearance was the controlled factor. Whereas one might have doubtful control over bearing clearance in a type (v) bearing, perhaps quite definite control could be established over the pad loading. Under such a system pads would have to be allowed to move in a radial direction, but their position and the amount of clearance would now be dependent variables. The significance of this can be demonstrated as follows. As is shown in Appendix II, the basic relation for hydrostatically lubricated pads fed with a constant flow of lubricant is

$$W \propto \frac{1}{h^3}$$

W and h being the pad load and clearance respectively. If h is the independent or controlled variable, as it is in conventional type (v) bearings, then clearly large variations in W will follow small variations in h. Added to this is the great uncertainty in h because of the difficulties described above.

If on the other hand W is the controlled variable, small changes in W will cause even smaller changes in h. In addition one might hope for close control of W in which case variations in h will be very small indeed.

The only effect temperature would have under these conditions would be to alter the lubricant viscosity. As is also shown in Appendix II

$$h \propto \sqrt[3]{\mu}$$

so that resulting changes in h will be considerably smaller than the change in viscosity causing it.

The requirements of rigidity and alignment imply that control of pad loading would have to be made somehow dependent on measurements of tilt angle and alignment, or alternatively, dependent on the net forces on the bearings. In the latter case the tilt angle would be measured indirectly by measuring the reaction to the magnetically produced torque on the rotor.

Persuance of this approach revealed that there were other advantages also. These are:

(i) The use of radially moveable pads (which could also rock slightly) meant that the bearing assembly could be relatively crudely aligned with the rest of the machine, the final attained alignment now falling back on the measuring system.

(ii) Instead of having to thread a heavy shaft through bearings only a few mils larger in diameter, there was the chance of being able to move the pads back a fraction of an inch to facilitate the shaft installation.

(iii) The overall rigidity could be made independent of the component rigidities. For example it was conceivable to control the pad loading so that bearing reaction torque was proportional to the rotor tilt angle. In this case the overall rigidity would depend only on the proportionality factor. The mechanical elements between the pole and rotor would merely transmit forces and their rigidities would be irrelevant.

(iv) Having direct control over such important parameters as bearing loading and rotor position was attractive in an experimental machine where many features would need further development. The fact that a large part of a bearing's performance could be made dependent on an easily accessible and quickly changeable piece of apparatus external to the homopolar generator was also attractive. It meant that many parameters could be altered without having to disassemble and modify the cumbersome mechanical parts.

The realization of such a scheme depended mainly on whether or not a suitable pad could be designed. A summary of the required features is as follows.

It must be in principle a hydrostatic type of pad. It must be radially moveable and capable of being loaded in a controllable way.

Preferably it should be capable of rocking about a point so that it may match the shaft wherever the shaft's operating position might be. This feature would enable the full realization of advantage (i) above and save considerable manufacturing and assembly time. On the other hand it would call for a pad design which took into account the particular nature of the point support.

It was decided to study the design of such pads and develop them if found feasible.

Brief History of Development: From the outset the pole bearings were conceived as a set of pressure fed, radially moveable pads, servo controlled in order to maintain the rotors in the desired position. The first concept of such a servo system involved returning a rotor to a position of zero torque. The direction of the rotor axes would then be defined by the magnetic characteristics of the machine and would be undefined at zero field. It was later realized that it would also be undefined at high rotor speeds so that a secondary system would be necessary.

In any case the proposal for a servo was vetoed by the Director on the grounds of complication, it being proposed to substitute manual operation instead. On this basis pole bearings were designed and constructed.

It was not until after the two failures described below, during which the lack of continuous pad load control contributed to if not caused the major part of the damage, that a servo system was built. In this system actual rotor displacements from a predetermined datum position were used to control the rotor restoring forces.

For the elimination of any metal to metal contacts between pads and shaft, a technique for gluing 1/16" sheets of asbestos based bakelite with an epoxy resin to the pad faces was developed and tried out on a set of six pads in the magnetic field. At the same time a set of six conventional

bronze pads were tried to test the possibility that the oil film itself might prove an adequate insulator.

The bronze pads seized at 430 R.P.M. whereas the insulated pads appeared to behave reasonably well up to this speed. Although this seemed to be evidence that the failure was the result of an electrical phenomenon, the sets of pads differed considerably in respects other than electrical insulation, e.g. size, shape, accuracy, so that the possibility of other mechanisms of failure could not be ruled out. For instance it was shown (Appendix III) that pads whose faces were machined so inaccurately as to cause incipient contact with the shaft over areas having long vertical dimensions became thermo-mechanically unstable above a certain speed. The mechanism of failure involved the transfer of load from the supporting oil films to the incipient contact regions brought about by the lowering of viscosity as the oil absorbed heat from the contact regions mainly via the shaft surface.

Whether the failure was initiated by an electrical or mechanical mechanism, it was clear that the subsequent progress of the failure was governed mainly by mechanical friction processes. Calculations of effective coefficient of friction, records of pressure, and deceleration all pointed to this being true. Consequently an extensive theoretical investigation of the mechanical stability of the pads was undertaken and this led to the modified design which was adopted and has so far proved successful.

SELECTION OF PARAMETERS

Before proceeding to a theoretical discussion of design, it would be well to clarify some of the terms to be used. A set of six pads forming a ring around the shaft is referred to as a bearing. Each pad spans a little less than 60° around the shaft and is of such a length as to make the developed

concave face of a pad approximately square. Each pad has a depression or plenum in the middle of the face which is surrounded by the lands. The plenum of each pad is fed from a separate fixed displacement pump giving a practically constant oil flow independent of pressure. The back of each pad forms a piston which fits into a shallow cylinder fixed to a pole. The pistons are fitted with o-ring gaskets and are relieved to allow a small amount of rocking in the cylinders. Each pad can therefore be regarded as being pivotted at a point in the centre of its back, this point being henceforth known as the pivot point. The piston and cylinder form a hydraulic ram which provides the means of radially adjusting and loading each pad. These rams are connected hydraulically to a set of manual valves and the servo control system.

If the developed face of a pad were a circle of radius R, with a concentric plenum of radius r, it can be shown (Appendix IV) on simple theoretical grounds that the power required from the plenum supply pump to support a given pad load at constant clearance minimizes at $r = 0.538\,R$. However most of the bearing friction is developed at the lands where the clearance between pad and shaft is least. An increase in r over the above figure will therefore lower the friction power at the expense of an increase in pump power. To make a final choice of land width one must consider other factors such as the desired maximum friction of the machine, power supplies to pumps, the size of pumps, the availability and size of the oil cooling system. The same applies to a square pad and one will find an optimum proportioning similar to the circular pad. Fig. 6.3 shows the dimensions adopted.

As is shown in Appendix II, the force exerted by a pad on a shaft is related to the clearance by $W \propto \frac{1}{h^3}$ when the oil feed is constant, and $\frac{dW}{dh} = -\frac{3W_o}{h_o}$. The zero subscripts refer to the state of balanced pad forces on the shaft.

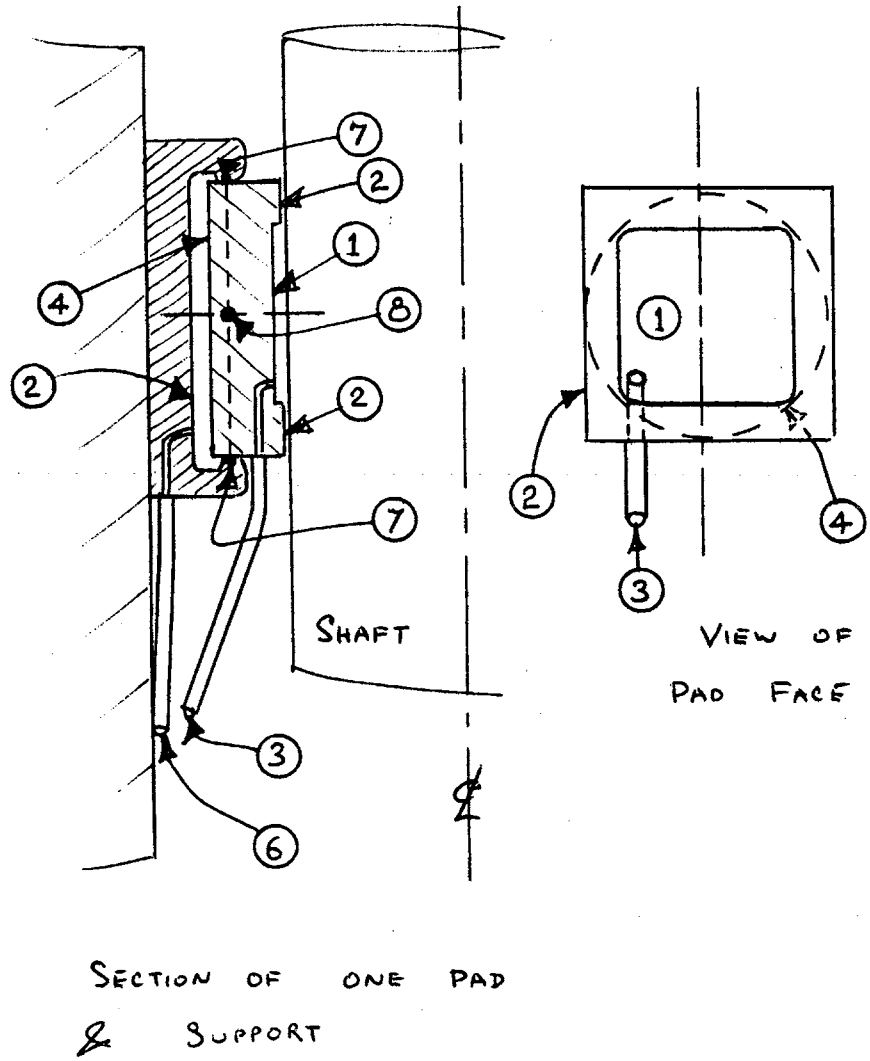

Figure 6.1 Diagram illustrating terms used.

(1) Plenum
(2) Lands
(3) Connection between plenum and constant flow source
(4) Piston
(5) Cylinder
(6) Connection between cylinder & external loading system
(7) O-ring gasket
(8) Pivot point

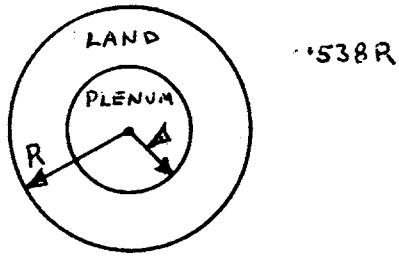

Figure 6.2 Proportions of circular pad face for maximum ratio of

$$\frac{\text{pad load}}{\text{lubricant power}}$$

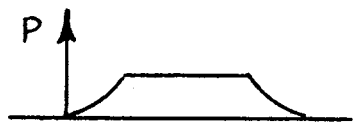

Graph of pressure distribution
across a diameter.

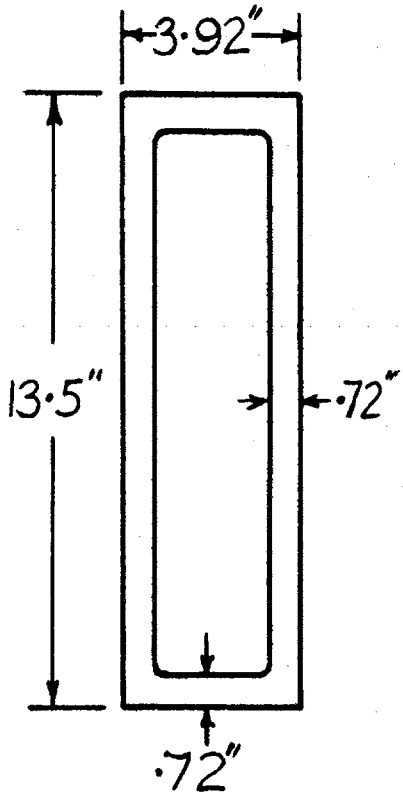

"Small" Pad

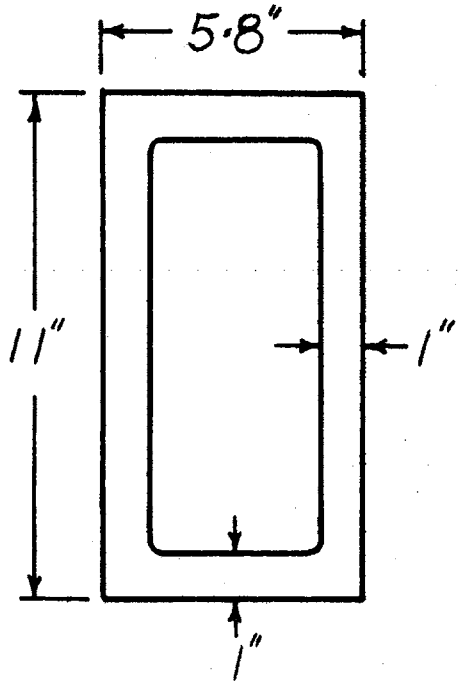

"Large" Pad

Figure 6.3

The rigidity of a six pad bearing is $\frac{9 W_o}{h_o}$ for all radial directions of loading relative to pad configuration. This can be shown as follows:

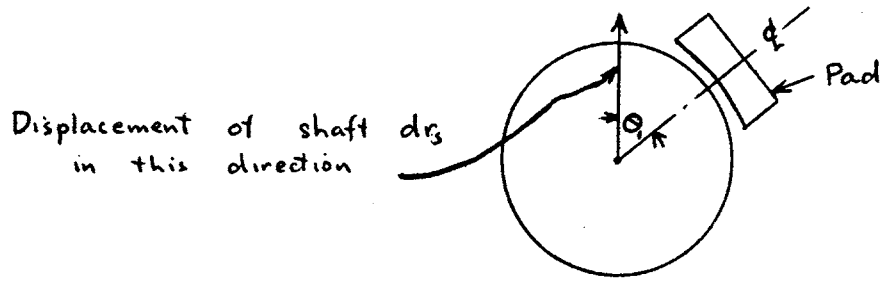

Consider a pad and a radial shaft displacement dr_s. Choose cylindrical co-ordinates so that $\theta = 0$ corresponds to the direction of the displacement dr_s, and let the pad be located at $\theta = \theta_1$, as shown in the diagram. The component of radial displacement affecting the pad is then

$$dr_1 = \cos \theta_1 \, dr_s$$

The change in radial pad load is therefore

$$dW_1 = - \frac{3 W_o}{h_o} \times \cos \theta_1 \, dr_s$$

and the component of this force in the direction of dr_s is

$$dW_{1s} = - 3 \frac{W_o}{h_o} \cos^2 \theta_1 \, dr_s$$

For each of the five other pads, the same relation holds except that the angle θ_1 must be replaced by $\theta_1 + \frac{n\pi}{3}$, n taking on values 1 to 5.

Hence the total rate of change in force in the direction dr_s is

$$\frac{dW_s}{dr_s} = - \frac{3 W_o}{h_o} \sum_{n=0,\,5} \cos^2 \left(\theta_1 + \frac{n\pi}{3} \right)$$

$$= \frac{9\,W_o}{h_o} \quad \text{in the opposite direction to } dr_s. \qquad (6.1)$$

The sum of the components of force at right angles to dr_s is zero. This follows directly from the component for one pad which is

$$dW_{1\perp s} = \frac{3\,W_o}{h_o} \cos\theta_1 \sin\theta_1 \, dr_s$$

The corresponding rate of change of total force is therefore

$$\frac{d\,W_{1\perp s}}{d\,r_s} = -\frac{3\,W_o}{h_o} \sum_{n=0,\,5} \cos\left(\theta_1 + \frac{n\pi}{3}\right) \cdot \sin\left(\theta_1 + \frac{n\pi}{3}\right)$$

$$= 0$$

Typical values for the Canberra H.P.G. are W_o = 5 tons; h_o = 3 mils; making $\frac{d\,W_s}{d\,r_s}$ = 15 tons/mil.

It is useful to study the relation between the various major parameters of a bearing so that one may be able to arrive at the best compromise between conflicting requirements. Quite often such knowledge may be used in conjunction with a particular design to produce a better design. Without such knowledge the correction of one fault in a design may produce a series of new faults.

The following inter-relations may be derived from the bearings under consideration.

We find for a bearing having a total land area A_L, oil viscosity μ, and a maximum shaft linear velocity U, that the maximum friction power P_F = (friction force) x (velocity).

$$\text{i.e.} \quad P_F = \frac{\mu U A_L}{h_o}$$

For bearings of similar geometry characterised by the shaft radius R, and the same maximum velocity,

$$U \propto R$$

$$A_L \propto R^2$$

$$\therefore \quad P_F \propto \frac{\mu R^4}{h_o} \tag{6.2}$$

Also for a particular pad face geometry, the pressure is independent of the scale factor as is shown in Appendix II (equation 16). Hence for the pad load:

$$W_o \propto \frac{\mu Q R^2}{h_o^3} \tag{6.3}$$

Combining (6.1), (6.2) and (6.3) we have,

$$Q \cdot P_F \propto \left(\frac{dW_s}{dr_s}\right) h_o^3 R^2 \tag{6.4}$$

This relation describes the particular conditions of the H.P.G. One obviously must seek the lowest possible product $Q \cdot P_F$ and therefore the minimum values of all variables on the R.H.S. of (6.4). The reduction of R however is limited by considerations of strength. h_o was probably taken too low since the variations in shaft and pad circularity turned out to be a considerable fraction of 3 mils.

$Q \cdot P_F$ has therefore an unalterable minimum value and one must decide on the balance between Q and P_F. This decision depends on such factors as oil heating (and consequent viscosity changes), oil cooling, allowable friction power (considering its effect on the desired performance of the machine) and cost of coolers and pumps. In general it is less expensive to allow a reasonably large P_F and a small Q. Such a choice enables oil

temperature rises to be high and consequently the coolers to be small. It also reduces the size and cost of pumps. Such factors determined the choice on the H.P.G.

Once P_F and Q are chosen, the ratio of $\frac{P_F}{Q}$ fixes the value of μ as can be seen by combining (6.1), (6.2), and (6.3).

$$\frac{P_F}{Q} \propto \frac{\mu^2 R^6}{h_o^5 \left(\frac{dW_s}{dr_s}\right)}$$

When considering the general design of this type of bearing, a limitation other than R may arise. For instance, coupled to the above relation (6.4) is that for plenum pressure.

Since $p \propto \frac{W_o}{R^2} \propto \frac{W_o}{h_o} \times \frac{h_o}{R^2}$

we have for this pressure $p \propto \left(\frac{dW_s}{dr_s}\right) \times \frac{h_o}{R^2}$ (6.5)

The requirement in (6.4) for a small R may therefore lead to high pressure.

One may have to limit pressure for practical reasons, so in such a case the following expression would be more relevant. This expression is obtained by combining 6.4 and 6.5.

$$Q \cdot P_F \propto \frac{h_o^4}{p} \left(\frac{dW_s}{dr_s}\right)^2 \qquad (6.6)$$

Again it is seen that a minimum value of $Q \cdot P_F$ is set by the limitations on the basic parameters, in this case minimum clearance, minimum permissible rigidity of oil film and maximum allowable pressure.

SECTION 7

STABILITY THEORY OF CENTRALLY PIVOTED PRESSURIZED PADS

Hydraulic Forces Acting on a Pad Face

The facility of radial motion of the pads implies that they must be supported in such a manner as to be freely rotatable about any axis, and it has been shown that the method of support adopted essentially allows this.

It is necessary to ensure therefore that with this method of support a pad will take up a stable position relative to the shaft such that the land clearance is as near as possible constant over the surface of a pad, since this is the condition of minimum friction force.

We must therefore study the torques acting on a pad as a function of the inclination of the pad to the shaft. Component torques about the following three mutually perpendicular axes will be considered:

(a) an axis parallel to the shaft axis. (parallel axis)

(b) an axis in the direction of a shaft radius. (radial axis)

(c) an axis parallel to a tangent to the shaft. (tangential axis)

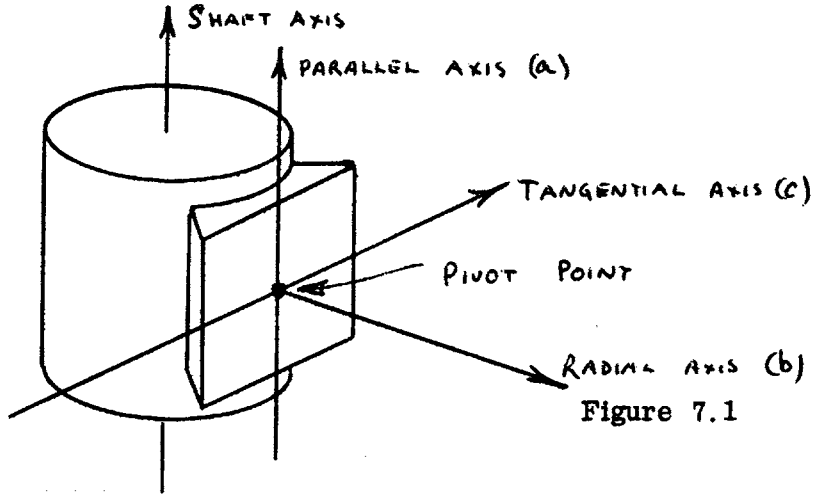

Figure 7.1

All three axes may be considered as intersecting at the pivot point of the pad.

Component (a) will be studied in detail, (b) and (c) being mostly inferred from the results of (a).

TORQUES ABOUT THE PARALLEL AXIS

It is convenient to consider the shaft surface as being transformed into a plane surface, and the pad surface into a slightly undulating one, clearance between the two being preserved during the transformation. The tangential dimensions of the lands are considered small enough to enable the lands to be regarded as plane in this transformation.

Rectangular co-ordinates will be used as defined in the Fig. 7.2. The x direction is in the direction of the velocity U.

A pad face consists of a plenum surrounded by four relatively narrow lands. Those lands whose longer dimension is in the x direction will be called x lands (or θ lands in cylindrical co-ordinates) and the others y lands (z).

The y lands are far more effective in producing torques about the parallel axis for three reasons: -

(a) Their moment arm is the maximum possible throughout their length whereas this is not true for the x lands;

(b) In the H.P.G. bearings the y lands were longer than the x lands;

(c) As is shown (V. 5), torques essentially result from differences in h and grad h. Since h will be for the lands a smoothly varying function of x and y, the differences in h and grad h will be extreme between

the y lands, but progressively less between opposite elements of the x lands having the same distance from the parallel axis, as this axis is approached.

In the following treatment therefore, the x lands will be neglected and the y lands will be treated two dimensionally, i.e. end leakage effects will be neglected.

It is shown in Appendix II that, provided h is small compared with the other dimensions of the oil film and dimensions of anomalies, the following equations apply to the oil film,

$$\overline{V} = \frac{U}{2} - \frac{h^2}{12\mu} \text{ grad } p \qquad \text{(III. 11)}$$

$$\text{div } (\overline{V}\, h) = q \qquad \text{(III. 12)}$$

Here $\overline{V}$ is the <u>average</u> velocity of all points in the oil having the same x, y co-ordinates (or z, θ co-ordinates in cylindrical geometry),

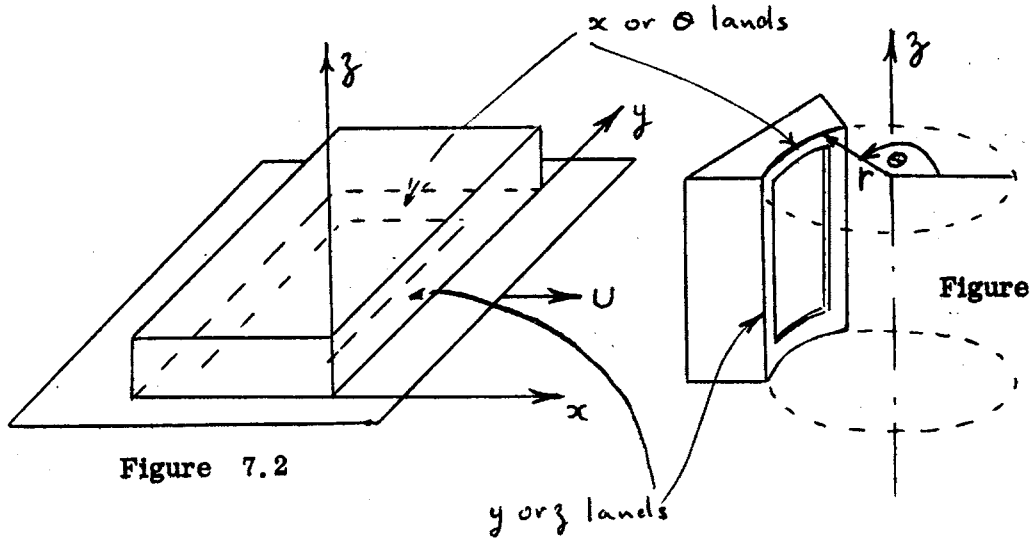

Figure 7.2

Figure 7.3

h and μ are in general functions of x, y, and q is the oil feed per unit area of pad surface (e.g. cubic feet per second per square foot).

These two equations may be combined,

$$q = \text{div} \frac{Uh}{2} - \text{div} \left(\frac{h^3}{12\mu} \text{grad } p \right) \qquad (7.1)$$

Let us now consider three separate sets of particular conditions, each one giving a certain pressure distribution. We require to select these three particular cases for ease in visualization and computation and so that the sum of the pressure distributions equals the actual pressure distribution. The pressure distributions of these three particular cases may be termed component pressure distributions.

Let us consider an actual case where q, p, h and μ distributions are q_a, p_a, h_a and μ_a respectively and $U = U_a$. In general q_a, p_a, h_a and μ_a may be functions of $x, y (z, \theta)$, but in our case $q_a = O$ except at the oil feed inlet hole. Then from 7.1 the following is true

$$q_a = \text{div} \frac{U_a h_a}{2} - \text{div} \left(\frac{h_a^3}{12\mu_a} \text{grad } p_a \right) \qquad (7.2)$$

Consider now the following three sets of particular conditions and the corresponding equations derived from 7.1 .

When dealing with (ii) and (iii) we may consider two loss-less narrow slots along the border of the plenum adjacent to the parallel lands.

(i) $U = O$, $q = q_a$, $h = h_a$, $\mu = \mu_a$.

The pressure distribution p_i is given by,

$$q_a = - \text{div} \left(\frac{h_a^3}{12\mu_a} \text{grad } p_i \right) \qquad (7.3)$$

(ii) $U = U_a$. The q distribution q_{ii} is such that $q = 0$ everywhere except at the imaginary slots at the edges of the parallel lands adjacent to the plenum. Here q is defined by the pressure distribution p_{ii}. p_{ii} is such that $p = 0$ at the slots.

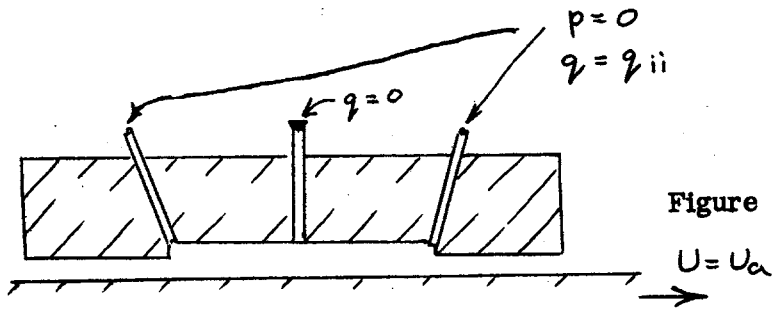

Figure 7.4

$$q_{ii} = \text{div } \frac{U_a h_a}{2} - \text{div } \left(\frac{h_a^3}{12\mu_a} \text{ grad } p_{ii}\right)$$

(iii) $U = 0$

$q = -q_{ii}$

Then p_{iii} is given by,

$$-q_{ii} = -\text{div } \left(\frac{h_a^3}{12\mu_a} \text{ grad } p_{iii}\right)$$

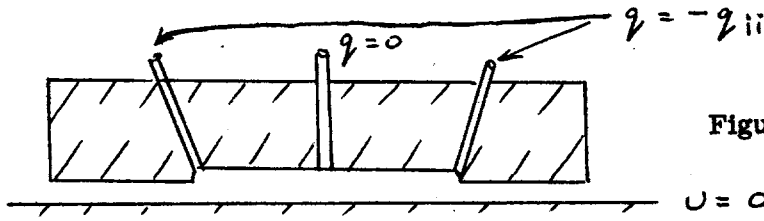

Figure 7.5

If the three equations 7.3, 7.4, 7.5 are added we find: -

$$q_a = \text{div } \frac{U_a h_a}{2} - \text{div } \frac{h_a^3}{12\mu_a} \left[\text{grad } (p_i + p_{ii} + p_{iii})\right] \qquad (7.6)$$

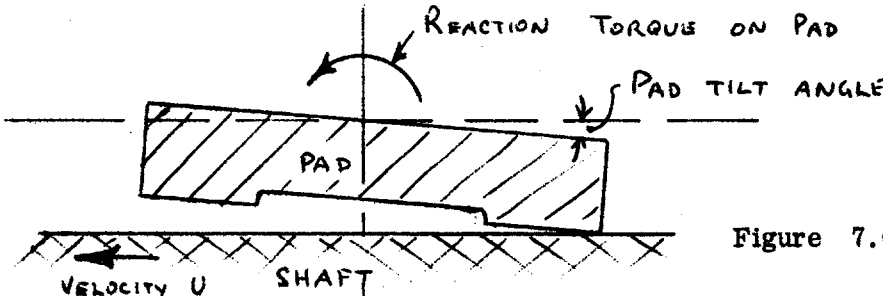

Figure 7.6

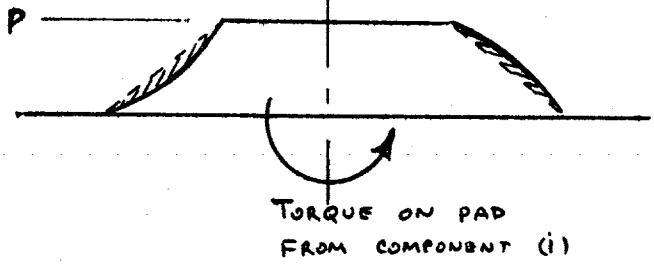

Shaded region is perturbation from case where lands are parallel to shaft (zero torque case).

Component (i) $U = O$
$P \neq O$

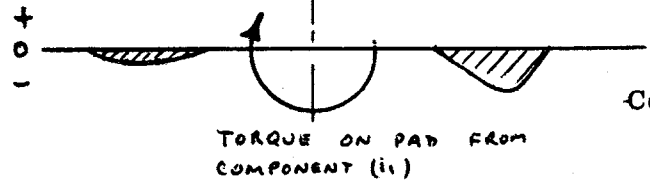

Component (ii) $U \neq O$

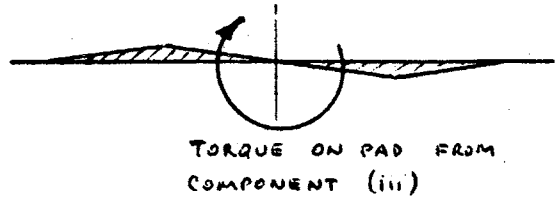

Component (iii) $U \neq O$
$P = O$

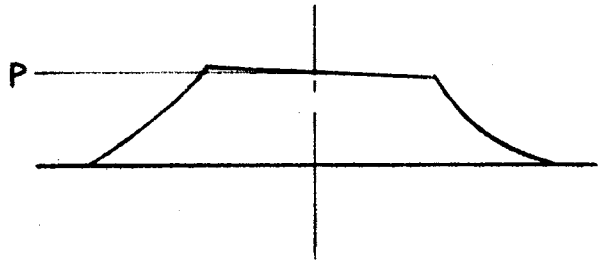

Composite pressure distribution = sum of all components.

From 7.2 and 7.6 it is evident that,

$$p_i + p_{ii} + p_{iii} = p_a$$

i.e. the actual pressure distribution is the sum of the components.

Each of these components will now be considered.

(i) Perturbation of the pressure gradient across the lands, the plenum being pressurized and U = 0.

Consider the inclined surface Fig. 7.7 whose average clearance is h_1, length L, and which has an inclination, defined in the figure of α. X is defined by $X = \frac{x}{L}$, the origin of X being through the centre of the surface as shown in Fig. 7.7, and Q is the oil flow ($-x$ direction) per unit length (into the paper in Fig. 7.7).

The average velocity in the x direction is given in Appendix II as,

$$\bar{V}_x = \frac{U}{2} - \frac{h^2}{12\mu} \frac{\partial p}{\partial x} \qquad \text{II. 9}$$

For component (i), U = 0, and $\bar{V}_x h = -Q$. Also we take $V_y = 0$, and $p = 0$ at $X = -\frac{1}{2}$,

then $$Q = \frac{h^3}{12\mu} \frac{dp}{dx}$$

and $$p = 12\mu Q L \int_{-\frac{1}{2}}^{X} \frac{dX}{h^3}$$

But $$h = h_1 (1 + \alpha h)$$

Therefore $$p_s = \frac{12\mu Q L}{h_1^3} \int_{-\frac{1}{2}}^{X} \frac{dX}{(1 + \alpha X)^3} \qquad (7.7)$$

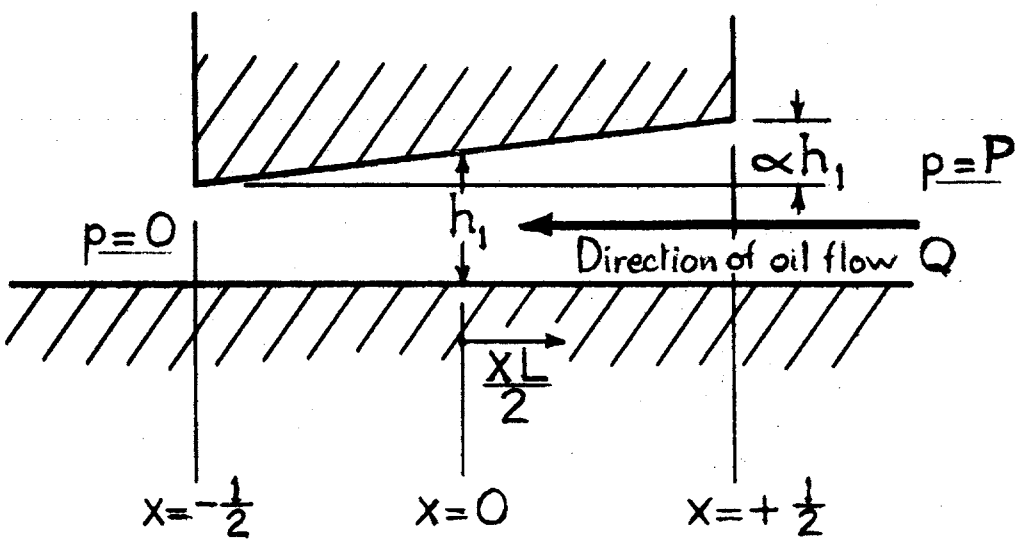

Figure 7.7

If at $x = +\frac{1}{2}$, $p = P$; the solution of 7.7 integrated over the length to give a force leads to the following expression for force per unit length of land,

$$F = \frac{PL}{2}\left(1 + \frac{\alpha}{2}\right) \tag{7.8}$$

We now consider two lands acting together whose centre lines are separated by D. This is illustrated in Fig. 7.8. The dimension k measures the concavity of the pad face. We introduce a factor N defined by $N = \frac{kD}{hL}$ which is a measure of the relative concavity of a pad, and assign subscript 1 to symbols referring to the leading edge land, 2 to the trailing edge ones. The inclination of the pad as a whole is represented by β also defined in Fig. 7.8.

The following relations are derived from the geometry making the usual approximations for small angles;

$$\alpha_1 = \frac{L}{D}\,\frac{N + \beta}{1 - \frac{\beta}{2}}$$

$$\alpha_2 = \frac{L}{D}\,\frac{N - \beta}{1 + \frac{\beta}{2}} \tag{7.9}$$

After substitution of these values in 7.8 and regarding the centre of action of force as being through the centre of the land (a small error introduced here), the torque is derived as,

$$T_s = \frac{D}{2}(F_1 - F_2)$$

$$= \frac{PLD}{8}(\alpha_1 - \alpha_2)$$

$$= \frac{PL^2}{4}\,\frac{1 + \frac{N}{2}}{1 - \frac{\beta^2}{4}} = PL^2 J_s \tag{7.10}$$

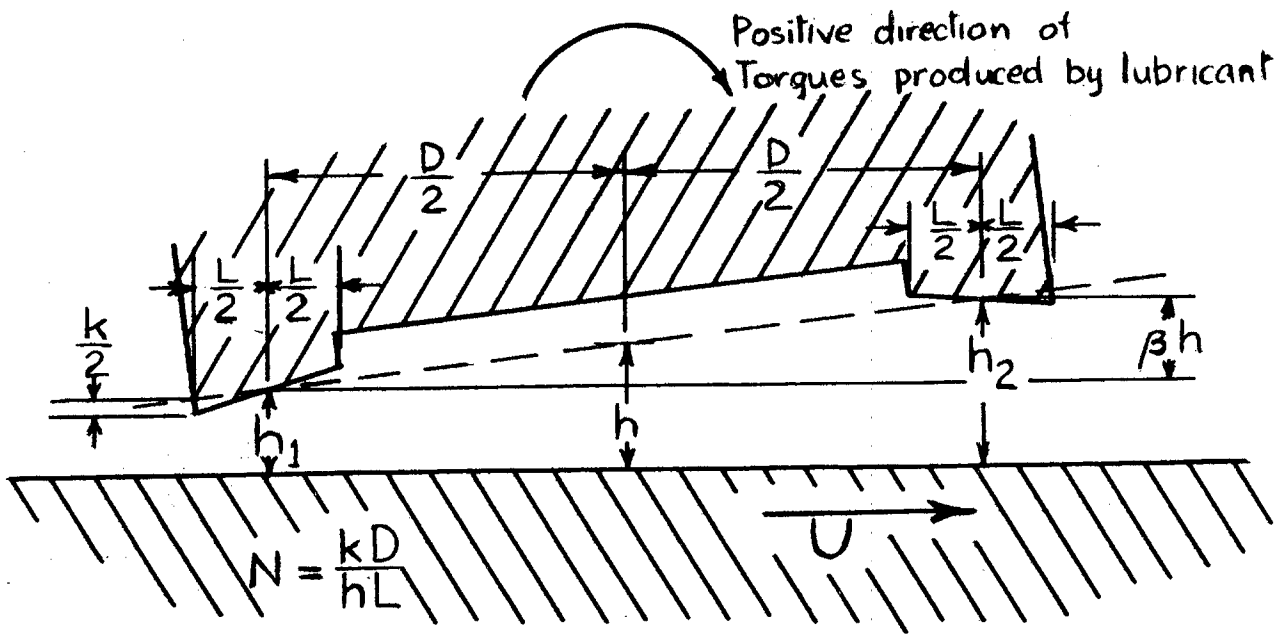
Positive direction of
Torques produced by lubricant
D/2
D/2
L/2
L/2
L/2
L/2
k/2
h1
h
h2
βh
U
N = kD/hL

Figure 7.8

The positive direction of torque is here established as being clockwise as shown in Fig. 7.8. J_s is plotted in Fig. 7.9 as a function of β for various values of N.

(ii) Torques arising from considering the "γ"lands as hydrodynamic tilting pads. U non zero; P = 0.

The general two dimensional equation for hydrodynamic flow (equation 9, Appendix V) is:

$$\frac{h^3}{6\mu}\frac{dp}{dx} = U\,(h - h')$$

Substituting the nomenclature of Fig. 7.7 (i.e. for x and h) and considering the positive direction of U being that of positive x, this equation becomes,

$$\frac{h_1\,(1+\alpha X)^3}{6\mu L}\frac{dp}{dX} = U\,(1+\alpha X - \delta) \qquad (7.11)$$

in which $h' = \delta h_i$.

The integral of this equation is:

$$p = \frac{6\mu UL}{h_1^2}\left[\alpha\int_{-\frac{1}{2}}^{X}\frac{X\,dX}{(1+\alpha X)^3} + \int_{-\frac{1}{2}}^{X}\frac{dX}{(1+\alpha X)^3}\right] \qquad (7.12)$$

where $\gamma = 1 - \delta$

Evaluating the integrals we have:

$$p = \frac{6\mu UL}{h_1^2}\left[\frac{1-\gamma-2(1+\alpha X)}{2\alpha(1+\alpha X)^2} + K\right]$$

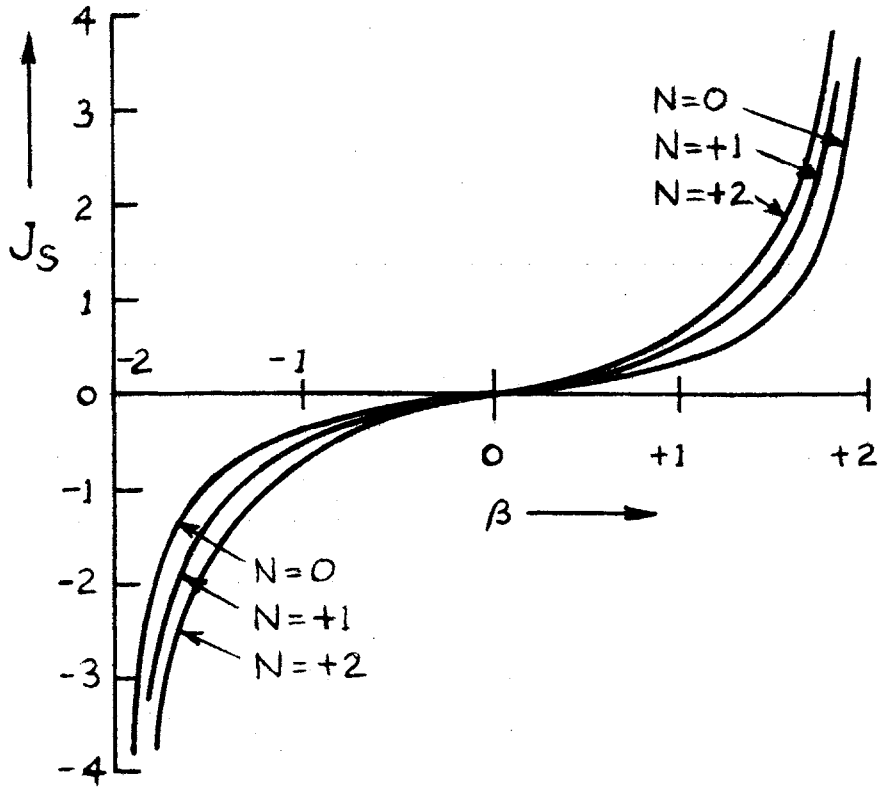

Figure 7.9

The boundary conditions $p = 0$ for $X = \pm \frac{1}{2}$ give $\gamma = \frac{\alpha^2}{4}$ and the constant of integration $K = \frac{1}{2\alpha}$.

The solution is therefore,

$$P_{D1} = \frac{3\mu UL}{h_1^2} \alpha_1 \frac{(X^2 - \frac{1}{4})}{(1 + \alpha_1 X)^2} \tag{7.13}$$

where the subscript "1" refers now to values for the leading land.

The expression 7.13 integrated over the land width gives the force F_1. Thus:

$$F_1 = \frac{6\mu UL^2}{h_1^2} \left[\frac{1}{\alpha_1} - \frac{2 \tanh^{-1} (\frac{\alpha_1}{2})}{\alpha_1^2} \right] \tag{7.14}$$

The substitution for α_1 (7.9) is made and also $h_1 = h (1 - \frac{\beta}{2})$ 7.14 then becomes:

$$F_{D1} = \frac{3\mu UL^2}{h^2} \cdot \frac{D}{L} \left[\frac{1}{(1 - \frac{\beta}{2})(\frac{\beta}{2} + \frac{N}{2})} - \frac{D}{L} \frac{\tanh^{-1} \left[\frac{L}{D} \left(\frac{\frac{\beta}{2} + \frac{N}{2}}{1 - \beta/2} \right) \right]}{(\beta/2 + N/2)^2} \right] \tag{7.15}$$

It is convenient to write the dimensionless quantity,

$$\frac{L}{D} \cdot \frac{\left(\frac{\beta}{2} + \frac{N}{2} \right)}{(1 - \frac{\beta}{2})} = g \tag{7.16}$$

and the quantity,

$$\frac{\mu UL}{h^2} = P_h \tag{7.17}$$

P_h has the dimensions of pressure.

The torque per unit length of land about the parallel axis is:

$$T_{D1} = \frac{F_{D1}\, D}{2}$$

Hence making substitutions of g and P_h,

$$T_{D1} = \frac{3}{2} D^2 P_h \cdot \frac{L^2}{D^2} \cdot \frac{(\frac{\beta}{2} + \frac{N}{2})}{(1 - \frac{\beta}{2})^3} \left[\frac{g - \tanh^{-1} g}{g^3} \right] \qquad (7.18)$$

or $$T_{D1} = P_h L^2 J_{D1} \qquad (7.19)$$

where $$J_{D1} = \frac{3}{2} \cdot \frac{\frac{\beta}{2} + \frac{N}{2}}{(1 - \frac{\beta}{2})^3} \cdot \left[\frac{g - \tanh^{-1} g}{g^3} \right] \qquad (7.20)$$

The conditions at the trailing edge may be reproduced at the leading edge by changing the sign of β and U. These substitutions in 7.15 will give F_{D2} but in 7.19 will give $-T_{D2}$ for the torque about the parallel axis.

Hence $$T_{D2}(\beta) = P_h L^2 J_{D1}(-\beta) \qquad (7.21)$$

The total torque is therefore,

$$T_D(\beta) = T_{D1} + T_{D2}$$

$$= P_h L^2 \left[J_{D1}(\beta) + J_{D1}(-\beta) \right] \qquad (7.22)$$

$$= P_h L^2 J_D$$

$J_D = J_{D1}(\beta) + J_{D1}(-\beta)$ is plotted in Fig. 7.10 for

$\frac{L}{D} = 1/5.$

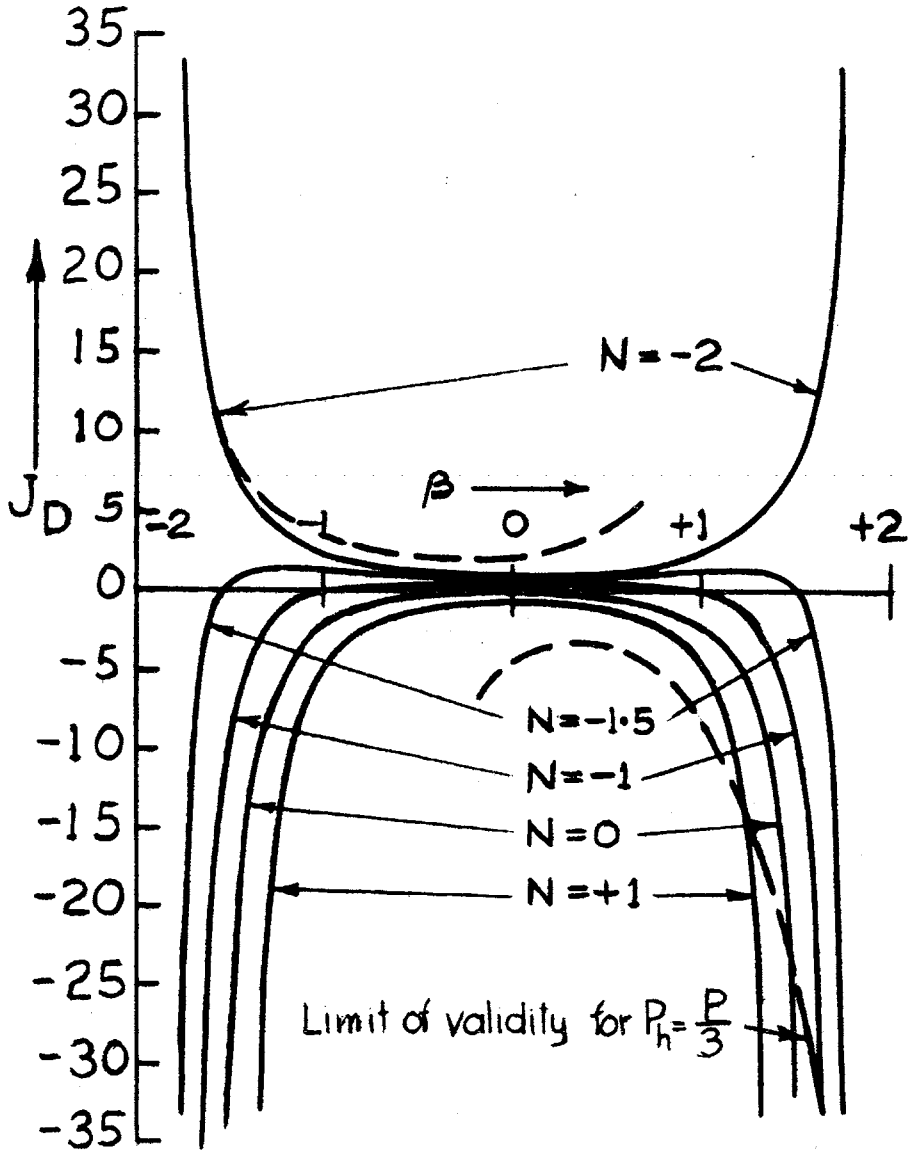
35
30
25
20
15
10
5
0
-5
-10
-15
-20
-25
-30
-35
J_D
-2
-1
0
+1
+2
β
N=-2
N=-1·5
N=-1
N=0
N=+1
Limit of validity for $P_h = \frac{P}{3}$

Figure 7.10

Limits of Validity of Equation 7.22

The validity of 7.22 depends on the magnitude of the net pressure everywhere under the lands. We will take the criterion that the net pressure must be positive and consider only the components (i) and (ii).

For the leading edge (Fig. 7.11) this will evidently be so for α_1 negative through zero to a positive value of α_1 such that,

$$\frac{dp_s}{dx_{-\frac{1}{2}}} = -\frac{dp_D}{dx_{-\frac{1}{2}}}$$

which leads to the relation,

$$\frac{3P_h}{P} = \frac{\left(1 - \frac{\alpha_1}{2}\right)\left(1 + \frac{\alpha_1}{2}\right)^2}{\alpha_1} \qquad (7.23)$$

Similarly for the trailing edge (Fig. 7.12) validity occurs for positive α_2 values through zero to a negative value such that,

$$\frac{dp_s}{dx_{-\frac{1}{2}}} = \frac{dp_D}{dx_{-\frac{1}{2}}}$$

This leads to:

$$\frac{3P_h}{P} = -\frac{(1 - \frac{\alpha_2}{2})(1 + \frac{\alpha_2}{2})^2}{\alpha_2} \qquad (7.24)$$

The relations 7.23 and 7.24 are plotted together in Fig. 7.13. The two limiting values of α_1 and α_2 respectively, determined for a particular value of $\frac{P_h}{P}$ can be substituted in 7.9 to give two new equations relating N in terms of β. These equations can then be plotted on the curves of Fig. 7.10 to form the boundaries of the region of validity.

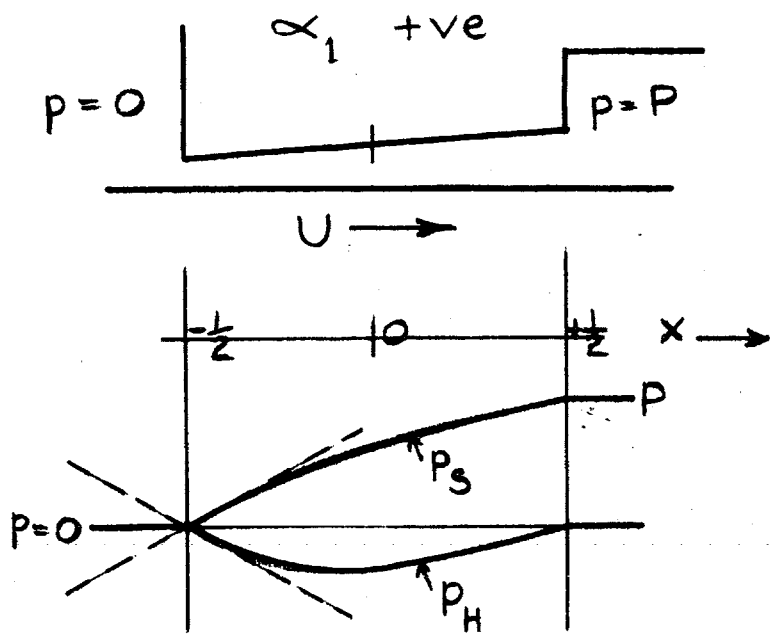

Figure 7.11

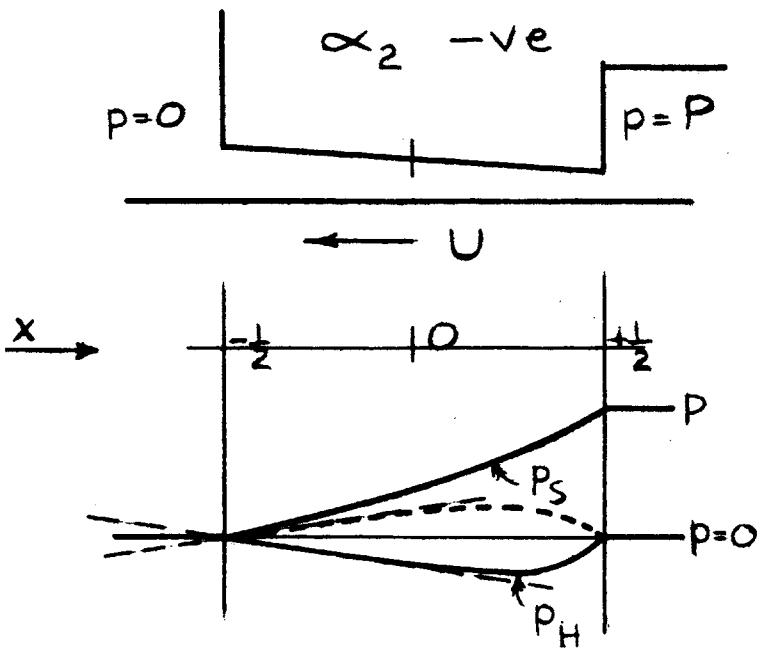

Figure 7.12

By way of example boundary curves are shown for $\frac{P_h}{P} = \frac{1}{3}$ and $\frac{L}{D} = \frac{1}{5}$

For high values of $\frac{P_h}{P}$, the limits of validity in Fig. 7.10 close in to such an extent as to seriously limit its usefulness unless one can estimate the J_D function in the "invalid" region.

The limiting values of J_D in this region can be calculated as follows:

We assume that as $P_h \rightarrow \infty$, component (ii) grows large compared with other components. The limiting condition may therefore be taken as $p_D \geq 0$ everywhere. J_{D1} and J_{D2} may be modified then to new values J'_{D1} and J'_{D2} remembering that $F_D \not< 0$. Thus

if	$J_{D1} > 0$, $J'_{D1} = J_{D1}$	i.e. $J'_{D1} \geq 0$
"	$J'_{D1} < 0$, $J'_{D1} = 0$	
"	$J_{D2} > 0$, $J'_{D2} = 0$	i.e. $J'_{D2} \leq 0$
	$J_{D2} < 0$, $J'_{D2} = J_{D2}$	

Limiting values of $J'_D = J'_{D1} + J'_{D2}$ have been calculated and are shown in Fig. 7.14.

(iii) Torques arising from the stepped geometry of the pad face.

We proceed by the method of superposition as outlined previously. Consider first the geometry with the two hypothetical apertures either side of the plenum as already described, and U non zero. Since in component (ii), the apertures, along with the outer edges of each pad are at the same pressure (the outlet pressure) we have in effect three independent tilting pads.

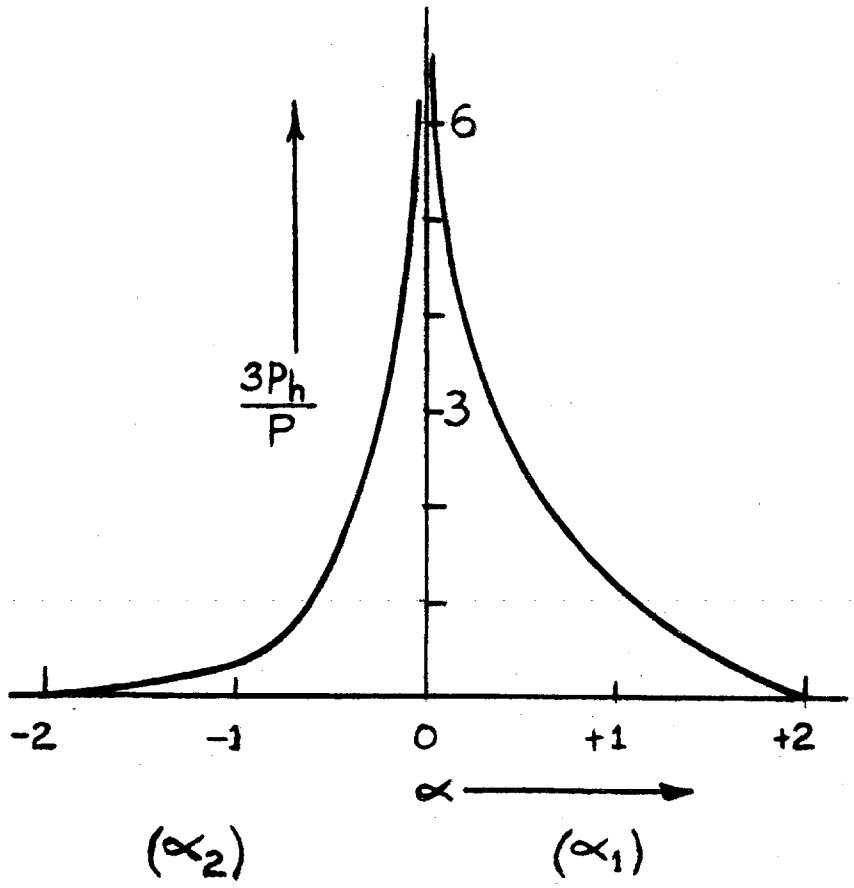

Figure 7.13

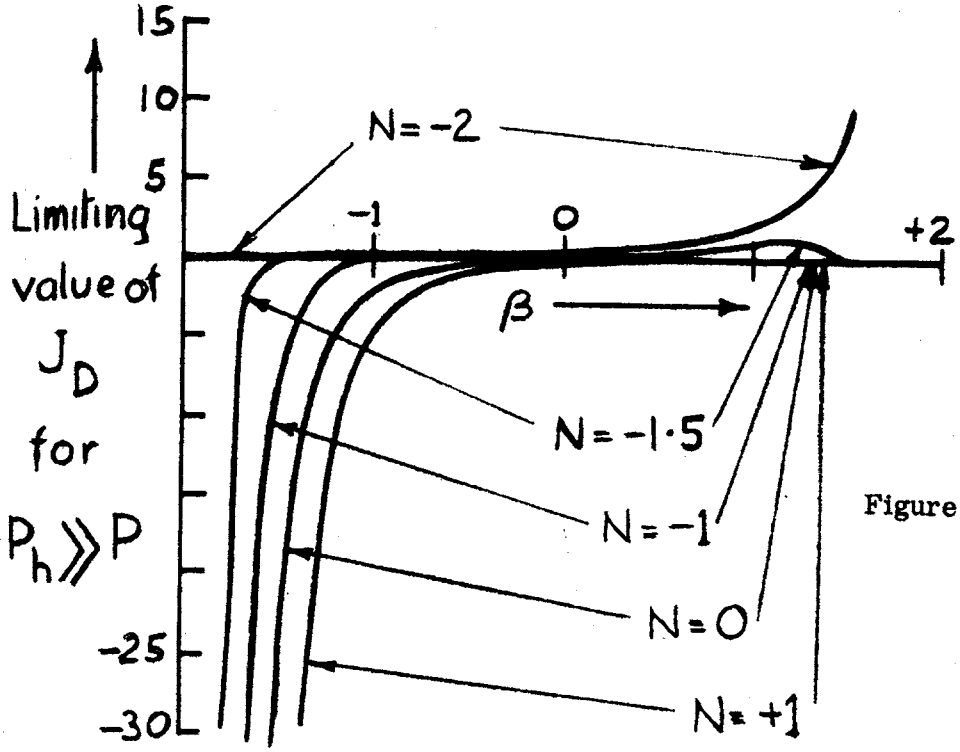

Figure 7.14

According to Appendix V equation 10 the oil flow per unit length under a tilting pad is $\frac{Uh'}{2}$ where h' is a mean value of clearance approaching the average clearance for small angles of inclination and approaching the minimum value of clearance for large angles of inclination. Let h'_1, h'_2, and h'_3 be these mean clearances for the leading and trailing lands and plenum respectively. The q_{ii} distribution is therefore such that $q = 0$ everywhere except at the apertures where, using the established subscript terminology, the oil flows (inwards) per unit length are:

$$Q_1 = \frac{U}{2}(h'_3 - h'_1)$$
$$Q_2 = \frac{U}{2}(h'_2 - h'_3) \qquad (7.25)$$

Component (iii)

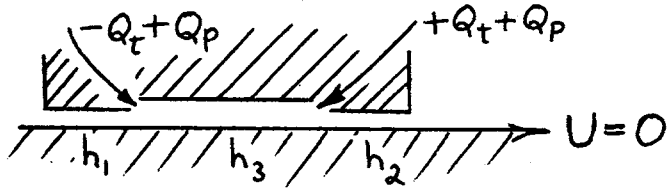

Fig. 7.15.

The q_{iii} distribution then has respective aperture flows of $-Q_1$, $-Q_2$.

It is convenient to define two new flows Q_t and Q_p thus:

$$\left.\begin{aligned} Q_1 &= Q_t - Q_p \\ Q_2 &= -Q_t - Q_p \end{aligned}\right\} \text{ i.e. } Q_t = \frac{Q_1 - Q_2}{2} = \frac{U}{4}(2h'_3 - h'_2 - h'_1) \text{ and } Q_p = \frac{-Q_1 - Q_2}{2} = \frac{U}{4}(h'_1 - h'_2) \qquad (7.26)$$

and to regard the q_{iii} distribution as the sum of two sub-components made up respectively of the Q_t and Q_p flows. The following table will clarify this idea.

	Aperture 1 (leading)	Aperture 2 (trailing)
Subcomponent flow (iiia)	$-Q_t$	$+Q_t$
Subcomponent flow (iiib)	$+Q_p$	$+Q_p$
Component flow (iii) (iiia + iiib)	$-Q_t + Q_p = -Q_1$	$+Q_t + Q_p = -Q_2$

It is convenient to define n here as $n = \dfrac{2\,h'_3}{h'_1 + h'_2}$

or since

$$h \backsimeq \frac{h'_1 + h'_2}{2} \; ; \quad n \backsimeq \frac{h'_3}{h} \tag{7.27}$$

System (iiia) is therefore one having a predominant flow across the plenum in the opposite direction to U of almost Q_t in value provided n is greater than about 5, since that part of Q_t which will flow under the lands will be of the order $\dfrac{Q_t}{n^3}$. The pressure gradient across the plenum will therefore be close to,

$$\frac{dp}{dx} = \frac{12\mu Q_t}{h'^3_3}$$

and provided the variations in plenum clearance are not too great when the pad is inclined, (as will be the case for large n) the pressure difference across the plenum will be:

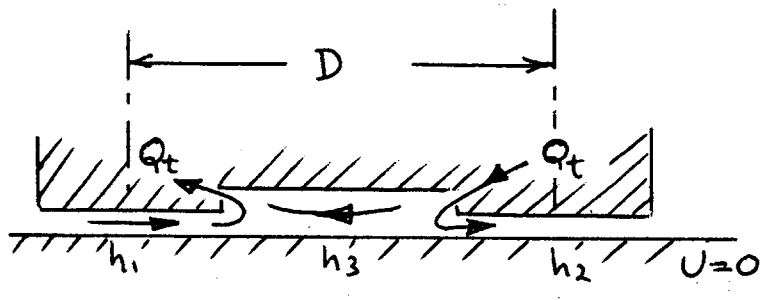

Fig. 7.16.

Component (iiia)

$$p_p \backsim \frac{12\mu}{h'^3_3} \cdot \frac{U}{4} (2h'_3 - h'_2 - h'_1)(D - L)$$

i.e.
$$p_p \backsim \frac{6\mu U}{h^2} \cdot \frac{(n-1)}{n^3} \times (D - L) \qquad (7.28)$$

and a torque will result of,

$$T_p = -\frac{\mu U D}{2h^2} \left[\frac{n-1}{n^3}\right]\left[D^2 - L^2\right] \qquad (7.29)$$

Provided $\beta \backsim 0$ there will be no other effect attributable to Q_t. However, for large positive β values, Q_t causes a negative average pressure component over most of the plenum, this negative pad loading resulting in an overall decrease in h to enable compensation. For negative values of β, the effect is reversed. The extent of this can be gauged by comparing P_D with P.

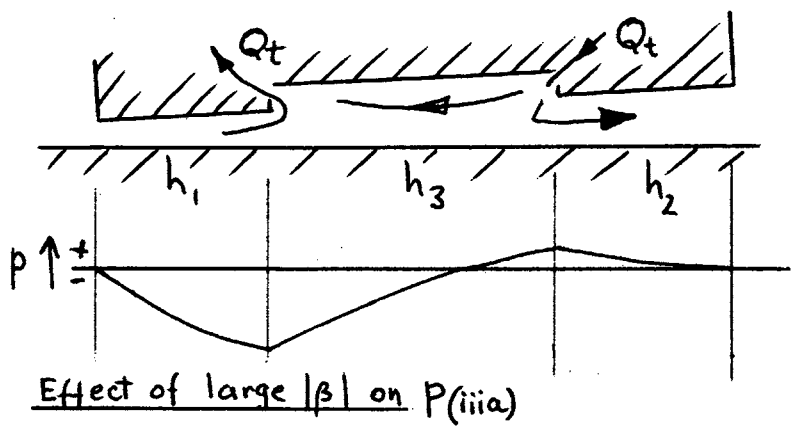

Fig. 7.17.

Subcomponent (iiib) is in essence a case of pressurizing the plenum by means of forced flow inwards of $2Q_p$ $(= \frac{U}{2}(h'_1 - h'_2))$.

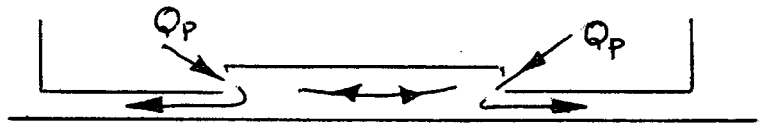

Fig. 7.18.

Component (iiib)

Since

$$\frac{Q_p}{Q_t} = \frac{h'_1 - h'_2}{2h'_3 - h'_2 - h'_1} \qquad \frac{\beta_h}{2nh - 2h} = \frac{\beta}{2} \times \frac{1}{(n-1)}$$

and $\beta_{max} = 2$, then $\frac{Q_p}{Q_t} < \frac{1}{n-1}$

Also the maximum flow <u>across</u> the plenum caused by Q_p occurs when $|\beta| = 2$.

The effect of Q_p on the pressure gradient across the plenum will therefore be neglected for large n values and also any resulting torque component. The major effect of Q_p will be in modifying h since it will add to or subtract from the oil supply $\overline{Q}$ giving a modified net effective oil feed into the plenum.

Therefore when Q_p is positive ($h_1 > h_2$), h must increase to accommodate the increase in flow since the pad loading is constant. Similarly when $h_2 > h_1$, h must decrease.

The extent of this modification can be gauged from the comparison of $2\,Q_p$ and $\overline{Q}$.

The main purpose of 7.28 and 7.29 is of course to estimate the effect of any chosen n value with the aim of increasing n to the extent that

p_p and T_p become unimportant. Their approximate derivation is therefore adequate.

It is useful to express 7.29 also in terms of the pressure P_h and ratio $r = \frac{D}{L}$. Thus for large n values,

$$T_p \sim - \frac{P_h L^2 r (r^2 - 1)}{2 n^2} = P_h L^2 J_p \qquad (7.30)$$

$\frac{P_h}{n^2}$ tending to remain constant and equal to the value at $\beta = 0$.

One further small component of torque must be mentioned; that due to the viscous friction on the pad face acting about the pivot point. If the effective moment arm is m, and n is large, this torque can be expressed as,

$$T_f = -2 P_h mhK = P_h L^2 \left[- \frac{2mhK}{L^2} \right] = P_h L^2 J_f \qquad (7.31)$$

where K is a constant of the order of 2 or so which takes into account the effect of end lands. Obviously J_f is quite small being of the order of $\frac{h}{L}$.

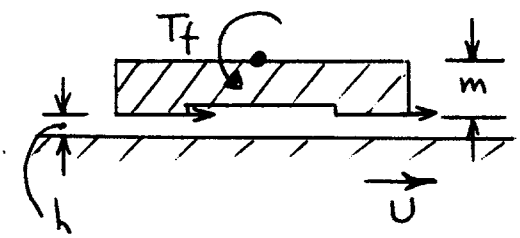

Fig. 7.19.

STABILITY

Four components of torque T have been calculated. They are

$$T_s = P L^2 J_s \qquad (7.10)$$

$$T_D = P_h L^2 J_D \qquad (7.22)$$

$$T_p = P_h L^2 J_P \qquad (7.30)$$

$$T_f = P_h L^2 J_f \qquad (7.31)$$

T_s may be put in a form similar to the other components. Thus

$$T_s = P_h L^2 J_{su}$$

where $$J_{su} = J_s \times \left(\frac{P}{P_h}\right)$$

J_{su} is therefore the only J function which varies with speed. The ratio $\frac{P}{P_h}$ is not constant with respect to variations in β .

Its magnitude can however be estimated by considering the particular value of P_h (P_{ho}) at $\beta = 0$. As shown in Appendix VI eqn. 4

$$\frac{P_{ho}}{P} \lesssim \frac{U'}{6}\left(\frac{a}{b} + 1\right)$$

where U' is the "normalized speed".

and $\frac{a}{b}$ is the pad aspect ratio.

The T components are expressed in a form in which their relative magnitudes may be easily compared by comparison of the J function only.

For the pole bearings the maximum value of U' was 3 so that, taking $\frac{a}{b} \approx 1$, the maximum value of $\frac{P_{ho}}{P} \approx 1$.

Hence $J_{su} \lesssim J_s$ in this case and it will be seen by comparing the graphs of J_s and J_D that in this case J_{su} is insignificant compared to J_D. It gains significance however as speed is reduced.

Of the three components other than T_s, it will be seen that T_D may easily be made the predominant component as it is with the pole bearing design.

For example at $\beta = +1$ and $N = 0$

$$J_D \lesssim -2.4$$

$$J_p \lesssim -.1$$

$$J_f \lesssim -.036$$

In discussing stability further, therefore, T_p and T_f will be neglected. Of the two remaining components T_s predominates at zero and low speeds up to say $U' = .4$ (roughly the condition for $|T_s| = |T_D|$ at $\beta = 1$ and $N = 0$) and T_D predominates at higher speeds, in our case up to $U' = 3$.

The sum of all significant torque components is a torque T which is a function of θ the angle of tilt of the pad. Considering the convention adopted for the directions of torques and angles, it will be evident that the conditions for equilibrium of a pad is $T = 0$, and that this equilibrium is stable if $\frac{\partial T}{\partial \theta_u}$ is positive; unstable if negative.

However, the torque components are expressed in terms of a relative inclination β and contain a factor P_h which is itself a function of β.

It will now be shown that these features are not complicating ones and that ultimately stability may be expressed in terms of J functions and β.

Thus the condition will be shown to be,

$$\Sigma J = 0 \text{ for equilibrium.}$$

$$\frac{\partial}{\partial \beta} \Sigma J > 0 \text{ for stable equilibrium.}$$

The calculation of stability for any configuration may therefore be greatly simplified by having only to deal with J functions.

At any particular speed we have,

$$T = P_h L^2 (J_{su} + J_D + J_p + J_f)$$

$$= P_h L^2 J$$

Since P_h and L^2 do not change sign as β varies

when $T = 0$

$J = 0$

The condition for equilibrium is therefore $J = 0$.

Also $\frac{\partial T}{\partial \theta} = \frac{\partial T}{\partial \beta} \cdot \frac{\partial \beta}{\partial \theta}$ (the partial derivative denote U constant)

now $\theta = \frac{h\beta}{D} = \left(\frac{ho}{D}\right) h'\beta$

Hence θ can easily be calculated from graphs such as VI. 4 (h' vs. β). Further $\frac{\partial \beta}{\partial \theta}$ cannot change sign unless it goes through either zero or infinity as β varies. Considering the curves of VI. 4 they

clearly contain no parts where $d\beta \to 0$, $\frac{\partial \beta}{\partial h'} = 0$ hence $\frac{\partial \beta}{\partial \theta}$ is never zero.

Also if $\frac{\partial \beta}{\partial \theta} \to 0$, $d\theta \to 0$ and hence $h'\beta$ = constant. Several curves of $h'\beta$ = constant have been dotted in on VI.4 to show that in our case at least this condition does not occur. Hence $\frac{\partial \beta}{\partial \theta}$ does not change sign (and is positive). Therefore when,

$$\frac{\partial T}{\partial \theta} > 0, \quad \frac{\partial T}{\partial \beta} > 0$$

A similar argument may be applied with regard to P_h

$$\frac{\partial T}{\partial \beta} = \frac{\partial}{\partial \beta} \left[P_h L^2 J \right]$$

$$= L^2 \left[P_h \frac{\partial J}{\partial \beta} + J \frac{\partial P_h}{\partial \beta} \right]$$

The particular condition we are interested in is $J = 0$.

Hence $$\frac{\partial T}{\partial \beta} = L^2 P_h \frac{\partial J}{\partial \beta}$$

$P_h L^2$ does not change sign with variations in β.

Hence when $$\frac{\partial J}{\partial \beta} > 0$$

$$\frac{\partial T}{\partial \beta} > 0$$

and $$\frac{\partial T}{\partial \theta} > 0$$

The conditions for stable equilibrium are therefore,

$$J = 0, \quad \frac{\partial J}{\partial \beta} > 0$$

Two difficulties should be mentioned at this point.

(i) The variations in h with β as discussed in VI imply that the relative concavity N is also a function of β ($N = {}^{kD}/_{hL}$). Strictly then, a curve representing a component of J for a pad should be drawn across the N = constant curves of graphs such as Figs. 7.9 and 7.10. However, for many discussions of stability the precise nature of the variations in N are not required, especially at low speeds where the variations introduce symmetrical modifications with respect to the vertical axis through $\beta = 0$.

It should be noted however that there is an abrupt change in the nature of J_D depending on whether N is greater or less than -2. At high speeds therefore the assymmetry in the h' vs β curve (Fig. VI.4) may cause differences between the values of N at the extreme values of β. If for example $N = -2$ at $\beta = 0$, then for $\beta > 0$, $|N| > 2$ and for sufficiently high U', $|N| < 2$ for $\beta < 0$. The resulting curve representing a pad would then have the form:

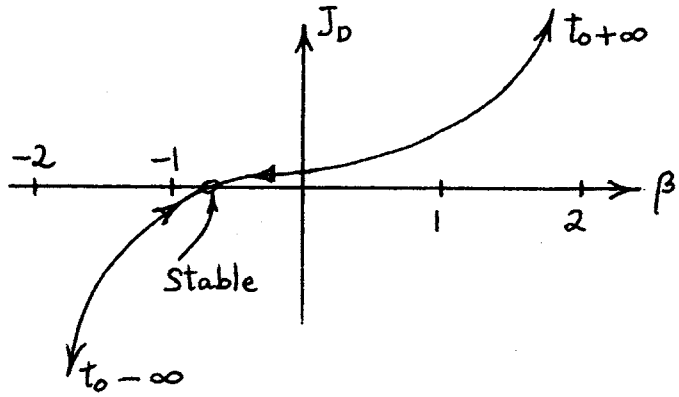

Fig. 7.20.

This happens to be quite stable especially when combined with J_S.

However at lower speeds J_D would revert to the inherently unstable form:

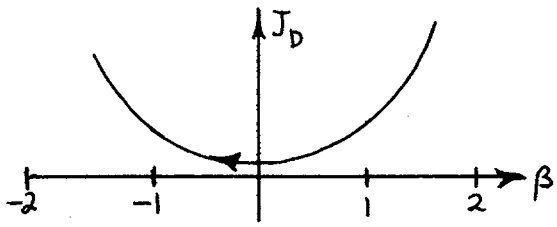

Fig. 7.21.

(ii) The second difficulty is the nature of J_{su}.

We have by definition,

$$J_{su} = J_s \times \frac{P}{P_h}$$

$$= J_s \times \frac{P}{P_{ho}} \times \frac{P_{ho}}{P_h}$$

By using VI. 4, and 7. 17, this becomes,

$$J_{su} \approx J_s \left[\frac{6}{U'(\frac{a}{b} + 1)}\right] \times \frac{1}{(h')^2}$$

Hence J_{su} is a function of β because h' is a function of β .

It has been pointed out above that J_{su} is only significant for $U' < .4$. It will be seen from the curves of VI. 4 that for this condition, h' is practically a symmetrical function of β and not significantly different from the curve for $U' = 0$. It is possible therefore to derive J_{su} from J_s for any particular aspect ratio. For example if $\frac{a}{b} = 1$,

$$J_{su}(\beta) \approx \frac{J_s(\beta)}{U'} \times \frac{3}{\left[h'(\beta)_{U'=0}\right]^2}$$

By way of example J_{su} is plotted for $U' = .3$, $N = 0$ and $\frac{a}{b} = 1$ in Fig. 7.22.

It is now possible to discuss the design of a pad face which is required to be stable over a range of speed.

The entire speed range may be divided into 3 regions defined by the relative magnitudes of T_s and T_D (we assume other T components negligible).

These regions are:

1. $T_s \gg T_D$ (e.g. $.1 > U' > 0$)

2. Transitional region (e.g. $1.6 > U' > .1$)

3. $T_D \gg T_s$ (e.g. $\infty > U' > 1.6$)

The major design parameter to be selected is of course N or specifically N_o the value for $\beta = 0$.

We will deal only with speed regions 1 and 3 and show that there is no value of N_o that is satisfactory over these two regions. Since the range of U' for the pole bearings falls in all three regions we conclude that it is not possible to choose a satisfactory N_o for these bearings without introducing other stabilising features.

Speed Region 1. The torque reduces to,

$$T \rightarrow T_s = P L^2 J_s$$

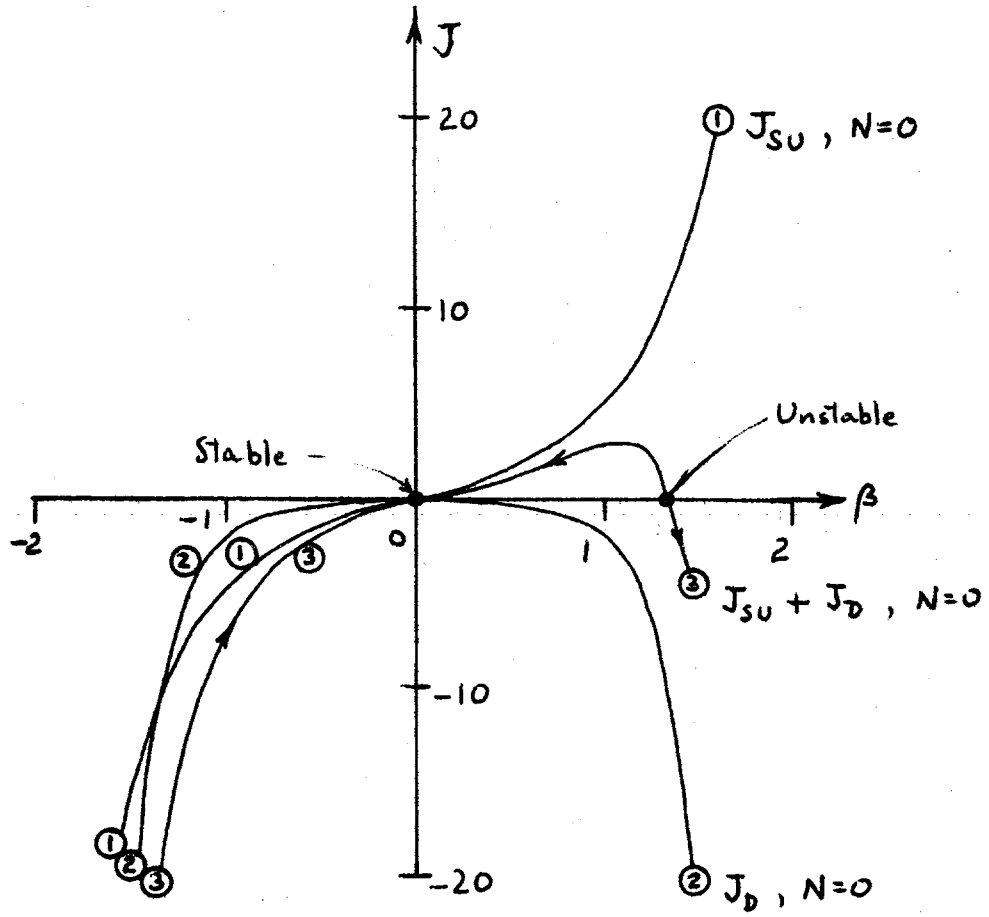

$$\frac{\alpha}{h} = 1$$

$$J_{SU} = \frac{J_S}{U'} \cdot \frac{3}{\left(h'_{U'=0}\right)^2}$$

$U' = .3$

$N = 0$

Figure 7.22

It will be seen from Fig. 7.9 and equation 7.10 that stability at $\beta = 0$ occurs provided $N \pm 2 > -2$. The subscript ± 2 indicates that the N value at $\beta = \pm 2$ is the important value. From previous considerations of N vs. β, it is seen that the approximate corresponding condition for N_o is $N_o > -1.4$.

Speed Region 3. Here we consider only the predominant J function J_D. Characteristic curves of J_D vs. β for various ranges of N, (N_o) may be determined from consideration of Fig. 7.10 and the limiting case $U' \rightarrow \infty$ illustrated in Fig. 7.14.

The entire N_o range has been divided below into four cases. In each case a characteristic curve is drawn, with shading indicating where the curve may lie between the two extremes of Fig. 7.10 and 7.14. Arrows show the direction of response of a pad to a displacement.

(a) $N_o = 0$

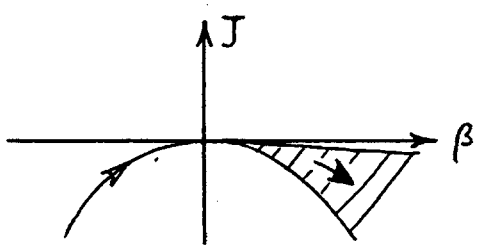

Fig. 7.23.

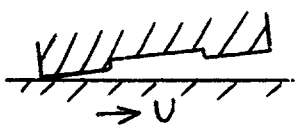

Stability - unstable

(b) $N > 0$

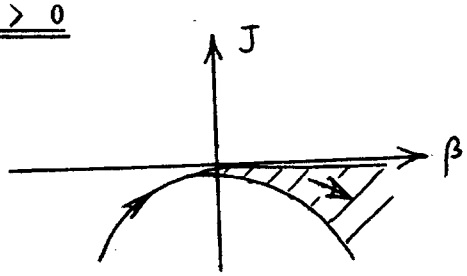

Fig. 7.24.

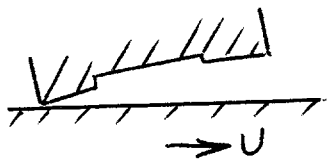

Stability - unstable

(c) $0 > N > -2$

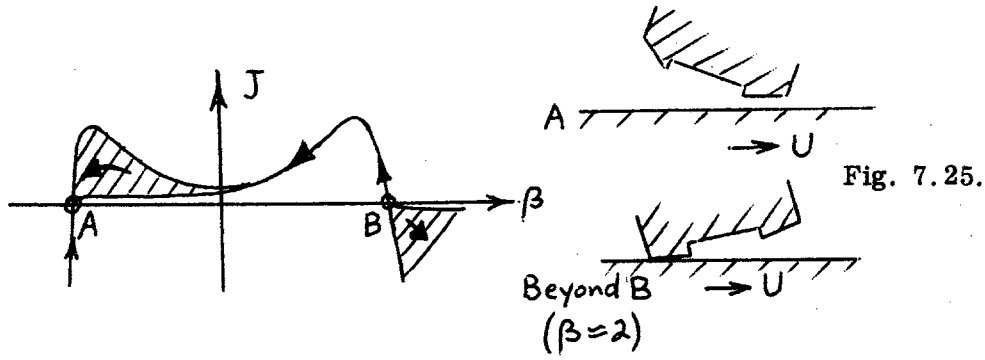

Fig. 7.25.

Stability - A is stable,

B unstable.

(d) $-2 > N$

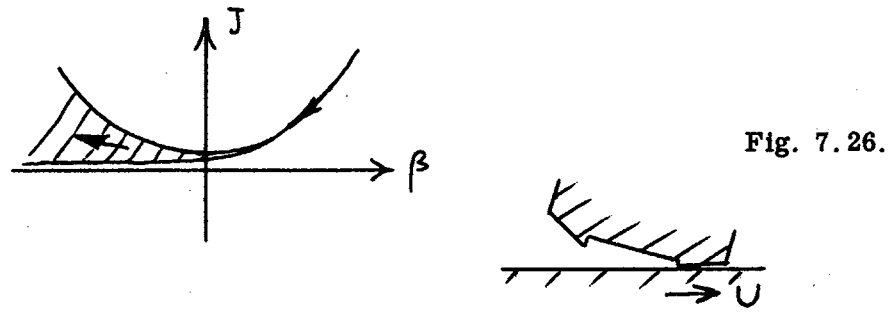

Fig. 7.26.

Stability - unstable

In addition there are possibly some special cases where N crosses from one of the above cases to another as β varies. These special cases cannot involve a change in sign of N. For large U', they involve $|N|$ for positive β being greater than $|N|$ for negative β. The one significant special case already considered elsewhere, is where there is cross over between (c) and (d).

Special case (e) $N_o \lessapprox -2$

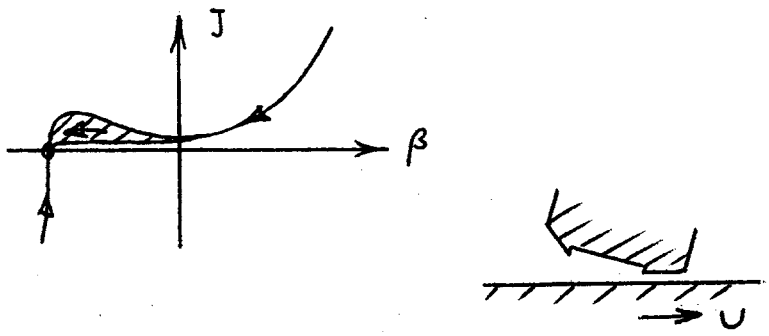

Fig. 7.27.

Stability - stable

Of all these cases, only two, viz. (c) and (e) have a stable operating point and of these only (e) is unambiguously stable.

However the condition for stability viz. $N_o \lessapprox -2$ is incompatible with the requirement for $U' \to 0$ viz. $N_o > -1.4$.

Hence it is not possible to select N_o such that a pad is stable over the entire range of U'.

SECTION 8

THEORY OF CYLINDRICAL STABILIZING LANDS

It seemed reasonable to the author to try to introduce into the pad design a stabilising feature that was hydrodynamic in nature to meet the essentially hydrodynamically produced unstabilizing torques. In this respect the action of a pair of surfaces cylindrically convex relative to the shaft was investigated.

Each of these surfaces should provide a pressure under the leading portion followed by cavitation towards the trailing edge. Since the forces would be a function of clearance, a stabilizing effect should result.

No mechanism capable of working in either direction of speed could be envisaged unless cavitation were allowed. Since most damage attributed to cavitation appeared to result from severe pressure fluctuations caused by insufficient damping of an inherently unstable situation, it was hoped that the small clearance and the large ratio of length to width (reducing the possible deleterious effects of end leakage) would provide sufficient damping to eliminate trouble of this nature. So far inspection has borne out this hope.

Pressure and Forces on a Cylindrical Surface of Infinite Extent.

The stabilizing lands are long compared with their width. End effects are therefore neglected and each is considered part of an infinitely long surface.

We consider the case of a moving plane surface, velocity U in the x direction. The x and y axes are fixed but are contained in the moving surface. The stationary cylindrical surface has its cylindrical

axis in the y direction and the z axis passes through the cylindrical axis. The origin of co-ordinates is in the moving plane. z is the clearance between the two surfaces. The stationary curved surface is bounded by two lines parallel to the y axis and equidistant from it.

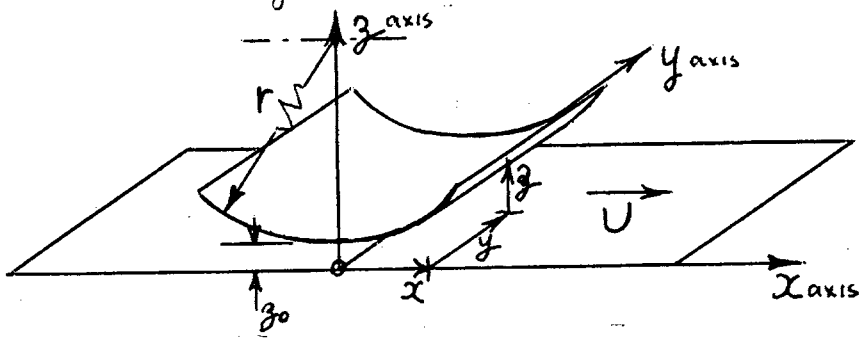

Fig. 8.1

Let z_0 be the minimum clearance. Then using the parabolic approximation for arcs of small angle we may write

$$\frac{z}{z_0} = 1 + \xi^2 \qquad 8.1$$

where

$$\xi = \frac{x}{\sqrt{2rz_0}} \qquad 8.2$$

and r is the radius of curvature of the stationary surface.

The general equation for pressure is shown in the Appendix VIII to be

$$p = 6\mu U \sqrt{\frac{2r}{z_0^3}} \times J(\xi, \epsilon) + K \qquad \text{VIII.4}$$

where

$$J = \left[\frac{1}{2} - \frac{3\epsilon}{8}\right]\left[\tan^{-1}\xi + \frac{\xi}{1+\xi^2}\right] - \frac{\epsilon\xi}{4(1+\xi^2)^2} \qquad \text{VIII.3}$$

J is thus a dimensionless form factor which depends on relative position (ξ) and ϵ. ϵ is a dimensionless number expressing the ratio of the average oil flow to the oil flow that would occur if $z = z_0$ everywhere (couette flow). i.e. the average oil flow is

$$\bar{Q} = \frac{\epsilon \beta_0 U}{2}$$

8.5

K is a constant. Both ϵ and K are set by boundary conditions which in our case are complicated by cavitation.

The Nature of Cavitating Fluid.

It is assumed here that a cavitating fluid consists of an intimate mixture of the liquid and small bubbles of its vapour in two phase equilibrium. We ignore possible temperature changes due to thermodynamic processes. The pressure throughout the mixture is equal to the vapour pressure. Hence $\text{grad} p = 0$.

The law of continuity of (volume) flow does not apply since the fluid is no longer incompressible. However, we assume that the density of the vapour is negligible and therefore that the law of continuity of flow applies to the liquid component.

Because of the intimate nature of the mixture, the flows of the components (liquid and vapour) are in the same direction as the flow of the fluid mixture.

Viscosity is indeterminate. However, we may postulate that $\frac{\partial \mu}{\partial z} = 0$ i.e. there is no variation in the number, density and size of the vapour bubbles in the z direction, and therefore the effective mixture viscosity is constant for a given x, y .

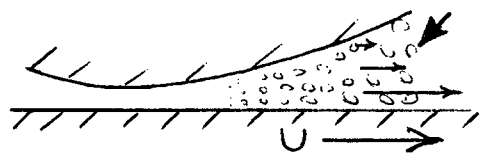

Cavitating fluid, an intimate mixture of liquid and vapour bubbles. Fig. 8.2

Since there is no pressure gradient, the only forces to be considered acting within the fluid are simple shearing forces. It follows that there will be a linear variation with z of V_x at a given x, y from O to U and

$$\bar{Q}_f = \bar{Q}_v + \bar{Q}_L = \frac{U z}{2} \qquad 8.6.$$

where $\bar{Q}_f$ is fluid mixture flow.
$\bar{Q}_v$ is vapour flow.
$\bar{Q}_L$ is liquid flow.

The Boundary Between Normal Lubricant and the Cavitating Fluid.

In the normal region $p > p_v$ (vapour pressure) and

$$\frac{z^3}{12\mu} \frac{dp}{dx} = \frac{U z}{2} - \bar{Q}_L \qquad V.9.$$

and V.10.

Hence at the boundary (continuing with 8.6)

$$\bar{Q}_L = \frac{U z_b}{2} - \frac{z_b^3}{12\mu} \frac{dp}{dx} = \frac{U z_b}{2} - \bar{Q}_v$$

or

$$\bar{Q}_v = \frac{z_b^3}{12\mu} \frac{dp}{dx} \qquad 8.7.$$

As explained, $\bar{Q}_v$ and $\bar{Q}_L$ must be of the same sign and therefore cannot be negative. Neither can $\bar{Q}_v$ be positive because $\frac{dp}{dx}$ would then be positive and p would be less than p_v immediately before the boundary.

$\bar{Q}_v$ must therefore be zero.

Hence

$$\frac{dp}{dx} = 0$$

For simplicity p_v will be taken as zero.

The boundary conditions for determining ϵ and K in 8.3 are therefore

$$\left.\begin{aligned} p &= 0 \\ \frac{dp}{dx} &= 0 \end{aligned}\right\} \quad \text{at the cavitation boundary, } (\xi = \xi_b)$$

$p = 0$ at the leading edge (negative extreme of ξ, $\xi = \xi_1$)

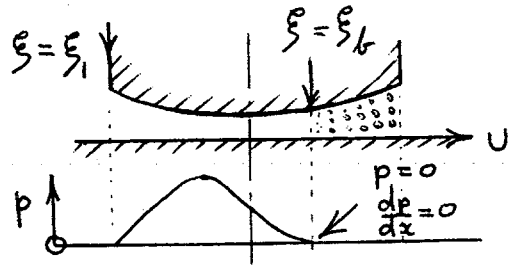

Fig. 8.3

It is worth noting that the treatment so far has been confined to the left hand side boundary of the cavitation region (Fig. 8.3) . The right hand boundary is discussed in more general terms and at some length in Appendix VII.

Solution of the equation for pressure in the non-cavitating (normal) Region

It will be noticed that Equation VIII. 3 for $\mathcal{J}$ has odd symmetry about the axis $\xi = 0$, and that in general on the left hand side of the axis there is a maximum peak and on the right hand side a corresponding minimum trough ($\mathcal{J} = \mathcal{J}$ min.)

The above discussed boundary conditions will therefore be met by choosing ϵ such that

$$\mathcal{J}_{\xi = \xi_1} = \mathcal{J}_{min} \qquad 8.9$$

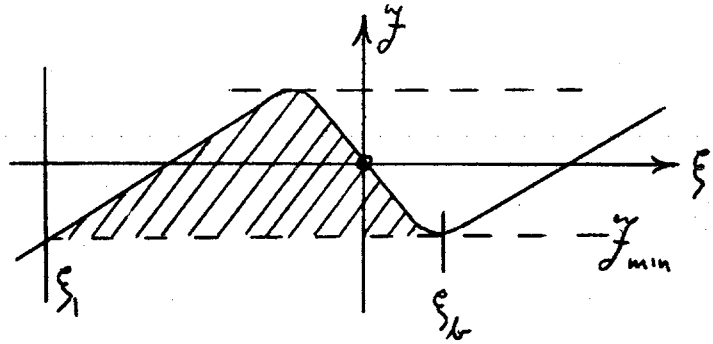

Fig. 8.4

The constant K then assumes the value

$$K = -6\mu U\sqrt{\frac{2r}{z_0^3}} \times \mathcal{J}_{min} \qquad 8.8$$

Hydrodynamic force on a cylindrical surface.

The force per unit length (y direction) on the surface is

$$F_1 = \int p\, dx$$

or by substitution of 8.2 and then VIII. 4

$$F_1 = \sqrt{2r z_0}\int p\, d\xi$$

$$= \frac{12\mu U r}{z_0}\left[\int_{\xi_1}^{\xi_b} \mathcal{J}\, d\xi - \mathcal{J}_{min}(\xi_b - \xi_1)\right]$$

i.e. $$F_1 = \frac{12\mu U r A}{g_0} \qquad 8.10$$

where $$A = \int_{\xi_1}^{\xi_b} \mathcal{J}\, d\xi - \mathcal{J}_{min}(\xi_b - \xi_1) \qquad 8.11$$

It will be seen that A corresponds to the area of the shaded part of Fig. 8.4. It will also be seen that A is a unique function of ξ_1 only, since for each value of ξ_1, there is only one value of ϵ which satisfies the condition 8.9.

The A.N.U. computer was programmed by the author to compute the relation between A and ξ_1. The actual programme involved computing A and ξ_1 from a succession of values of ϵ. The results of this computation were used in the preparation of Fig. 8.6.

Torques.

The configuration adopted to stabilize pads of the basic design already described was to place two cylindrical surfaces on either side of the pad and separated from it by grooves. The nominal clearance for these surfaces ($\beta = 0$) was the same as for the pad.

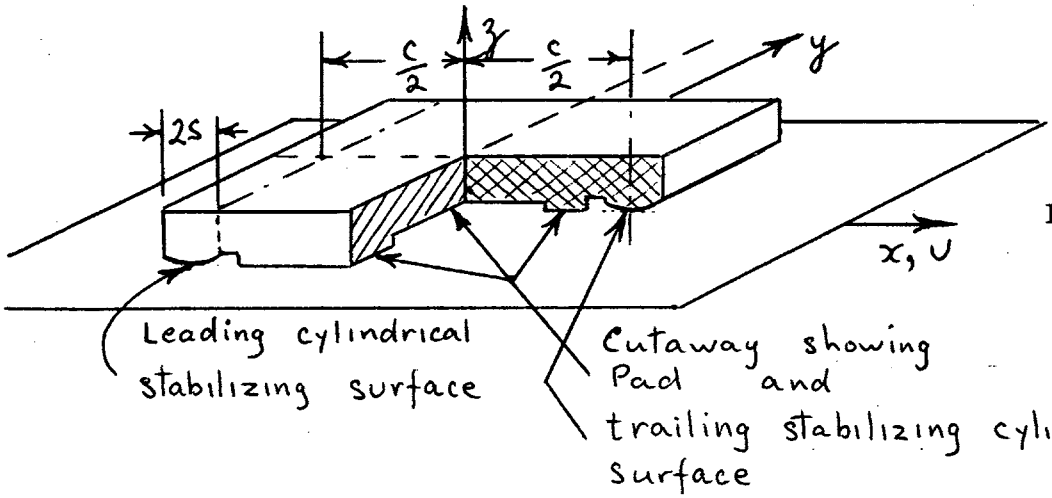

Fig. 8.5

The torque about the pivot point for the leading surface is therefore approximately:

$$T_1 = F_1 \frac{c}{2} \qquad 8.12.$$

Now F_1 is a function of A which in turn is a function of ξ_1 and therefore of z_0 and S, where $2S$ is the cylindrical surface width (in the x direction).

Thus from 8.2

$$\xi_1 = \frac{S}{\sqrt{2r z_0}} \qquad 8.13.$$

Also from the geometry it will be seen that β is now physically limited to β_{max} such that $\beta_{max} = \frac{2D}{c}$ 8.13a

Further the relation between z_0 and parameters previously used in the pad theory is

$$z_0 = h\left[1 - \frac{\beta}{\beta_{max}}\right] \qquad 8.14.$$

It is also useful to define a new term ξ_0 which can be regarded as the normal or most desirable value of ξ (at $\beta = 0$).

Thus

$$\xi_0 = \frac{S}{\sqrt{2rh}} \qquad 8.15.$$

Combining 8.13, 8.14 and 8.15 we find

$$\xi_1 = \frac{\xi_0}{\sqrt{1 - \frac{\beta}{\beta_{max}}}} \qquad 8.16.$$

and $$\gamma_0 = h \frac{\xi_0^2}{\xi_1^2}$$ 8.17.

Substituting 8.10 for F_1 and 8.17 for γ_0 in 8.12 we obtain

$$T_1 = 6\mu \frac{UrC}{h} \frac{\xi_1^2}{\xi_0^2} A(\xi_1)$$ 8.18.

This may be rendered into a form similar to that of other torque components by the subsitution for P_h (equation 7.17).

Then

$$T_1 = P_h L^2 \left(\frac{hr}{L^2}\right)\left(\frac{C}{L}\right) \frac{6\xi_1^2}{\xi_0^2} A_{(\xi_1)}$$

or $$T_1 = P_h L^2 J_{c_1}$$ 8.19.

where $$J_{c_1} = 6\left(\frac{hr}{L^2}\right)\left(\frac{C}{L}\right) \frac{\xi_1^2}{\xi_0^2} A_{(\xi_1)}$$

or substituting 8.15

$$J_{c_1} = \left(\frac{s^2}{L^2}\right)\left(\frac{C}{L}\right) \left[3\left(\frac{\xi_1}{\xi_0}\right)^2 \frac{A_{(\xi_1)}}{\xi_0^2}\right]$$ 8.20.

Each of the ratios in the square brackets can be expressed as functions of $\left(\frac{\xi_1}{\xi_0}\right)$, (the right hand one being also a function of ξ_0) and therefore of $\frac{\beta}{\beta_{max}}$ by using equations 8.16. It is convenient to redefine the quantity in square brackets by ψ_1.

Thus

$$\psi_1\left(\frac{\beta}{\beta_{max}}\right) = 3\left(\frac{\xi_1}{\xi_0}\right)^2 \times \frac{A}{\xi_0^2}$$ 8.21.

and then

$$J_{c_1} = \frac{S^2}{L^2} \times \frac{C}{L} \times \psi_1 \qquad 8.22.$$

It should be noted that $\psi_1 \to \infty$ as $\beta \to \beta_{max}$. In fact if

$\beta = (\beta_{max} - \delta)$

$$\psi_{1\,\delta \to 0} \longrightarrow 3 \frac{\beta_{max}}{\delta} \frac{A_\infty}{\xi_0^2} \qquad 8.23.$$

where A_∞ is a limiting value which approaches approximately .20.

The resultant torque from two stabilizing surfaces is

$$T_c = T_1 + T_2 = P_h L^2 J_c \qquad 8.24.$$

where

$$J_c = \frac{S^2}{L^2} \frac{C}{L} (\psi_1 + \psi_2) \qquad 8.25.$$

ψ_2 and ψ_1 are related by

$$\psi_2(\beta) = -\psi_1(-\beta) \qquad 8.26.$$

Plots of $\psi = (\psi_1 + \psi_2)$ for various values of ξ_0 appear in Fig. 8.6.

Optimum value of ξ_0

In order to create stable operation at $\beta = 0$ with maximum possible rate of production of restoring torque with change in β it is necessary to maximize $\frac{\partial T_c}{\partial \beta}$ at $\beta = 0$ with respect to the shape of the cylindrical surface.

From 8.24 and 8.25 we have

$$T_c = P_h S^2 \frac{C}{L} \psi$$

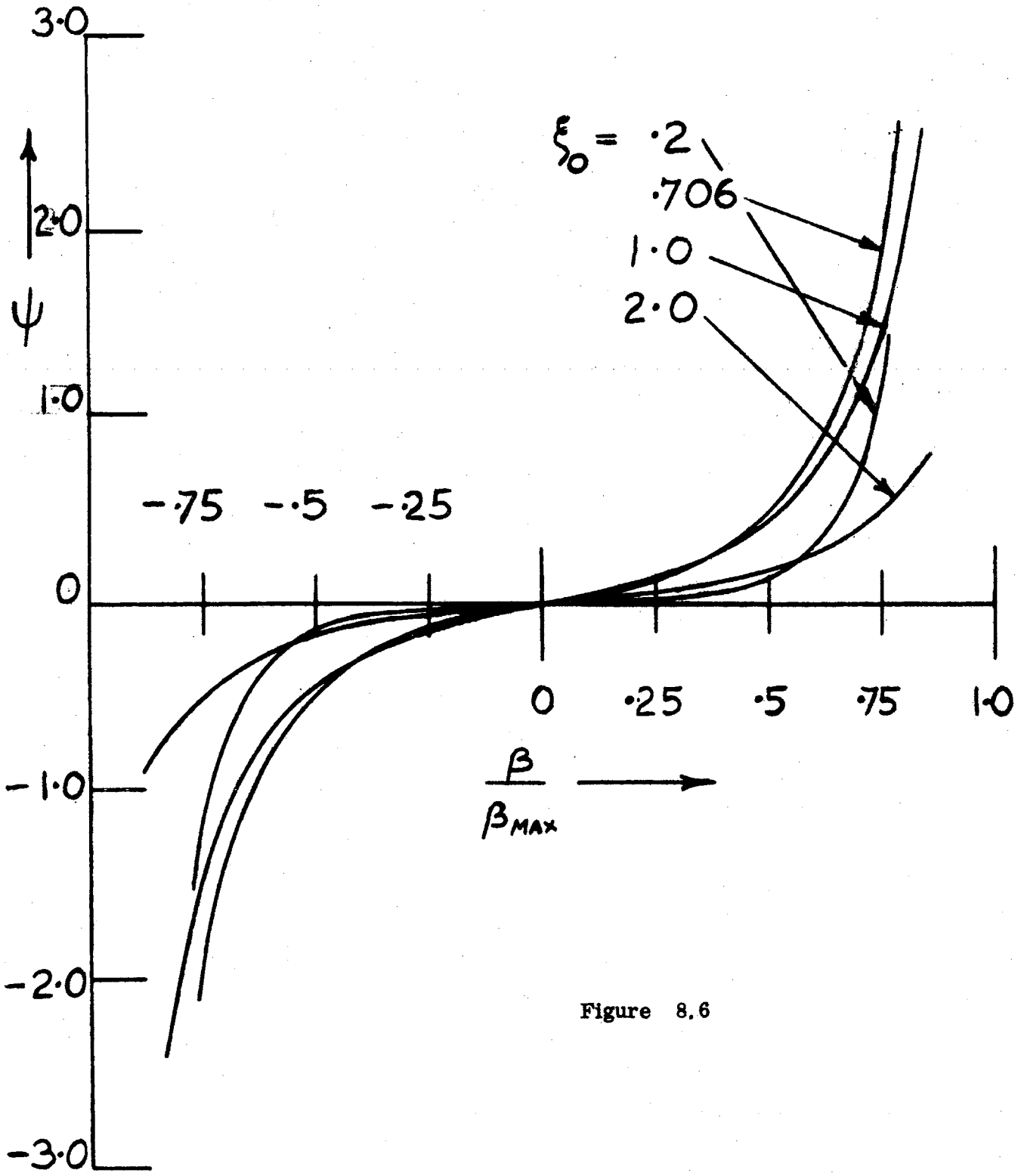

Figure 8.6

i.e. $$\frac{\partial T_c}{\partial \beta} = P_h S^2 \frac{C}{L} \frac{\partial \psi}{\partial \beta} \qquad 8.27$$

The partial derivatives denote r and s constant. To maximize $\frac{\partial T_c}{\partial \beta}$ it is therefore necessary to maximize $\frac{\partial \psi}{\partial \beta}$.

From 8.26

$$\psi = \psi_1 + \psi_2$$
$$= \psi_1(\beta) - \psi_1(-\beta)$$

and
$$\frac{\partial \psi(\beta)}{\partial \beta} = \frac{\partial \psi_1(\beta)}{\partial \beta} + \frac{\partial \psi_1(-\beta)}{\partial \beta}$$

At $\beta = 0$ we have therefore

$$\frac{\partial \psi(0)}{\partial \beta} = 2 \frac{\partial \psi_1(0)}{\partial \beta} \qquad 8.28.$$

Now
$$\frac{\partial \psi_1}{\partial \beta} = \frac{\partial \psi_1}{\partial \xi_1} \times \frac{\partial \xi_1}{\partial \beta}$$

From 8.21

$$\frac{\partial \psi_1}{\partial \xi_1} = \frac{3}{\xi_0^4} \left[\xi_1^2 A' + 2 \xi_1 A \right]$$

where A' denotes $\frac{\partial A}{\partial \xi_1}$

and from 8.16

$$\frac{\partial \xi_1}{\partial \beta} = \frac{\xi_1^3}{2 \beta_{max} \xi_0^2}$$

Hence
$$\frac{\partial \psi}{\partial \beta} = \frac{3}{\beta_{max}} \frac{\xi_1^3}{\xi_0^3} \left[\frac{\xi_1^2 A'}{\xi_0^3} + \frac{2 \xi_1 A}{\xi_0^3} \right]$$

At $\beta = 0$, $\xi_1 = \xi_0$ and we write A_0 for A, A_0' for A'

Therefore

$$\frac{\partial \psi(0)}{\partial \beta} = \frac{6}{\beta_{max}} \left[\frac{A_0'}{2 \xi_0} + \frac{A_0}{\xi_0^2} \right]$$

or
$$\frac{\partial \psi(0)}{\partial \beta} = 6 \left[\frac{A_0'}{2 \xi_0} + \frac{A_0}{\xi_0^2} \right] \qquad 8.29.$$

where $\beta' = \frac{\beta}{\beta_{max}}$ 8.30.

The computer programme giving A vs. ξ_1 , (or A_0 vs. ξ_0) also gave the relation 8.29 .

The maximum was found to be close to .534 and occurred at $\xi \approx .85$.

Comparable curves are shown on Fig. 8.6. Also evident from this figure is the effect of ξ_0 on ψ near β_{max} previously determined in equation 8.23. It might be considered better to reduce ξ_0 below .85 in order to improve still further the restoring torque at large β .

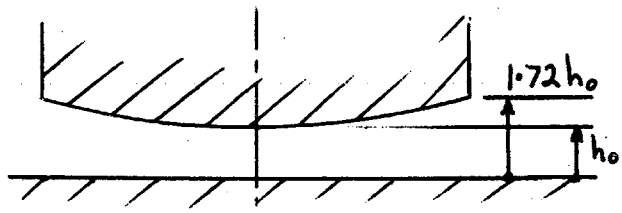

Fig. 8.6a

Optimum profile $\xi_0 = .85$.

STABILITY OF PAD WITH STABILIZERS.

The procedure for proportioning a composite pad of the shape of Fig. 8.5 is as follows. We assume at first that N is independent of β i.e. $N = N_0$. All the various torque components have been expressed in the form $T = P_h L^2 J$. Hence we consider only the J functions and the combined curve may be calculated and drawn for all components except the stabilizer component. This is illustrated in Fig. 8.7. where curves 3, 4 and 5 are the components J_s, J_p and J_D respectively for the "large" pads of the Pole Bearings. J_f is negligible in comparison.

The maximum value of $\left(\frac{\partial \psi}{\partial \beta'}\right)_0$ has been indicated as .534.

Hence using equation 8.22 et seq., the maximum $\frac{\partial J}{\partial \beta'}$, possible may be determined thus:

$$\left(\frac{\partial J}{\partial \beta'}\right)_{max} \approx \frac{S^2 C}{2L^3} \qquad 8.31$$

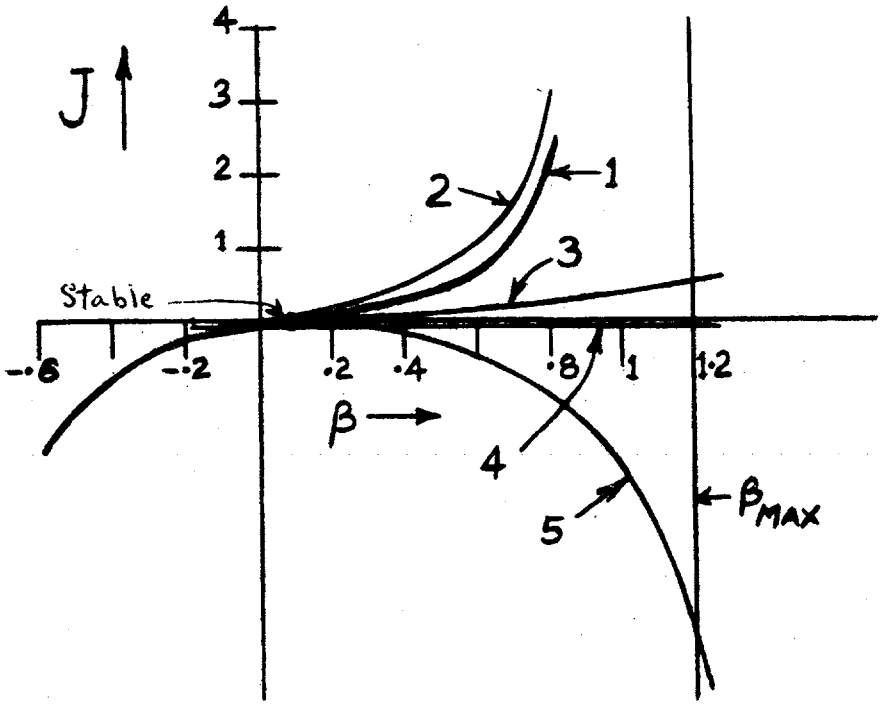

Figure 8.7

1 Combined curve

2 Component from stabilizing surfaces J_c

3 Component J_s $(P=P_{h_o})$.

4 Component J_p $(\eta = 25)$.

5 Component J_D

Curves are for large pad. $N_o = O$

$U' = 4$

$\frac{a}{b} = .5$

One may proceed by selecting a value of β_{max} and sketching in, with the aid of the curves of 8.6, what would be a satisfactory stabilizing J using the oriteria already discussed in Section 7. The slope of this sketched curve at $\beta = 0$ determines the quantity $\frac{S^2C}{L^3}$ according to the approximation 8.31. The selection of β_{max} determines C by equation 8.13a. Hence the required S may be found. This process may be repeated and refined until a satisfactory design is established.

The radius of curvature of the stabilizing surfaces (in plane geometry) is found from 8.15 with $\xi_o = .85$ or other selected value.

In Fig. 8.7. curve 2 is the J curve for the stabilizing surfaces for $\xi_o = 1.4$ and curve 1 is the combined J curve showing a stable operating point at $\beta \approx .05$.

Selection of N_o

Due to the fact that a pair of stabilizing surfaces acting alone stabilize at $\beta = O$, it is best to arrange the sum of all other J components at $\beta = O$ to be zero. Hence the selection $N_o = O$ is indicated. However, if J_p is significant, N_o might be made slightly negative to cancel J_p at $\beta = O$. In what follows the optimum value of N_o will be taken as zero.

SOME SPECIAL CONSIDERATIONS OF THE STABILITY THEORY FOR CYLINDRICAL CONFIGURATIONS.

The theory so far has been especially developed for plane moving surfaces. Provided the angle subtended by each pad is not large and the pad radial dimensions are not large, there will be little error in applying the theory directly to the cylindrical case.

The truth of this statement will be illustrated by reference to the H. P. G. pole bearings where the angle subtended by each pad is slightly less than 60^{o} .

We will consider only the case where $N_o = O$ and ignore variation in h in the first instance.

Three more or less obvious effects will be considered -

(a) The effect on moment arm in the torque calculations.

(b) Variation of N with β

(c) Effect on the calculation of β_{max}

(a) <u>Moment Arm.</u>

All previous dimensions used

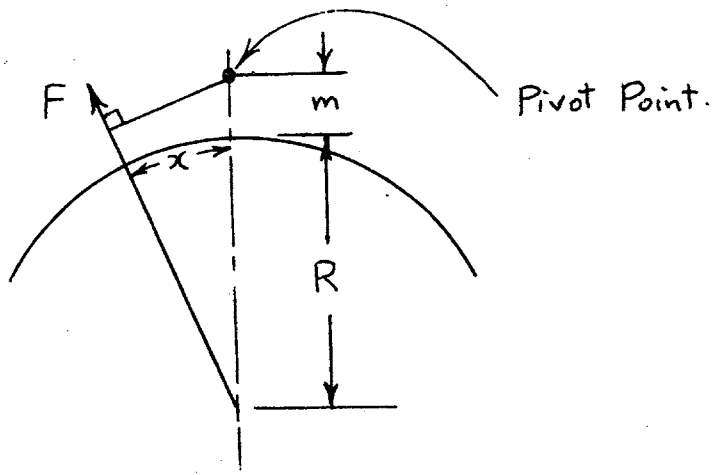

Fig. 8.7a

in the plane geometry theory will be considered as measurements along the surface of the cylindrical moving member.

It will be clear from the Figure 8.7a that the torque may be represented as

$$T = F(m + R)\sin\frac{\alpha}{R}$$

Here m is the measurement to the pad pivot point, α a typical dimension (e.g. C, D), R the shaft radius, and F a typical force.

All the forces considered except those on the stabilizing surfaces have $\alpha = \frac{D}{2}$. The stabilizing surfaces have $\alpha = \frac{C}{2}$. We are therefore concerned with the relative effect of these two groups of components.

The ratio of the torques of the two groups may be written:-

$$\left(\frac{T_1}{T_2}\right)_{Cyl} = \frac{F_1 \sin\frac{C}{2R}}{F_2 \sin\frac{D}{2R}}$$

This must be compared with the ratio in plane geometry, viz.

$$\left(\frac{T_1}{T_2}\right)_{plane} = \frac{F_1 C}{F_2 D}$$

In applying plane geometry theory to the cylindrical case, a correction factor must therefore be applied to J_c of

$$\frac{D}{C} \times \frac{\sin\frac{C}{2R}}{\sin\frac{D}{2R}}$$

(b) Variation of N with β .

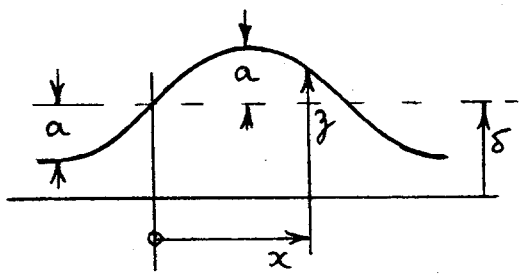

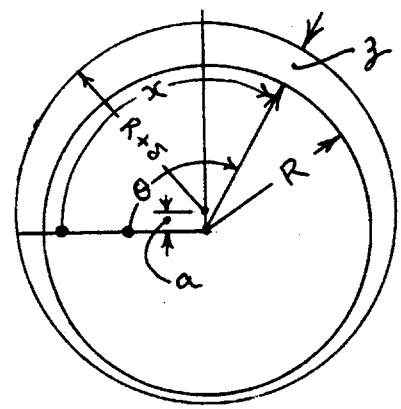

Fig. 8.8.

$$\Theta = \frac{x}{R}$$

The clearance between two cylindrical surfaces with parallel axes may be written

$$z = \delta + a \sin\frac{x}{R}$$

for $\frac{z}{R} \ll 1$ 8.32.

Here δ is a constant for a given pair of surfaces and a is a variable depending on the relative position of the surfaces.

Any pad face machined as a cylindrical surface may be represented by a section, of appropriate length, of any one of a series of curves having the same δ .

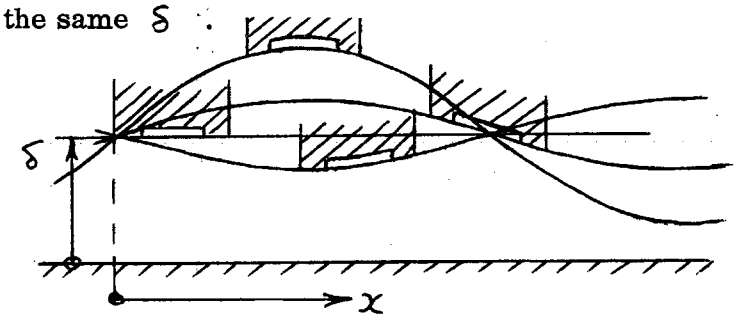

Fig. 8.9.

This is illustrated in Fig. 8.9 where each of the diagrams represent an allowable curve of z vs x for a particular pad/shaft combination machined with a certain δ . Each of the diagrams exemplifies a particular combination of β and h and it will be seen that to obtain $N_o = O$ (i.e. no concavity when there is no tilt) we must have

$$\delta = h_o$$

The particular conditions for $N_o = O$ and $h = h_o$ are shown in Fig. 8.10.

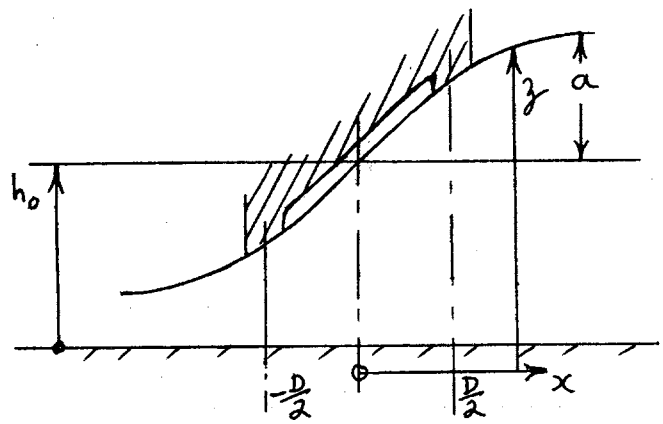

Fig. 8.10.

Using previous definitions and equation 8.32 with $\zeta = h_o$

$$\text{i.e. } \zeta = h_o + a \sin \frac{x}{R} \qquad 8.33.$$

$$\text{we find } \beta = \frac{2a \sin \frac{D}{2R}}{h_o} \qquad 8.33a$$

Also at $\frac{D}{2}$, $\frac{d\zeta}{dx} = \frac{a}{R} \cos \frac{D}{2R}$

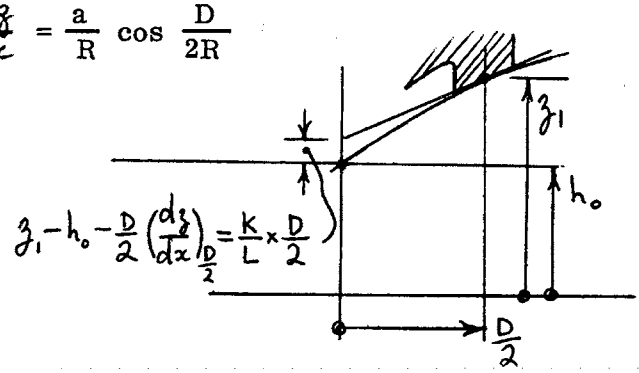

Fig. 8.11.

Recalling the original definition of $N \left(= \frac{KD}{hL}\right)$ we see that

$$\zeta_1 - h_o - \frac{D}{2}\left(\frac{d\zeta}{dx}\right)_{x_1} = \frac{K}{L} \times \frac{D}{2}$$

or $$a \sin\left(\frac{D}{2R}\right) - \frac{Da}{2R} \cos\left(\frac{D}{2R}\right) = \frac{K}{L} \times \frac{D}{2}$$

or $$N = \frac{2a}{h_o}\left(\sin\left(\frac{D}{2R}\right) - \frac{D}{2R} \cos\left(\frac{D}{2R}\right)\right)$$

However, on substituting the equation for β we have

$$N = \beta\left(1 - \frac{D}{2R} \cot \frac{D}{2R}\right) \qquad 8.34.$$

N is therefore proportional to β. The proportionality factor $(1 - \frac{D}{2R}\cot\frac{D}{2R})$ in the case of the Pole Bearings is .04 so that the effect is considered negligible.

(c) Calculation of β_{max}

In the development of the theory for plane geometry, β_{max} was taken as (8.13a) $\beta_{max} = \frac{2D}{C}$. This relation is important in that it relates the clearances at the pad lands and the stabilizing surfaces, e.g. refer to eqn. 8.14.

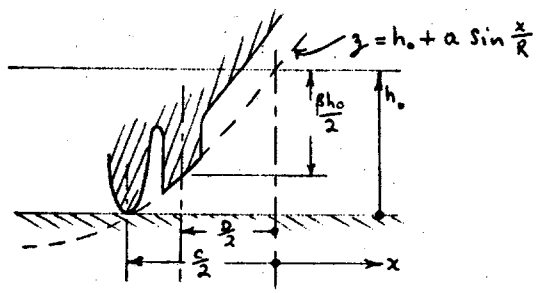

Fig. 8.12.

Referring to Fig. 8.12, it will be seen that the maximum value of β is characterized by

$$a \sin \frac{C}{2R} = h_0$$

and $$a \sin \frac{D}{2R} = \beta_{max} \frac{h_0}{2}$$

Hence $$\beta_{max} = \frac{2a \sin \frac{D}{2R}}{h_0} = \frac{2 \sin \frac{D}{2R}}{\sin \frac{C}{2R}}$$

This must be compared with Eqn. 8.13a

$$\beta_{max} = \frac{2D}{C} \qquad 8.13a$$

The correction factor to be applied is therefore

$$\frac{C}{D} \times \frac{\sin \frac{D}{2R}}{\sin \frac{C}{2R}}$$

which is the inverse of that found in section (b) above.

The evaluation of

$$\frac{C}{D} \times \frac{\sin \frac{D}{2R}}{\sin \frac{C}{2R}}$$

for the Pole "large" bearings is 1.025 which is considered negligibly different from unity.

There seems little difficulty therefore in applying the derived theory to the cylindrical case.

Even if one includes the variation effect of h with β , the effect on N is not large. The extreme case of $h' \simeq .3$ and $\beta_{max} \simeq 1.5$ (corresponding to U' = 3 ; refer to Appendix VI. Fig. 4) is illustrated below for $N_o = O$. The extreme value of N (for the land closest to the shaft) is approximately - .2.

It will be seen by reference to the curves of Fig. 7.10 that such a small variation from $N_o = O$ is insignificant.

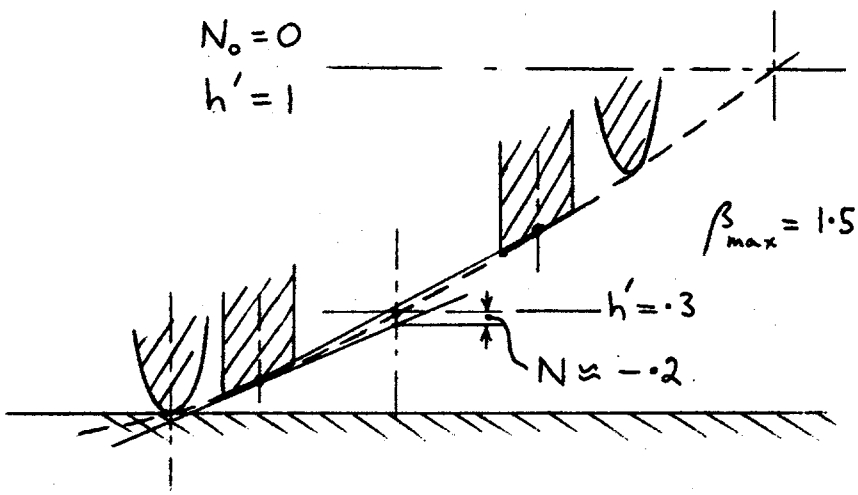

Fig. 8.13

TORQUES ABOUT THE RADIAL AXIS.

These torques form component (b) defined at the beginning of Section 7.

It is convenient to use standard cylindrical co-ordinates, the origin being the

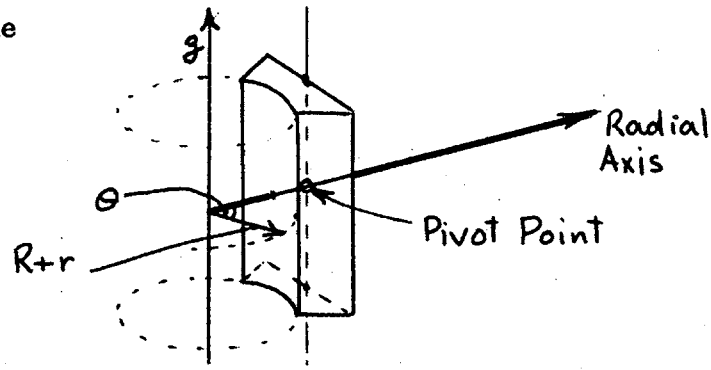

Fig. 8.14

intersection of the z axis and radial axis. Zero rotation about the radial axis is defined to exist when the axes of the cylindrical surface of pad and shaft are parallel, (and $\beta = 0$ everywhere).

It is shown below that a rotation about the radial axis causes changes in clearance which for any particular value of z are the same as if that part of the pad has a particular inclination (β).

Further it is shown that this β is proportional to z .
In our transformation to plane or quasi plane surfaces, the above rotation therefore causes a warping of the transformed pad surfaces. The extent of this warping is conveniently gauged by the maximum magnitude of inclination β_w occurring at the extremities of the pad.

Equation 8.33a gives the relation for β viz.

$$\beta = \frac{2a \sin \frac{D}{2R}}{h_o}$$

For a rotation γ about the radial axis

$$a = \gamma z$$

Hence

$$\beta = \frac{2\gamma z}{h_o} \sin\frac{D}{2R}$$

If the length of the pad in the z direction is $2W$ then

$$\beta_w = \frac{2\gamma W}{h_o} \sin\frac{D}{2R}$$

and therefore

$$z = \frac{\beta W}{\beta_w} \qquad 8.35.$$

Any <u>normal</u> force $F dz$ at θ will produce an elemental radial axis torque of

$$d\left|T_R\right| = F \sin\theta \cdot z \cdot dz \qquad 8.36$$

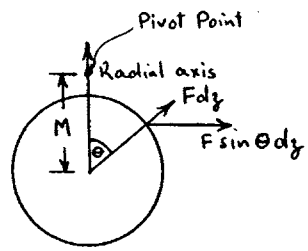

Fig. 8.15

Here $\left|T_R\right|$ represents torque in contrast to T_R which throughout has denoted torque per unit length (z direction). (Similarly F denotes force per unit length).

This must be compared with the elemental parallel axis torque

$$T_p = FM \sin\theta$$

where M is the distance from shaft centre to pivot point.

This may be substituted in 8.36 together with 8.35 for γ to give

$$d|T_R| = \frac{T_p}{M}\gamma\, d\gamma = \frac{W^2}{\beta_w^2}\frac{T_p}{M}\beta\, d\beta$$

Hence on integrating

$$|T_R| = \frac{W^2}{M\beta_w^2}\int_{-\beta_w}^{\beta_w} T_p \beta\, d\beta \qquad 8.37$$

T_p, it must be remembered is the torque per unit length (γ direction). We may relate the total torque $|T_R|$ to the total torque $|T_p|$ by substituting $|T_p| = T_p \times 2W$

Then

$$|T_R| = \frac{W}{2M\beta_w^2}\int_{-\beta_w}^{+\beta_w} |T_p|\,\beta\, d\beta \qquad 8.38$$

The value of this equation is that once the stability has been investigated about the parallel axis, this information may be used directly to examine the stability about the radial axis. One may perform the integration graphically and convert a graph of $|T_p|$ vs. β into a graph of $|T_R|$ vs. β_w.

If $|T_p|$ is regarded as a series of terms the n^{th} one being $|T_p|_n = a_n\beta^n$, then the corresponding term of $|T_R|$ will be

$$|T_R|_{n,\beta_w} = \frac{W}{M(n+2)}|T_p|_{n,\beta_w} \qquad 8.39$$

provided n is odd. If n is even $|T_R|_n = 0$. Consequently $|T_R|$ will have the same broad shape as $|T_p|$ but will lack local peaking near β_{max} (corresponding to terms with high n). In addition the coefficient $\frac{W}{M}$ will usually be a fraction of the order of $\frac{1}{2}$.

The $|T_R|$ characteristic therefore, although inherently as stable as the $|T_p|$ characteristic, provides less satisfactory restoring torques.

Torques about the Tangential Axis (component (c) defined at the beginning of Section 7). The total restoring torque about the tangential axis may be designated $|T_T|$ and is related to $|T_p|$ in a similar fashion to $|T_R|$. However, in this case the individual terms of $|T_p|$, e.g. $|T_p|_m$ must be dealt with separately according to the angle Q_m (Fig. 8.14) at which they act, and $|T_T|$ becomes equal to the sum of terms:

$$|T_T| = \frac{W}{M \beta_w^2} \sum \operatorname{cosec} \theta_m \int_{-\beta_w}^{\beta_w} |T_p| \beta \, d\beta \qquad 8.40.$$

β_w is defined consistently as

$$\beta_w = \frac{2(h - h_{min})}{h} \frac{D}{C} \qquad 8.41$$

so that in every mode of displacement a particular value of β_w corresponds to a particular ratio of minimum to maximum clearance. $|T_T|$ is generally similar to $|T_R|$ but 2 to 3 times greater.

SECTION 9

CONSTRUCTION OF BEARINGS

The following description refers to the upper rotor and pair of pole bearings.

Shaft. The shaft was machined from solid mild steel. The two bearing surfaces were belt ground and polished to within .0002 inches of a perfect cylinder. The uppermost surface is 13 inches nominal diameter and the lower bearing surface 18 inches nominal diameter.

Pads. The two sets of six pads are designated "small" and "large". The small pads are uppermost and bear on the 13 inch diameter shaft surface. The large pads bear on the 18 inch diameter surface.

Small Pads. These were machined from stainless steel castings and are faced with a high temperature asbestos based bakelite known as "ferrobestos".

The facing material was prepared from sheets machined to 1/16" thickness. It was then thin enough to be bent into the correct curve without breaking. Bonding to the stainless steel was by an epoxy resin, finally hot cured, the work being performed with the aid of jigs. This method of bonding was found to be stronger than the bakelite itself.

Prior to bonding, all other machining was carried out on the castings to ensure that after the bonding subsequent treatment would not affect the accuracy of the bearing surface.

The final machining of the ferrobestos was carried out on a jig borer, maching two pads at a time so that the diameter could be accurately measured.

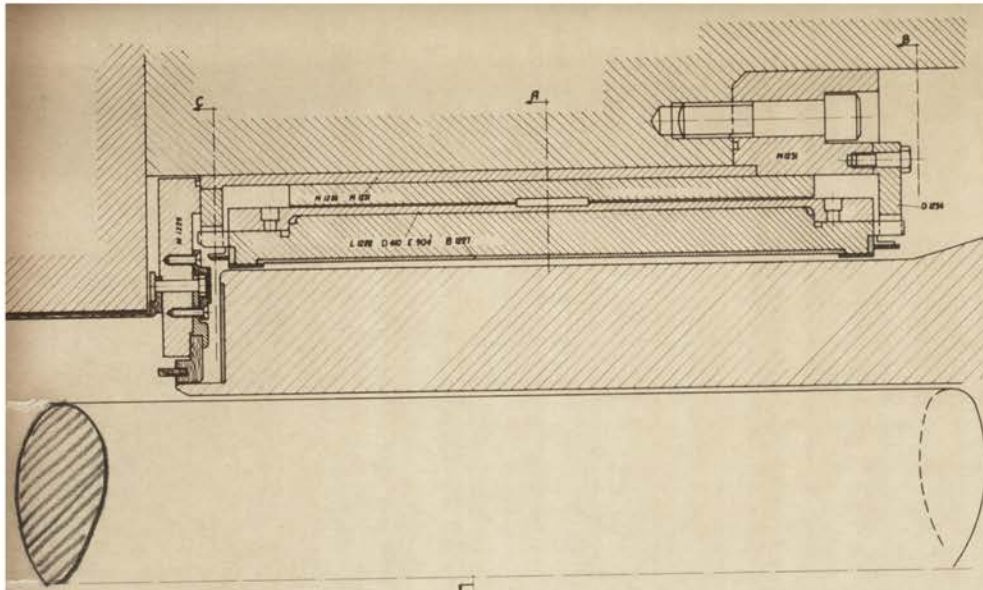

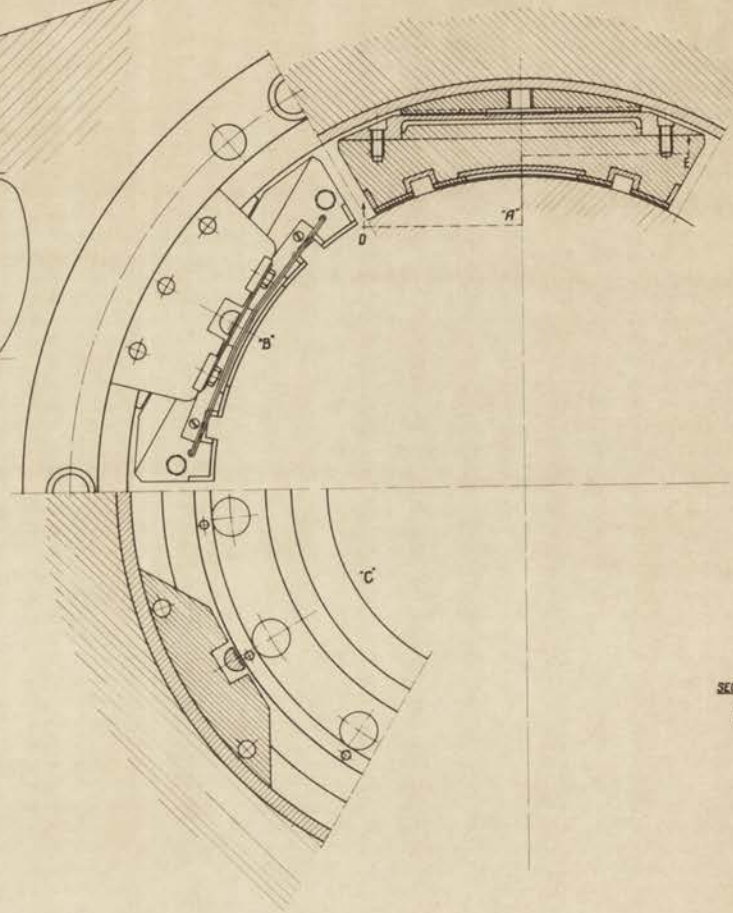

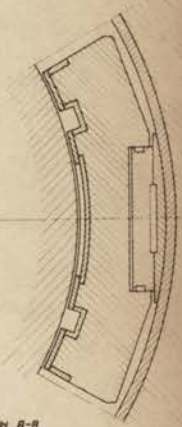

SECTION A-A
SHOWING MARK III
CYLINDER TYPE PRO.

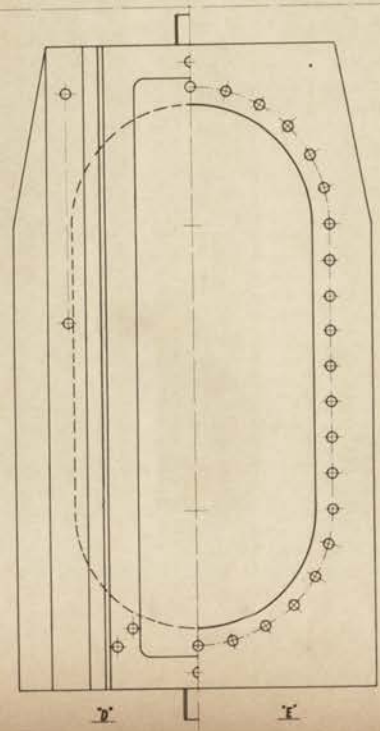

RESEARCH SCHOOL OF PHYSICAL SCIENCES
AUSTRALIAN NATIONAL UNIVERSITY

SMALL GUIDE BEARING SECTIONS

DRAWING NO. L 1226

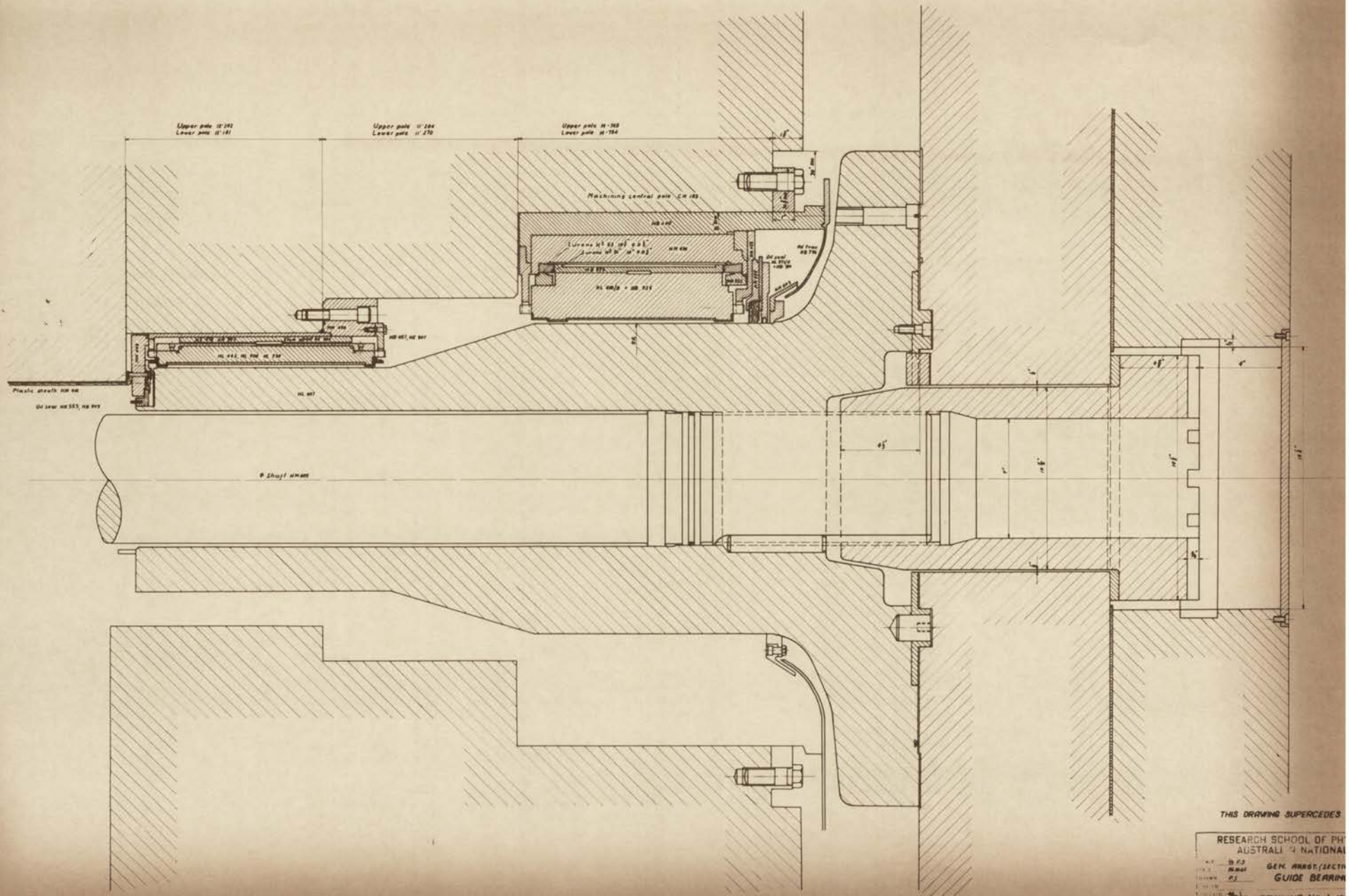

THIS DRAWING SUPERCEDES

RESEARCH SCHOOL OF PH
AUSTRALI N NATIONAL

GEN. ARRGT. (SECTI
GUIDE BEARIN

DRAWING No. L 12

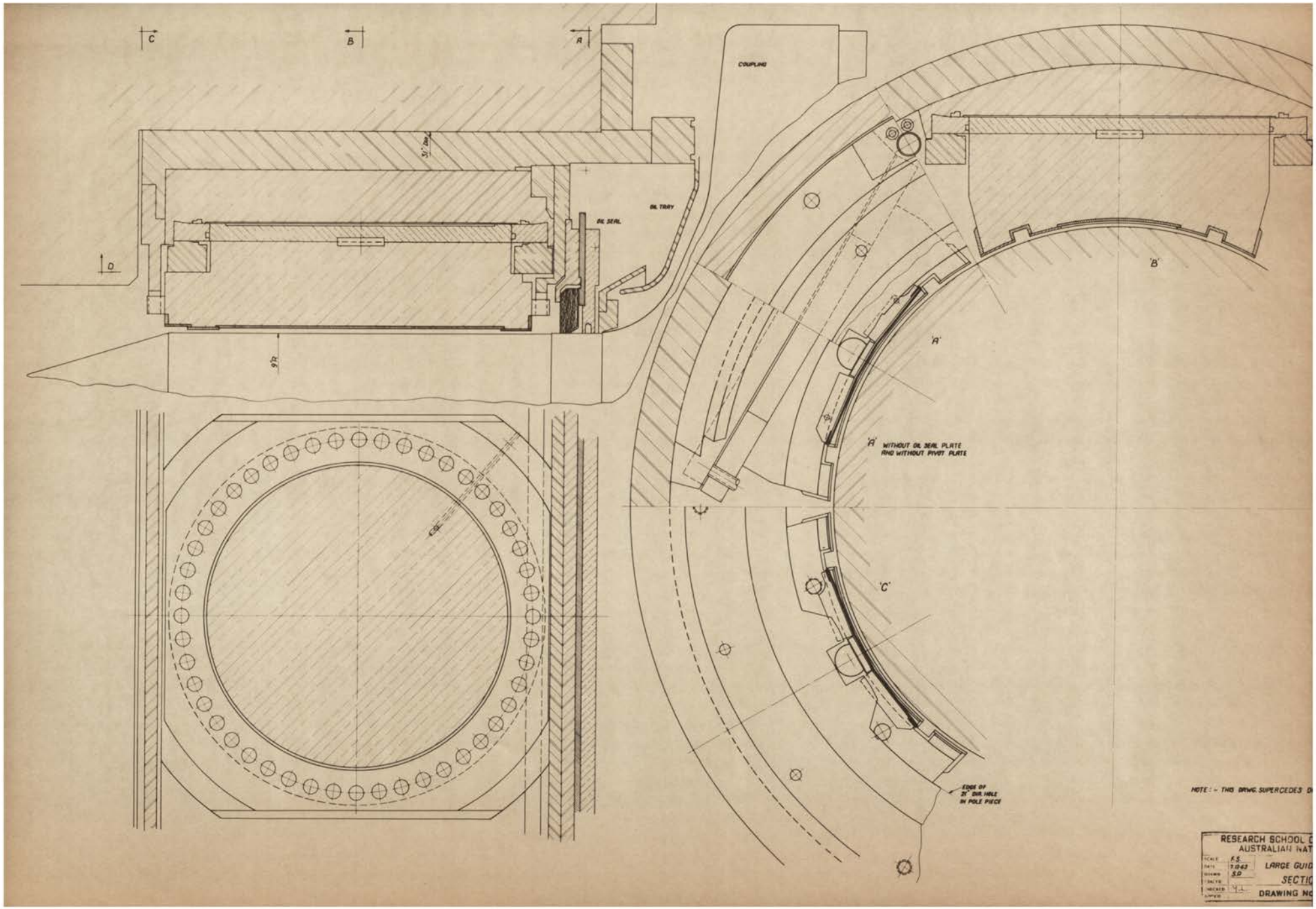
C
B
A
COUPLING
OIL TRAY
OIL SEAL
D
'B'
'A'
'A' WITHOUT OIL SEAL PLATE AND WITHOUT PIVOT PLATE
'C'
EDGE OF 2" DIA. HOLE IN POLE PIECE
NOTE :- THIS DRWG. SUPERCEDES
RESEARCH SCHOOL
AUSTRALIAN NAT
LARGE GUID
SECTIO
DRAWING NO

Due to the limited space available for the small pads, their radial dimensions could not be made adequate enough to prevent a small distortion under load. This distortion was due to the mis-match between the two loading patterns on either side of the pad, although this mis-match was reduced as far as practically possible. The distortion was calculated to be about 3 mils and would lead to solid to solid contact between bearing face and shaft if ignored.

The difficulty was overcome by machining the pad faces in two stages. The first stage was machining in the jig borer to within 4 mils of the final dimension. This was carried out in a special holding device which by adjusting appropriate screws, could flex the pad.

After the first stage the pad was flexed and the degree of flexing checked by an indicator on the tool arm measuring against the freshly machined surface.

The second stage machining was then carried out thus machining into the pad a distortion which would counteract the loading distortion.

Provision for oil feeds was made during general machining. These consisted of holes from either side of the lower end of the small pads. One set of drillings led to the pad face and another set to the opposite side to feed the ram operating there.

The rams, or more particularly the ram "cylinders" consisted of steel plates having shallow depressions (approximately $\frac{1}{4}$" deep) into which fitted the backs of the pads. There were make-up segments behind these to fill the space between the cylindrical bearing housing and the plane surface of the ram "cylinder".

The total allowable radial movement of each pad was 1/16 inch, most of which was taken up in retraction to facilitate entry of the shaft. Because of this small movement and the restricted dimensions, a special O-ring seal was designed and tested.

To facilitate assembly, each unit consisting of a pad and ram was retained against the bearing housing by means of two springs. The units rested between two flanges and were located circumferentially by the retaining springs. Once loaded, the units were firmly located circumferentially by virtue of the friction between ram backs and housing. They were however free to align themselves during the loading process, this aligning involving swivelling and sliding of the ram on the segments described above.

The attached drawings show the layout of these pads, the ram "cylinders", segments etc.

Large Pads. In principle these were similar to the small pads. However, there were differences due to the fact that much more space was available to enable more rigid units to be designed.

The material chosen for the pads was therefore bronze and as before, these were faced with ferrobestos. The machining was straightforward, being carried out on the jig borer with no provision for distortion being necessary.

Whereas the small rams and cylinders were not circular in shape necessitating the plane interface between cylinder and segment to enable rotation about a radial axis, the large rams could be made circular because of space considerations. The "cylinder" in this case was cylindrical.

Oil feed was to the pad for lubricating oil, and to the cylinder for

the loading oil.

The oil seal was a conventional O-ring but the cylinder adjacent to the O-ring groove was relieved to allow a limited rotation about the parallel and tangential axis as well as the radial axis.

Retaining springs were incorporated as before to hold the units back in the housings during assembly.

Oil Supply Lines. All lubricating oil was carried in steel pipes 3/8" O. D. which entered the housings from above, and passed between the small pad units to the region between the two bearings. Here the pipes ran around the housing a half or third revolution to provide a certain amount of flexibility. Loading oil pipes entered from below after travelling across the upper pole face. In the case of the small pads, sufficient flexibility had to be incorporated in these pipes also.

The oil connection to each pad was essentially a rotating one which added to the overall flexibility.

Instrumentation. Besides pressure gauges and sensing devices associated with the servo mechanism, bearing pad faces were monitored for temperature by fixing in them a number of small commercially available thermistors attached to small copper discs (1/8" approx. diameter).

Attached drawings show the layout of the large pad units, piping and thermistors.

THE SERVO CONTROL SYSTEM

We confine our attention here to the upper rotor and supporting guide bearings. It was desired to control both the direction and position of the rotor axis. There were, therefore, four degrees of freedom to be controlled by the four independent variables related to the orthogonal radial

co-ordinates of each bearing.

Rotor position sensing. In the selection of suitable probes, consideration had to be given to reliability, accuracy, and simplicity. The most serious environmental difficulty was by far the liquid metal NaK. This material was used in small accelerating jets during the relatively long period of acceleration as well as in large quantities during each current pulse. In both cases the spent NaK was allowed to spray from the jet areas in a partially confined manner making it difficult to locate the probes in suitable NaK free positions. It was finally decided to try using capacitive probes heavily covered with a layer of insulation to reduce the effect if a small puddle of Nak were to accumulate between rotor and probe especially whilst the former was stationary. It was hoped that a small rotational speed would be sufficient to clear such an accumulation; and that the amount of splashing during the acceleration period would not be troublesome. In fact positions were found fairly free from splashes during acceleration. It was decided to disconnect the servo system by valving off the hydraulic lines to the pad rams during a pulse as the effect of the NaK would almost certainly put the probes out of action temporarily.

This meant that after each pulse, the rotor would have to be left turning at 100 r.p.m. or more, otherwise the magnetic torques would be too severe. In practice this need not be an imposition since energy is proportional to the square of speed which meant, for instance, that pulsing from 400 r.p.m. to 100 r.p.m. would leave only 6% of the original energy. Further development of rotor sensing probes or methods of confining the Nak after leaving the jets, was anticipated.

In practice the probes behaved well and as expected. It was found that the servo system could be reconnected 10 or 20 seconds after a pulse.

Eight capacitive probes were used altogether. Four were placed at 90^{o} intervals around the rotor facing the upper surface near the circumference. Adjacent to these four were a similar number facing the cylindrical surface of the rotor. Opposite probes of each set were electrically connected to form four independent sources of information viz. two rectangular components of rotor tilt or rotor axis direction; and two similar components or radial position.

Each pair of probes formed part of the two arms of a conventional transformer bridge circuit which was powered by a 2,500 c.p.s. supply. The bridge unbalance was amplified electronically and phase sensitively rectified to provide currents to power four pairs of small electromagnets.

The hydraulic part of the servo loop was designed to minimize phase lag and so make improbable the occurrence of instability. At the same time it was necessary to devise a scheme whereby six pads could be controlled by two co-ordinate information.

The device used consisted of a cylinder about 1 in. diameter having a set of six radial holes drilled in the same plane. Each of these holes was fed via a throttle from a high pressure line so that the flow was practically constant no matter what constriction might be placed at the holes. This ring of holes was surrounded by a freely suspended metal ring which constricted the oilflow from each hole to a certain extent. The amount of constriction at any particular hole could be varied by applying a force to the ring, but the amounts of constriction and therefore the pressures at successive holes were related by a smoothly varying function. The pressure at each hole was tapped and fed to the appropriate pad ram via a length of capilliary tubing. Thus the co-ordinated motion of six pads could be controlled by applying a force on the constricting ring in the appropriate direction. This force was applied in two co-ordinates

by the above mentioned electromagnets.

Some consideration was given to the problem of what information should be fed to each bearing and to the problem of stability in a system having four controlled variables. The probe system and bearing motivation system enabled independent action in either co-ordinate so that the problem reduced to a two dimensional one. However any further reduction to two independent feedback loops seemed difficult; for example to arrange matters so that axial direction information caused only a change in axial direction, and position information a change in position, would involve a complicated cross-connection and division of information. A practically simple arrangement would be one where each set of information was connected to a separate bearing. It was shown that certain such connections are stable and others unstable. The connection shown diagrammatically in Fig. 9.1 was the one adopted. Fig. 9.2 illustrates a sequence of positions during return to zero position following a typical displacement.

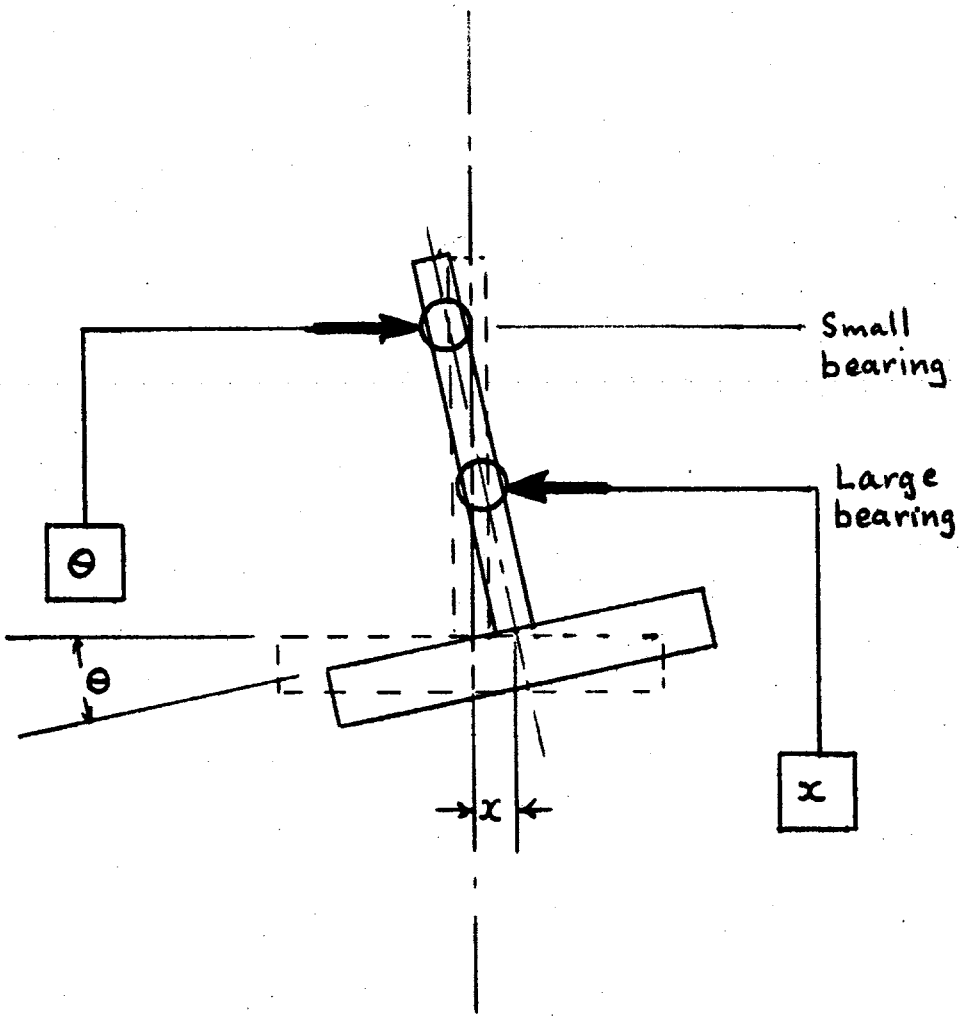
Small bearing
Large bearing
θ
θ
x
x
Dotted outline shows "zero position".

Figure 9.1

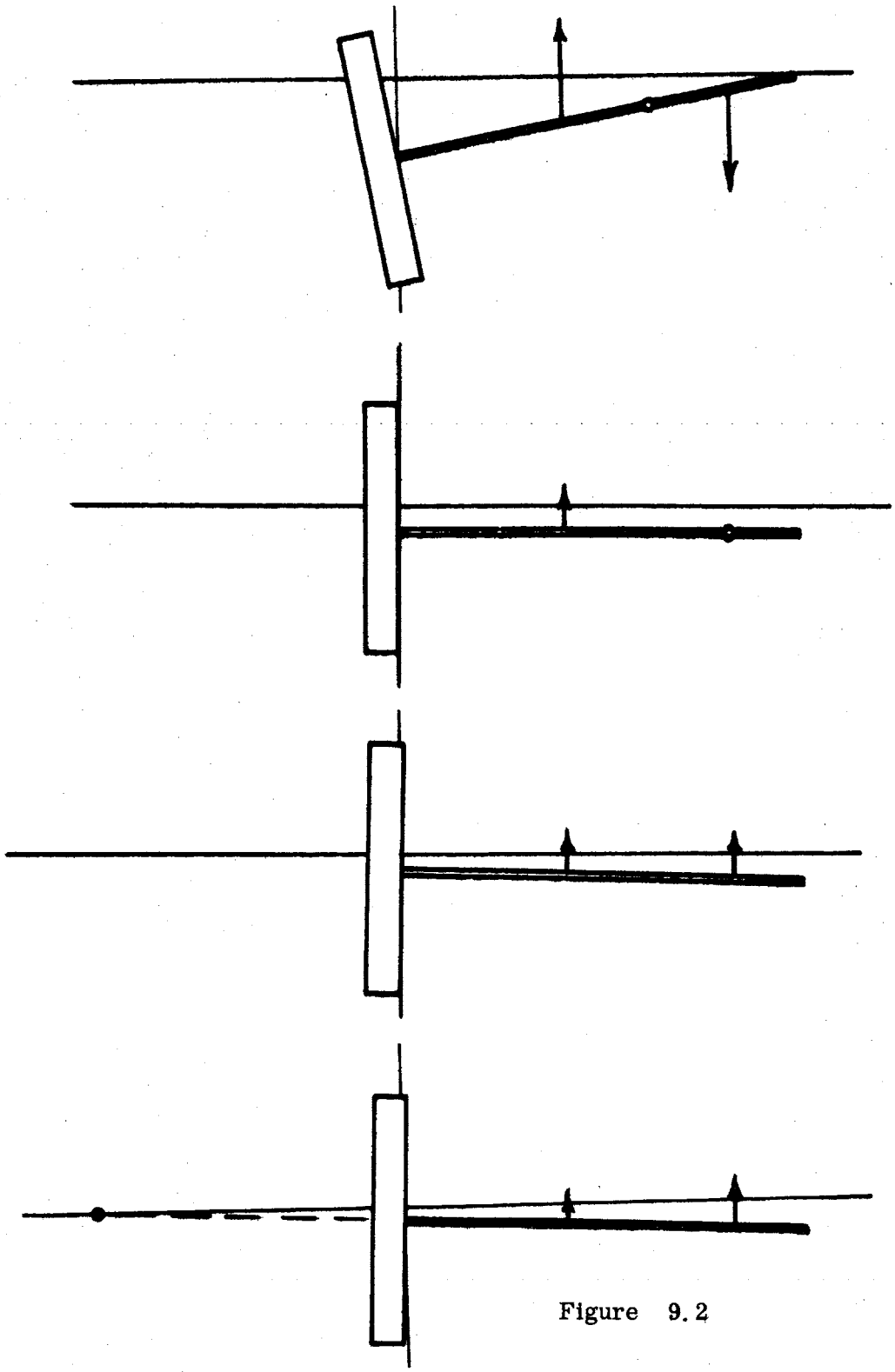

Figure 9.2

SECTION 10

OBSERVATIONS AND DISCUSSION

In 1962 the first set of bearings designed according to the principles in this paper were tried out. They were in the magnet yoke of the homopolar generator but without a rotor and with no field. This trial was in essence to examine their behaviour at high speed. The full design speed of 900 r.p.m. was reached and maintained for at least one hour. The behaviour of the bearings was quite satisfactory.

Since there was no rotor for these tests the servo system was inoperative and pad ram pressures had to be monitored and adjusted when necessary.

Later in the year the bearings received their first trials in a complete assembly. This assembly included one rotating rotor (the other being clamped stationary) and one set of NaK jets to carry current to and from the rotor. The trials went on for several months during which successively larger current pulses were taken, culminating in the largest pulse of 1.8 million amperes lasting approximately one second (Fig. 10.1).

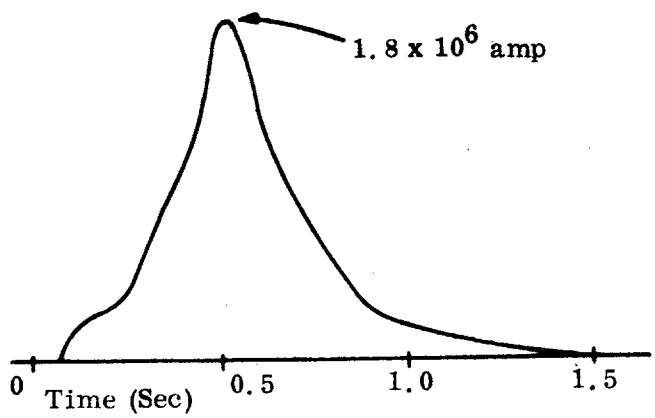

Fig. 10.1.

During this time the bearings were always under servo control except during a pulse as described in Section 9.

In this series of tests, speeds were limited to 550 r.p.m. because of the tendency of an oil seal to fling oil at higher speeds.

Four types of observations were taken.

1. Calorimetric observations on the oil to pole bearings and thrust bearing.

2. Pad face temperatures by means of thermistors in the pad faces.

3. Sundry measurements of oil pressure and the oil volume in the rams. This latter measurement was achieved by installing a number of small free pistons, one in each oil line to each ram and observing their movements by means of thin rods passing through oil seals and operating potentiometers.

4. Direct observation on dismantling.

The full speed calorimetric losses amounted to 50 k.w. measured with an accuracy of about $\pm$ 10%. Unfortunately, the oil from large and small bearings became mixed after discharge from the pad faces, so that it was not possible to measure the ratio of losses between the two sets.

This measured loss must now be compared with the value expected from calculation.

If one assumes uniform clearance over the whole pad face, then this uniform clearance h can be written

$$h = \sqrt[3]{\frac{12\mu QL}{pB}} \qquad 10.1$$

where B is the effective plenum circumference. Respective values for small and large bearings are 3.4 and 3.7 mils respectively assuming the oil supplier's value of μ at the operating temperature.

Again assuming uniform clearance, the friction power per pad can be written

$$P = \frac{\mu A U^2}{h} \qquad 10.2$$

where A is the effective area of the lands (including the stabilizing lands).

Using 10.2 and the above figures for h derived from 10.1, it is found that the small and large bearing losses should be 11.5 and 27.5 k.w. respectively.

The measured losses are therefore 11 k.w. higher than expected.

A small part of this discrepancy can be accounted for by losses due to friction in two oil seals and general turbulence of the discharged oil adjacent to the shaft. The discrepancy may be described another way. The "effective uniform clearance" may be defined from observations of pressure and oil flow using 10.1. We shall designate this effective value by h_p.

On the other hand a second value of "effective uniform clearance" may be calculated using 10.2 and observed values of friction powers. We shall designate this value by h_f

In our case the ratio of the two effective values is $\frac{h_p}{h_f} = 1.25$.

One probable explanation for this ratio not being unity is that clearances were not uniform. The effect of non uniformity will now be demonstrated.

Fig. 10.2 illustrates a pad simplified by having rather narrow lands.

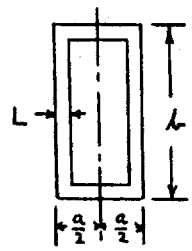

Fig. 10.2

If this pad were tilted by a certain β amount, the average clearance being h, then the clearance y around the perimeter x would be as in Fig. 10.3.

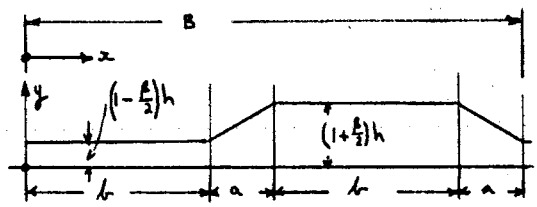

Fig. 10.3

Since the plenum is at uniform pressure, the oil flow will be found to be

$$Q \propto \oint y^3 dx$$

But by definition (10.1) $\quad Q \propto (h_p)^3 B$

$$\text{i.e.} \qquad h_p = \sqrt[3]{\frac{\oint y^3 dx}{B}}$$

$$\text{or} \qquad h_p \approx h \sqrt[3]{1 + \frac{3\beta^2}{4}} \qquad 10.3$$

On the other hand the friction loss over the lands will be

$$P \propto \oint \frac{L dx}{y}$$

but by definition (10.2) $\quad P \propto \frac{A}{h_f} \propto \frac{LB}{h_f}$

Hence $$h_f \propto \frac{B}{\oint \frac{dx}{y}}$$

or $$h_f \simeq h\left(1 - \frac{\beta^2}{4}\right) \qquad 10.4$$

Therefore the ratio $\frac{h_p}{h_f}$ is as follows:

$$\frac{h_p}{h_f} \quad \frac{\sqrt[3]{1 + \frac{3\beta^2}{4}}}{1 - \frac{\beta^2}{4}} \qquad 10.5$$

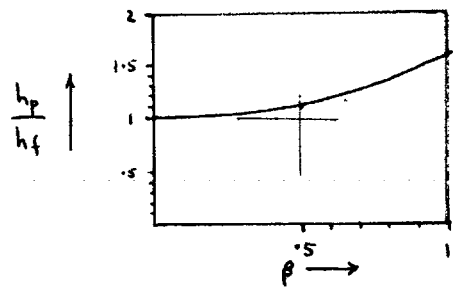

Fig. 10.4

A value of 1.25 corresponds roughly to $\beta = .65$.

If we include stabilizing lands, h_f is less than indicated by 10.4 and therefore the condition $\frac{h_p}{h_f} = 1.25$ will occur at a smaller value of β than .65.

Possible causes of non uniform clearance

1. O-ring friction

One of the most probable causes of non-uniformity is O-ring friction. Ideally the hydraulic support of each pad is identical to a ball pivot. However, the pivoting of a pad entails motion at the ram oil seal which is opposed by friction. It has been noticed that the friction of an O-ring seal in a simple ram-cylinder assembly is usually of the order of 5% of the ram force.

If we assume the same force acts when a pad pivots, friction torques of the order of 100 in lbs. per inch. of pad length can easily be

developed in a direction which is indeterminant. Reference to Figure 7.9. and the appropriate constants indicate that such torques can be developed at

$$\cdot 4 > \beta > -\cdot 2 \ .$$

It is reasonable to expect then that all the pads will not maintain an inclination close to zero but rather have a random distribution within this range. Indeed direct observation of the oil volumes in the rams by the method described earlier, while the shaft was rotated slowly and slightly eccentrically, indicated that the pads followed in steps. The resulting variations in film thickness were $\pm$ .5 to $\pm$ 1.5 mil. in most cases so that it would seem probable that variations of this order might always be present.

Other probable causes of non-uniformity are as follows:

ii. Machining errors in shaft and pads.

Although extreme care was taken, errors in non linearity of the order of $\pm \frac{1}{4}$ mil. are probable.

iii. Temperature gradients.

If heat flows from the pad face radially, the pad will become more convex. This will change its N value such as to make the pad stable at a slightly larger value of $|\beta|$ and also make it non parallel to the shaft in the axial direction. In the case of the small bearing which is axially long and only one inch thick, a temperature difference of 5°C is sufficient to cause a variation of clearance of $\pm$ 1 mil. However the presence of the insulation on the pad face will inhibit such gradients although the expansion of the insulation itself under 15°C temperature rise of the oil may cause considerable bowing. The lower bearing should however be comparatively free from this effect.

iv. Forces

Great care has been taken in the case of the flimsy small bearing to ensure no ill effects from the action of plenum and ram forces. These forces do not exactly cover the same areas so some bowing is inevitable. However this has been countered by machining into the pads a slight negative bow.

Observations of pad thermistors - further evidence for variation of clearance.

One or two of the thermistors embedded in the pad faces have shown temperatures in excess of 100°C indicating clearances as low as 1 mil. even supposing viscosity remained constant. There is no consistent evidence of an average value of β other than zero.

Effect of error in assumed value for viscosity.

Another explanation of the ratio $\frac{h_p}{h_f}$ being other than unity is that μ was not, in practice, the value assumed. From 10.1 and 10.2 we have

$$h_p \propto \sqrt[3]{\mu}$$

and $$h_f \propto \mu$$

i.e. $$\frac{h_p}{h_f} \propto \mu^{\frac{2}{3}}$$

To make $\frac{h_p}{h_f}$ unity, the assumed value of μ must be multiplied by .72. This suggests temperatures may have been higher than assumed. They certainly were in some places as indicated by the thermistors. On the other hand, no check measurement of viscosity was ever made.

Direct observation on disassembly.

After several months' running the homopolar generator was disassembled and the pads inspected. There was no indication of any wear that might result from solid to solid contact. It is evidence such as this that gives one confidence that the design is basically sound.

ACKNOWLEDGEMENTS

The author is indebted to the following staff members of the A.N.U.: to Mr. Y Ladyzhynsky for most of the draughting and some of the detailed design; to Mr. James and Mr. Edwards and their respective staffs for construction and installation; to Dr. Hibbard and Mr. Foster for installation of thermistors and some minor modifications to improve electrical insulation; and indeed to all members of staff, academic and otherwise, who helped, to varying degree, physically and with valuable advice.

REFERENCES

(1) Lubrication of Bearings; Butterworths London.
F. T. Barwell, 1956

(2) H. E. Swift; Stability of Lubricating Films in Journal Bearings.

Proc. Inst. Civil Engineers, Vol. 233, 1931-32, pp. 267-322

(3) E. O. Waters; Transactions American Society Mech. Engineers, 64, (1942), 711.

(4) Fluid Dynamics, G. H. A. Cole.

APPENDIX 1

Derivation of the expression $\frac{T}{\theta} = \frac{B^2 r^4}{16 g}$ for the rate of torque generation between two steel surfaces forming a gap in a magnetic circuit.

The steel is considered infinitely permeable and therefore the surfaces are equipotential surfaces. The gap is regarded as small compared to the rotor radius, and only small angular displacements from parallelism are considered. Thus edge effects and fringing field are small and are neglected.

The case where the surfaces are parallel and separated by g cms. provides the origins of all axes. The surfaces are circular and concentric of radius r. One surface is allowed to rotate about a fixed diameter, θ being the angle of rotation from the origin.

The fixed diameter is the y axis, the x axis being perpendicular and in the plane of the rotating surface in its original position. z is the gap distance at any point x, y
All distances are in cms.

At any point x, y

$$z = g - x\theta \qquad 1.$$

Between the equipotential surfaces

$$B z = \text{constant}$$

Let B_o be the uniform flux density (gauss) in the original case. At the origin, the gap is unchanged. Therefore $B_z = B_o g$

2.

Hence $$B = \frac{B_o g}{g - \chi\theta} = \frac{B_o}{1 - \frac{\chi\theta}{g}}$$

or making a small-angle approximation

$$B = B_o \left(1 + \frac{\chi\theta}{g}\right) \qquad 3.$$

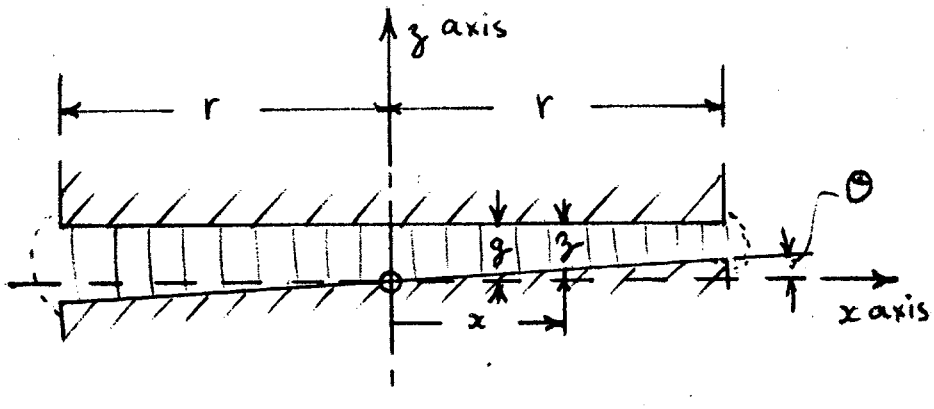

Figure I. 1

Illustrating symbols used in derivation

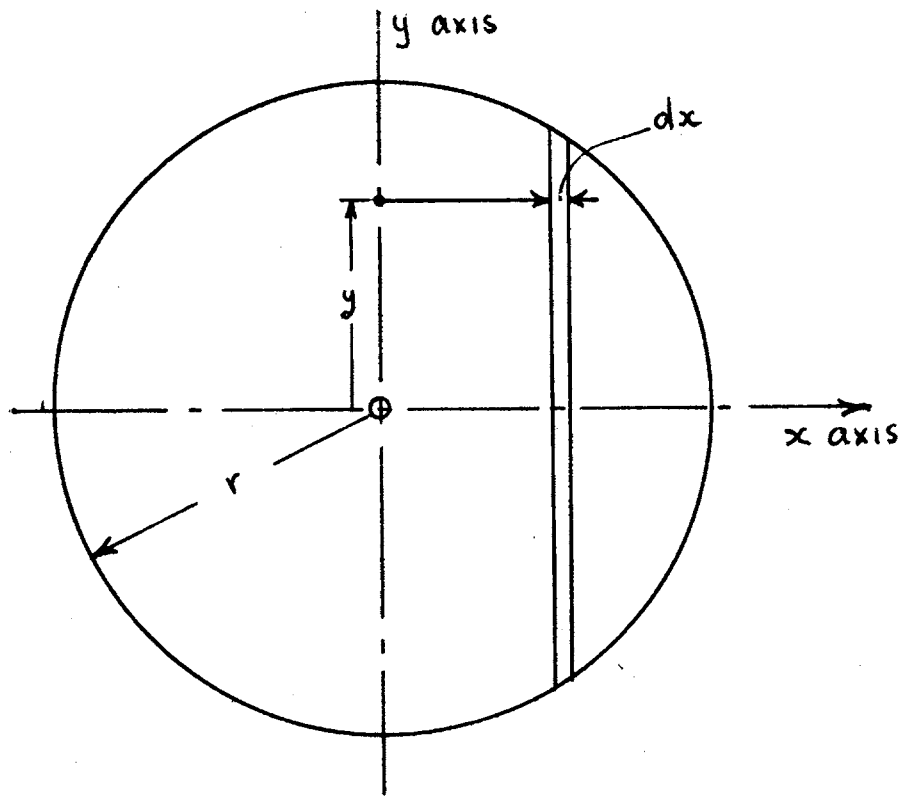

Plan View of one surface

The force dF on an element of surface $dx \cdot dy$ is

$$dF = \frac{B^2}{8\pi} \, dx \cdot dy \text{ dynes}$$

Substituting 3 and continuing to approximate for small angles we have therefore:

$$dF = \frac{B_o^{\,2}}{8\pi} \left(1 + \frac{2x\theta}{g}\right) dx \cdot dy \qquad 4.$$

We define an element of torque about the y axis as $dT = x\,dF$

Hence

$$dT = \frac{B_o^{\,2}}{8\pi} \left(1 + \frac{2x\theta}{g}\right) x \cdot dx \cdot dy \qquad 5.$$

5 is integrated to obtain the total torque

$$T = \frac{B_o^2}{8\pi} \int_{-r}^{+r} \int_{-\sqrt{r^2-x^2}}^{+\sqrt{r^2-x^2}} \left(1 + \frac{2x\theta}{g}\right) x \cdot dx \cdot dy = \frac{2B_o}{8\pi} \int_{-r}^{+r} \left(1 + \frac{2x\theta}{g}\right)\left(\sqrt{r^2-x^2}\right) x \cdot dx$$

$$= \frac{2B_o^2}{8\pi} \left[\int_{-r}^{+r} x\sqrt{r^2-x^2} \cdot dx + \frac{2\theta}{g} \int_{-r}^{+r} x^2\sqrt{r^2-x^2} \cdot dx \right]$$

The first integral is of an odd function between symmetrical limits. It is therefore zero. The second function integrates to $\frac{\pi r^4}{8}$

Hence

$$T = \frac{\theta B_o^{\,2} r^4}{16g}$$

or in the notation of the main body of the report

$$\frac{T}{\theta} = \frac{B^2 r^4}{16g}$$

APPENDIX II

Derivation of $W \propto \frac{\mu Q}{h^3}$ for hydrostatically lubricated pads with uniform and nearly uniform clearance

(a) The case of plane bearing surfaces, uniform clearance.

The Navier Stokes momentum equation for an incompressible fluid with constant ρ and μ is

$$-\frac{d\underline{V}}{dt} = \frac{1}{\rho} \text{grad } P + \underline{F} + \frac{\mu}{\rho} \nabla^2 \underline{V}$$

When viscuous forces predominate over inertial and body (gravitational) forces, this reduces to

$$\text{grad } P = -\mu \nabla^2 \underline{V}$$

which is equivalent to the three component equations:

$$\frac{\partial p}{\partial x} = \mu \left(\frac{\partial^2 V_x}{\partial x^2} + \frac{\partial^2 V_x}{\partial y^2} + \frac{\partial^2 V_x}{\partial z^2} \right) \qquad 1.$$

$$\frac{\partial p}{\partial y} = \mu \left(\frac{\partial^2 V_y}{\partial x^2} + \frac{\partial^2 V_y}{\partial y^2} + \frac{\partial^2 V_y}{\partial z^2} \right) \qquad 2.$$

$$\frac{\partial p}{\partial z} = \mu \left(\frac{\partial^2 V_z}{\partial x^2} + \frac{\partial^2 V_z}{\partial y^2} + \frac{\partial^2 V_z}{\partial z^2} \right) \qquad 3.$$

In general each second derivative $\frac{\partial^2 V_m}{\partial n^2}$ will be of order $\frac{V}{L^2}$ where L is the dimension of the fluid space in the n direction. For flow between parallel surfaces which are closely spaced (distance h) in the z direction, (1) and (2) may be closely approximated by

$$\frac{\partial p}{\partial x} = \mu \frac{\partial^2 V_x}{\partial z^2} \qquad 4.$$

and $$\frac{\partial p}{\partial y} = \mu \frac{\partial^2 V_y}{\partial z^2} \qquad 5.$$

Also we may put $V_z = 0$, in which case $\frac{\partial p}{\partial z} = 0$ 6.

It follows that $\frac{\partial p}{\partial x}$ and $\frac{\partial p}{\partial y}$ are functions of x and y only so that the solution of (4) becomes

$$V_x = \left(\frac{1}{\mu}\frac{\partial p}{\partial x}\right)\frac{z^2}{2} + b z + c$$

If the boundary conditions are $z = 0 \; ; \; V_x = U$
$z = h \; ; \; V_x = 0$

this equation becomes

$$V_x = \left(\frac{1}{2\mu}\frac{\partial p}{\partial x} - \frac{U}{zh}\right)(z^2 - zh) \qquad 7.$$

The co-ordinates may be chosen so that the moving surface has its velocity U in the x direction. Hence for V_y , the boundary conditions are:

$$z = 0 \; ; \; V_y = 0$$
$$z = h \; ; \; V_y = 0$$

whence

$$V_y = \frac{1}{2\mu}\frac{\partial p}{\partial x}(z^2 - zh) \qquad 8.$$

The average velocities $\bar{V}_x$ and $\bar{V}_y$ of the lubricant may be defined

respectively as

$$\bar{V}_x = \frac{1}{h}\int_0^h V_x \, dz$$

and

$$\bar{V}_y = \frac{1}{h}\int_0^h V_y \, dz$$

It follows by integration of (7) and (8) that

$$\bar{V}_x = \frac{U}{2} - \frac{h^2}{12\mu}\frac{\partial p}{\partial x} \qquad 9.$$

and $$\bar{V}_y = -\frac{h^2}{12\mu}\frac{\partial p}{\partial y} \qquad 10.$$

or simply for the average velocity

$$\bar{V} = \frac{U}{2} - \frac{h^2}{12\mu}\,\text{grad}\, p \qquad 11.$$

The law of continuity applies to $\bar{V}h$

i.e. $$\text{div}\,(\bar{V}h) = q \qquad 12.$$

where q is the oil flow supplied per unit area ot the pad face. Combining (11) and (12) we have

$$\text{div}\,(\bar{V}h) = q = -\frac{h^3}{12\mu}\nabla^2 p + \text{div}\,\frac{Uh}{2} \qquad 13.$$

The pads that we are considering have a central plenum to which oil is fed and which is surrounded by a "land" region where clearance is uniform. In the land region where no oil is supplied, we have then the Laplace equation.

$$\nabla^2 p = 0$$

The pressure equipotentials may be plotted in the usual way (e. g. sketching "flow nets" of curvilinear squares). Their geometry is independent of h and p .

Obviously these pressure equipotentials are independent of U . The pad load is therefore independent of U .

Also from (11), integrating the normal components around the boundary of the pad, and remembering that grad p is normal to the boundary

$$\oint V_n = \frac{Q}{h} = -\frac{h^2 P_o}{12\mu} \oint \left| \text{grad} \frac{p}{P_o} \right| \qquad 14.$$

where P_o is the plenum pressure and Q is the oil flow fed to the plenum. Since $\frac{p}{P_o}$ is a function only of x and y it follows that for any pad shape

$$Q \propto \frac{P_o h^3}{\mu}$$

Also the pad load $W = \int_A p dA = P_o \int_A \frac{p}{P_o} dA$ where the integral is over the pad area. Again $\frac{p}{P_o}$ is a function of x and y

Hence $$W \propto P_o$$

Therefore

$$W \propto \frac{\mu Q}{h^3} \qquad 15.$$

Another useful relation may be derived from (14) regarding a series of pads whose x, y dimensions are proportional. Each member of such a series may be defined by some characteristic linear dimension e. g. length L . At similar points on the boundaries of similar pads therefore

$$\text{grad} \frac{p}{P_o} \propto \frac{1}{L}$$

and the line integral around each boundary is:

$$\oint \text{grad} \frac{p}{P_o} \propto \frac{1}{L} \times L \qquad = \text{constant}$$

Hence for such a series

$$\frac{\mu Q}{P_o h^3} \qquad = \text{constant} \qquad 16.$$

(b) The case of bearing surfaces with non-uniform clearance, showing that in the symmetrical case W is independent of speed.

We will deal in the first instance with plane surfaces and only with cases having a y, z plane of symmetry through the centre of the pad.

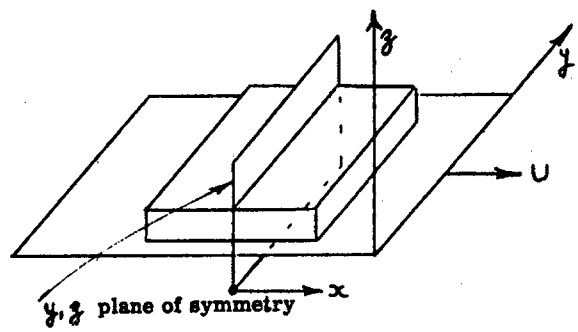

Let us measure the x co-ordinate from this plane.

Then for $x > 0$, h is some function of x and y, while for $x < 0$, h is the same function of $-x, y$.

i.e. for $x > 0; h = h(x, y)$

and $x < 0; h = h(-x, y)$ 17.

h is an even function of x . Its first and second partial derivatives are respectively odd and even functions of x.

Thus, if for $x > 0$; $\frac{\partial h}{\partial x} = h'_x(x,y)$; $\frac{\partial^2 h}{\partial x^2} = h''_x(x,y)$

then for $x < 0$; $\frac{\partial h}{\partial x} = -h'_x(-x,y)$; $\frac{\partial^2 h}{\partial x^2} = h''_x(-x,y)$ 18.

It is to be noted that any odd function of x has its first derivative an even function and second derivative an odd function.

Returning now to (9) and (10) and applying the condition for flow continuity over the lands

$$\left(\frac{\partial \bar{V}_x}{\partial x} + \frac{\partial \bar{V}_y}{\partial y} = 0\right)$$

we have $$\frac{U\partial h}{2\partial x} - \frac{1}{12\mu}\left[h^2\left(\frac{\partial^2 p}{\partial x^2} + \frac{\partial^2 p}{\partial y^2}\right) + 2h\frac{\partial h}{\partial x}\left(\frac{\partial p}{\partial x} + \frac{\partial p}{\partial y}\right)\right] = 0 \quad 19.$$

For $x > 0$ we have substitute the functions (17) and (18) for

$$h, \frac{\partial h}{\partial x}, \frac{\partial^2 h}{\partial x^2}.$$

Thus:

$$\frac{U}{2}h'_x(x,y) - \frac{1}{12\mu}\left[\{h(x,y)\}^2\left(\frac{\partial^2 p}{\partial x^2} + \frac{\partial^2 p}{\partial y^2}\right) + 2h(x,y)h'_x(x,y)\left(\frac{\partial p}{\partial x} + \frac{\partial p}{\partial y}\right)\right] = 0$$

and for $x < 0$ 20.

$$-\frac{U}{2}h'_x(-x,y) - \frac{1}{12\mu}\left[\{h(-x,y)\}^2\left(\frac{\partial^2 p}{\partial x^2} + \frac{\partial^2 p}{\partial y^2}\right) - 2h(-x,y)h'_x(-x,y)\left(\frac{\partial p}{\partial x} + \frac{\partial p}{\partial y}\right)\right] = 0 \quad 21.$$

Because of the change of sign of the first and third terms between these two equations, an odd p function satisfying (20) will also satisfy (21).

Thus, for $x > 0$ let $p = p_0(x,y)$; $\frac{\partial p}{\partial x} = p'_x(x,y)$; $\frac{\partial^2 p}{\partial x^2} = p''_x(x,y)$

Then for $x < 0$ $p = -p_0(-x,y)$; $\frac{\partial p}{\partial x} = p'_x(-x,y)$; $\frac{\partial^2 p}{\partial x^2} = -p''_x(-x,y)$

and for the partial derivatives with respect to y

for $x > 0$, let $\frac{\partial p}{\partial y} = p'_y(x,y)$; $\frac{\partial^2 p}{\partial y^2} = p''_y(x,y)$

then for $x < 0$ $\frac{\partial p}{\partial y} = -p'_y(-x,y)$; $\frac{\partial^2 p}{\partial y^2} = -p''_y(-x,y)$

By making the appropriate substitutions, it will be seen that such a function of (x,y) may satisfy both (20) and (21).

In addition, p = constant is a solution of (20) and (21),

So also is the <u>even</u> function $p = p_e(x,y)$ provided the sum of all the terms in the square brackets of (19) is everywhere zero. However, this is the condition for the pressure function when $U = O$, as is obtained by putting $U = O$ in (9) and applying the continuity law to (9) and (10).

Hence the complete solution of (19) is

$$p = p_o + p_e + \text{constant}$$

Boundary conditions usually reduce the constant to zero.

The pad load is the integral of this pressure over the land area plus the plenum pressure times the plenum area.

Thus

$$W = \int_A p\,dA + p_p A_p$$

$$= \int_A p_e\,dA + p_p A_p; \text{ Since } \int_A p_o\,dA = O$$

Now p_o must be zero for the plenum since it is an odd function and we will assume no pressure changes possible in the plenum. Then p_p must be the appropriate boundary value of p_e

Thus W is always a function of p_e only, which is the <u>zero speed</u> pressure function. Hence W is independent of speed.

Where the bearing surfaces are curved, they may be developed into plane or almost plane surfaces and the above arguments applied. The error will be small provided $\frac{h}{R_s}$ is small, where R_s is the radius of curvature of the surfaces.

(c) The case of cylindrical bearing surfaces.

In cylindrical co-ordinates let the pad extend from $z = 0$ to $z = l$, and in the θ direction to $\pm \theta_0$.

Let the shaft surface be

$$r_1 = R_s$$

and the pad surface be

$$r_2 = R_s + a + b\cos\theta$$

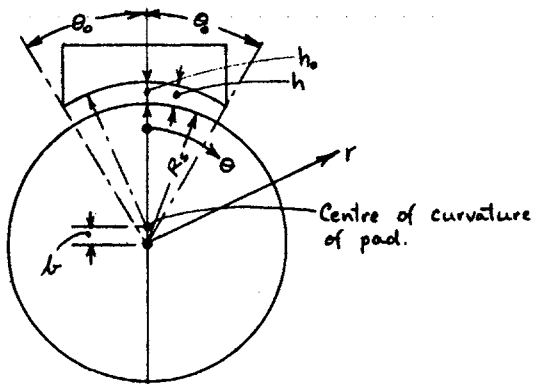

Here a is the difference in radius of curvature of the two surfaces and b is the eccentricity between the two centres of curvature. a is therefore a constant built into the geometry, whereas b may change with relative motion between pad and shaft. Let us choose $\theta = 0$ to be a plane of symmetry for the pad.

The clearance h is therefore

$$\begin{aligned} h &= r_2 - r_1 \\ &= a + b\cos\theta \end{aligned}$$

and at $\theta = 0$

$$h_o = a + b$$

Hence $h = h_o \cos\theta + a(1 - \cos\theta)$

It is convenient to write

$$\cos\theta = 1 - \alpha$$

since with the angles usually met with α will be small and appropriate approximations may be made.

Making this substitution

$$h = h_o(1 - \alpha) + a\alpha$$

or $$\frac{h}{h_o} = 1 - \alpha + \frac{a\alpha}{h_o}$$

A further simplification may be made by defining $\frac{a\alpha}{h_o} = \beta$. Here β is also small since a and h_o will be generally of the same order of magnitude.

Hence our working equation is

$$\frac{h}{h_o} = 1 - \alpha + \beta$$

Let us neglect the fact that in general the bearing surfaces will not be parallel, and treat the pad as being surrounded, on the $z = 0$ and $z = \ell$ side by lands where $h = h_o$; and on the $\theta = \pm \theta_o$ sides, by lands where $h = h_o(1-\alpha+\beta)$

Further assume that the land widths are small compared to their lengths so that they may be treated two dimensionally.

Also for simplicity assume a square pad surface (i. e. $2R_s \theta_o = \ell$)

For a plenum pressure P_o, the oil flow from the $z = 0$, ℓ ends

is therefore $Q_1 = K P_o h_o^3$

and for the $\theta = \pm \theta_o$ sides

$$Q_2 = K P_o h_o^3 (1 - \alpha + \beta)^3$$

where K is a constant and α and β are average values for these lands.

The total flow is therefore

$$Q = Q_1 + Q_2 = K P_o h_o^3 \left[2 - 3\alpha + 3\beta\right]$$

where an approximation has been made for small α and β. Since P_o is proportional to the pad load W (neglecting small effects due to the lands) we may also write

$$W \propto \frac{Q}{2h_o^3} \left(1 + \frac{3\alpha}{2} - \frac{3\beta}{2}\right)$$

The rate of change of W with h_o may be derived by differentiating, remembering that β only is a function of h_o

Thus

$$\frac{dW}{W} = -3 \frac{dh_o}{h_o} \left[\frac{1 + \frac{3\alpha}{2} - 2\beta}{1 + \frac{3\alpha}{2} - \frac{3\beta}{2}}\right]$$

or with approximations

$$\frac{dW}{W} = -3 \frac{dh_o}{h_o} \left(1 - \frac{\beta}{2}\right)$$

In the case of parallel plane surfaces, the similar relation is

$$\frac{dW}{W} = -3 \frac{dh_o}{h_o}$$

Hence the case with cylindrical surfaces may be approximated by the plane case provided h_o is not large i. e. provided β is not too small compared to the difference in radii of curvature a. For 60^o pads $\alpha \approx .13$. Hence since $\beta = \frac{a\alpha}{h_o}$, $|a|$ may for example be any value up to the steady design

value of h_o for the approximation $\frac{dW}{W} = -3\frac{dh_o}{h_o}$ to be within 13% for changes in h_o up to 50%.

APPENDIX III

A mechanism of bearing failure involving incipient contact areas.

The argument outlined here may generally apply to all types of "rigid" hydrodynamic or hydrostatic bearings. By "rigid" is meant "having features which are fixed" - as opposed to bearings having pivoted pads which may be termed "non-rigid". It also applies to non-rigid bearings having certain symmetrical features.

The argument depends on "incipient contact areas" i. e. areas where the clearance is reduced to zero but which do not normally transfer force between shaft and bearing. Such conditions would hardly result from the design but may occur because of faulty manufacture or operation under other than design conditions. In the latter case, there is real danger when friction is taken as the sole criterion of a bearing's behaviour. This is because incipient contact areas ideally produce no friction and cannot therefore be detected in this way. However as will be shown, they can lead to sudden and catostrophic breakdown.

Despite its generality, the argument will be confined to a particular case for the sake of clarity. This case is illustrated below and closely resembles the conditions of the seizure mentioned in the body of this report.

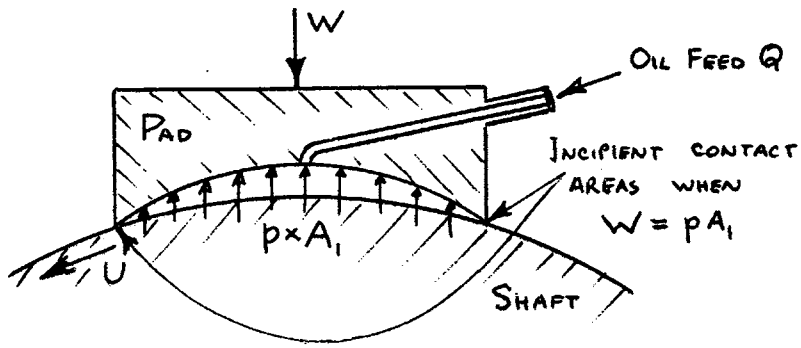

The following equations may be set up:

$$P_{\chi} = n(W - pA_1)\,Uf \qquad 1.$$

Here W is the pad load,

p is the average pressure under the pad,

A_1 is the pad area.

The force exerted on the pad by oil is therefore pA_1 and the solid to solid contact force at the contacts when they are no longer incipient is $(W - pA_1)$

U is the surface speed, f the coefficient of friction, and n the number of pads.

P_{χ} is therefore the total friction power produced at the contacts.

$$P_{\chi} = P_o + P_s \qquad 2.$$

Here all of P_{χ} is taken as flowing to the shaft surface. This is reasonable since the contacts are continually being presented with a relatively cool shaft surface so the temperature gradient strongly favours heat flow to the shaft. On the other hand, heat flow into the pad body will be inhibited by the continuous supply of heat to the same adjacent regions thus lowering the temperature gradient in this direction.

From the shaft surface, P_{χ} divides into P_o flowing to the oil by convection, and P_s flowing into the body of the shaft.

$$p = K_2 \mu \qquad 3.$$

Most of the oil feed Q is confined to the flow end-wise by the contacts. The pressure p is therefore developed as a result of the pressure gradient over the end lands. This gradient depends on Q , the pad dimensions (including h which is constant throughout this argument), and μ the viscosity at these lands.

$$\mu = V(T_o) \qquad 4.$$

This is simply the viscosity-temperature relation for the particular lubricant used. T_o is the oil temperature at the end lands or just before the oil leaves the pad. Both temperatures T_o and T_s are measured from the normal running value which is essentially the oil feed inlet temperature.

$$A_2 H(a T_s - T_o) = \frac{P_o}{n} \qquad 5.$$

Here $\frac{P_o}{n}$ is the heat flow to the oil for one pad. The major part of this transfer will occur under the pads because of the high velocities there. A_2 is the effective area for heat transfer to the oil for one pad and is roughly the same as A_1 . The temperature difference associated with heat transfer varies between T_s (oil inlet temperature is zero) and ($T_s - T_o$).

In general the mean temperature difference will be $\frac{\alpha T_s + \beta (T_s - T_o)}{\alpha + \beta}$ where α and β are appropriate weighting factors. This expression reduces to

$$\left[\frac{(\alpha + \beta) T_s}{\beta} - T_o \right] \times \frac{\beta}{\alpha + \beta}$$

The average heat per unit area is therefore

$\frac{h}{a} (a T_s - T_o)$ where $a = \frac{\alpha + \beta}{\beta}$ and h is the film transfer coefficient.

In (5) H is defined by $H = \frac{h}{a}$. Strictly H should be taken as a function of shaft speed but will be assumed constant for simplicity.

$$T_o = K_3 \frac{P_o}{n} \qquad 6.$$

This equation simply relates the final oil temperature rise to the heat input to the oil. K_3 is a function of oil density, specific heat, and flow rate Q .

The six equations preceding which contain seven unknowns may be reduced to one equation between the two unknowns P_s and T_s .

The result is

$$P_s = C_1 - C_2 V(C_3 T_s) - C_4 T_s \qquad 7.$$

where

$$C_1 = nUfW$$

$$C_2 = nUfA_1 K_2$$

$$C_3 = K_3 A_2 Ha/ (1 + K_3 A_2 H)$$

$$C_4 = nC_3/K_3$$

C_1 and C_2 are therefore proportional to U while C_3 and C_4 are essentially constant.

The diagrams on page 112 illustrate a typical viscosity-temperature curve and a consequent series of P_s vs. T_s curves for various speeds. All the curves go through $P_s = 0$, $T_s = 0$ since this is the condition for the contacts to be initially incipient.

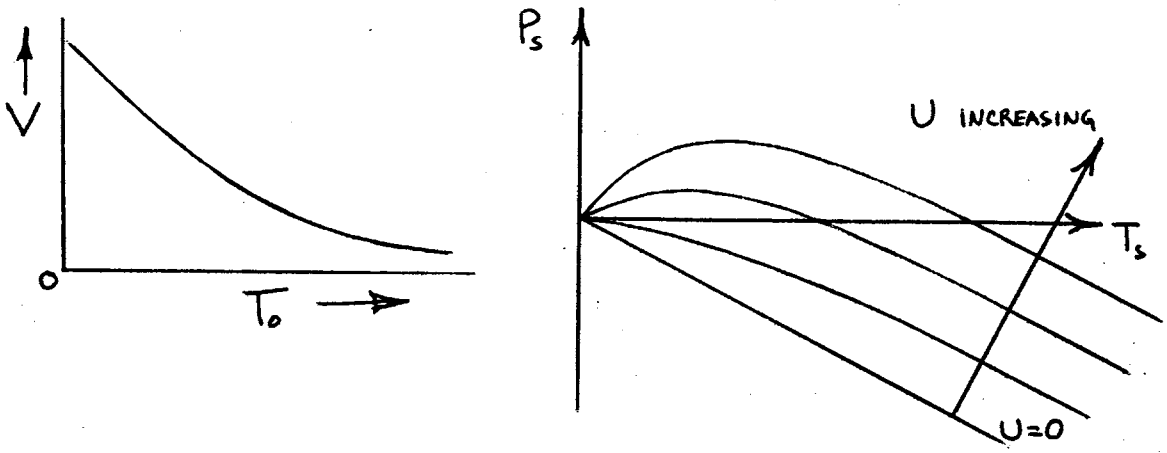

The interpretation of these P_s vs. T_s curves depends on the realization that each of them defines T_s as a function of time. The exact function involves solution of the Poisson equation

$$\nabla^2 T = \left(\frac{\rho s}{k}\right) \frac{\partial T}{\partial t}$$

with the boundary conditions $\quad \text{grad } T_s = \frac{1}{k} \frac{dP_s}{dS}$

(ρ specific gravity, s specific heat, k thermal conductivity, S shaft surface area).

However, the solution of this equation is not necessary since we are only interested in the general behaviour of T_s vs. t and whether in fact T_s can vary with t .

Some general properties of these P_s vs. T_s curves will now be discussed. For simplicity we idealize our problems to that of a cylinder of metal having all heat transfer restricted to the cylindrical surfaces between say $z = 0$ and $z = \ell$. Further, heat transfer in the z direction is taken as zero, and at every instant the cylindrical surface temperature T_s is uniform.

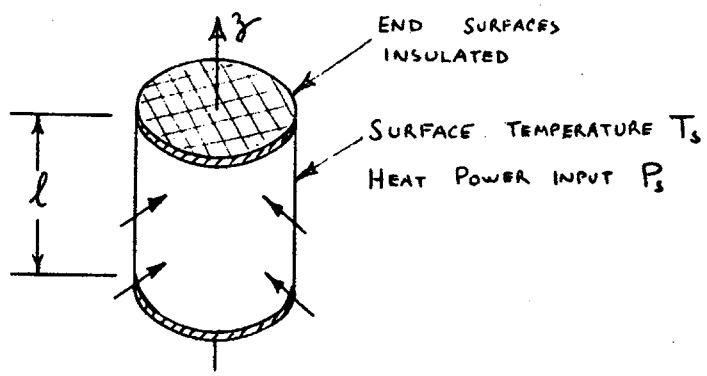

In this case then the following facts will be evident.

(a) $P_s - T_s$ curves in general have a definite beginning and end which represent the beginning and end of the period under consideration.

(b) In particular if a $P_s - T_s$ curve degenerates into a point and represents a process of finite time then such a point can only occur on the T_s axis and represents a state of thermal equilibrium. This follows from the definition of thermal equilibrium (no time or spatial change in temperature, heat transfer into and out of the system zero).

(c) Hence if a $P_s - T_s$ curve begins and ends on the axis, it represents a process which begins and ends in states of equilibrium. The period of time over which each of the equilibrium states extends is indeterminate. However, the time scale of the transition between the two equilibrium states is completely defined. The transition time t_t can be roughly estimated from:

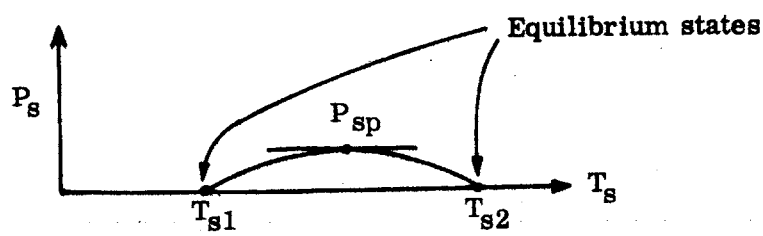

$$t_t > \frac{(T_{s2} - T_{s1})\, C}{P_{sp}} \qquad 8.$$

where C is the thermal capacity of the shaft and P_{sp} is the peak value of p_s .

(d) The direction of the transition from two equilibrium states is unambiguously determined by the sign of P_s . Thus in (8) if T_{s1} and T_{s2} are defined as the beginning and end states then the direction of the transition must be so that t_t is positive.

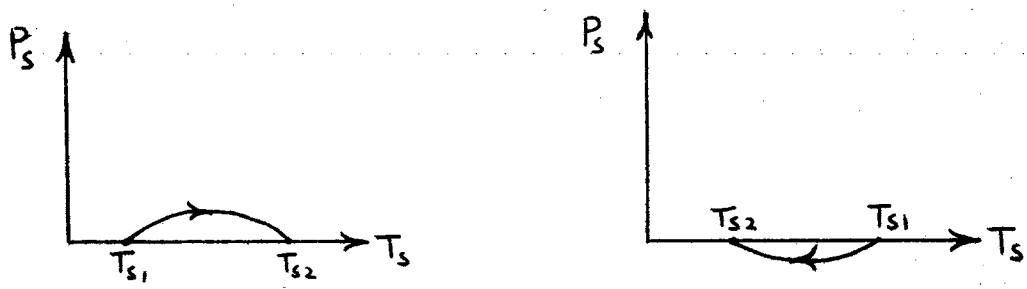

(e) A corollary of (d) is that any smooth $P_s - T_s$ curve which passes through the T_s axis represents parts of two processes which either start with or finish at a state of thermal equilibrium. In the former case the state of equilibrium is therefore unstable because at an undetermined time the process may travel along either path. In the same sense the latter case is stable.

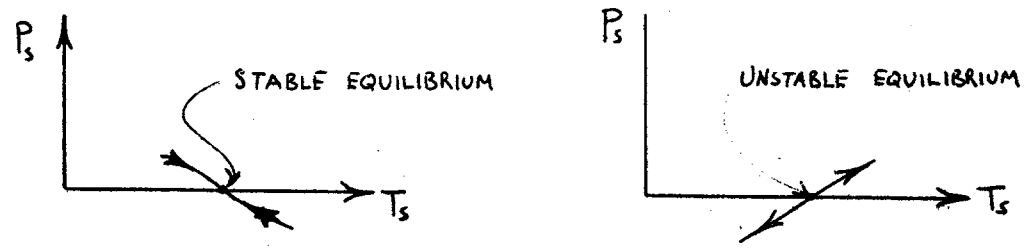

Similarly any equilibrium state can be described as stable or unstable depending on the slope $\frac{dP_s}{dT_s}$ of the $P_s - T_s$ curve emanating from the appropriate point on the T_s axis.

If $\frac{dP_s}{dT_s}$ is negative, the equilibrium is stable.

If $\frac{dP_s}{dT_s}$ is positive, the equilibrium is unstable.

Armed with these facts one may now analyse the previously obtained set of P_s, T_s curves with regard to the stability of the thermal equilibrium point $P_s = O, T_s = O$

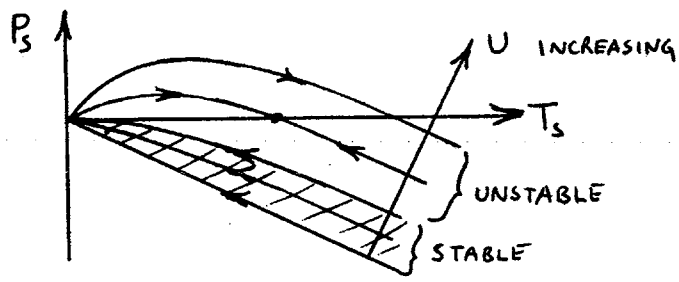

Clearly with U above a certain value, the point changes from stable to unstable. It should be noted that if the limiting speed is exceeded, it does not necessarily follow that equilibrium is immediately lost and T_s will rise. An "unstable" curve corresponds to equilibrium over an indefinite time which then undergoes a transition to another equilibrium state at a higher value of T_s. In practice this means that any slight change in operating conditions may cause the transition but it is quite possible that U may increase well beyond the stable limit without any apparent ill effect. Then without warning a sudden transition might occur leading to what is in fact a bearing seizure.

The condition for stability is evidently $\frac{dP_s}{dT_s} < O$ at $T_s = O$

$$\text{i.e.} \quad -V'(C_3 T_s) < \frac{C_4}{C_2 C_3}$$

$$\text{where} \quad V'(T) = \frac{d}{dT} V(T)$$

Substituting the values for the C's

$$-V'_{T=O} < \frac{1}{Uf A_1 K_2 K_3} \qquad 9.$$

Hence there is a critical speed U which depends on, amongst other more obvious factors, the rate of change of oil viscosity with temperature.

Typical approximate values for the bearings referred to in the body of this paper at the speed of failure were:

$U = 37$ ft/sec.

$f = 0.2$

$A_1 = 0.75\ \text{ft}^2$

$K_2 = 3.4 \times 10^{9}\ \text{sec}^{-1}$

$K_3 = 6.2 \times 10^{-3}\ {}^{o}\text{F sec/ft lb.}$

Hence $\frac{1}{Uf A_1 K_2 K_3} = 8.4 \times 10^{-9}\ \text{lb sec/ft}^2\ {}^{o}\text{F.}$

The oil viscosity was approximately 5×10^{-4} lb sec/ft^2, and

$V'_{T=O} \backsimeq 10^{-5}\ \text{lb sec/ft}^2\ {}^{o}\text{F.}$

Obviously then the conditions were unstable and a fast transition to a high temperature might be expected. This was the case.

APPENDIX IV

The optimum proportions of a circular plane pad with uniform clearance.

The problem may be set as follows. A circular pad of radius R is to support a given load W at a given clearance h . It is required to find the radius of the concentric plenum region such that the pumping power supplied to the lubricant is a minimum.

Assume the speed is zero. Following the arguments of Appendix II (a), pressure equipotentials will be concentric circles and flow will be radial.

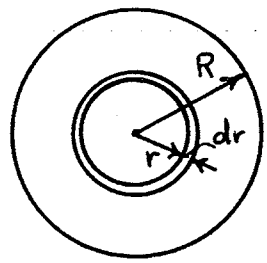

For any elementary ring of radius r and width dr we have

$$\frac{dp}{dr} = -\frac{12\mu\bar{V}}{h^2}$$

But $2\pi\bar{V}rh = Q$ the oil supplied to the plenum.

Hence $$\frac{dp}{dr} = -\frac{6\mu Q}{\pi rh^3}$$

or calling $$\frac{6\mu}{\pi h^3} = K$$ (a constant for this problem)

$$\frac{dp}{dr} = -\frac{KQ}{r} \qquad 1.$$

It is convenient to take the pad load as

$$W = \int_0^{p1} A_p \, dp$$

where A_p is the area enclosed by the equipotential p and p_1 is the highest pressure under the pad.

Hence taking p=O at $r = R$, $W = -\int_R^{r_1} (\pi r^2)\left(\frac{KQ}{r} dr\right)$

where r_1 is the radius of the equipotential p_1 .

Integrating

$$W = \frac{\pi KQ}{2}(R^2 - r_1^2) \qquad 2.$$

Since W is given, (2) shows Q as a function of r_1

$$\text{i.e.} \qquad Q = \frac{2W}{\pi K(R^2 - r_1^2)} \qquad 3.$$

(2) includes contributions to W of all pressure equipotentials of radius R to r_1 . It is therefore the load of a pad having a plenum (uniform pressure) of radius r_1 .

The plenum pressure p_p is found by integration of (1).

Thus

$$p_p = -KQ \int_R^{r_1} \frac{1}{r} dr$$

$$= KQ \ln \frac{R}{r_1} \qquad 4.$$

The pumping power P is

$$P = p_p Q$$

$$= KQ^2 \ln \frac{R}{r_1}$$

or substituting (3) for Q

$$P = \frac{4 \ell n \frac{R}{r_1} W^2}{\pi^2 K (R^2 - r_1^2)^2} \qquad 5.$$

The condition for P to minimise is therefore

$$-(R^2 - r_1^2) \frac{1}{r_1} = 2 \ell n \frac{R}{r_1} (R^2 - r_1^2)(-2r_1)$$

or

$$\ell n \frac{R}{r} = \tfrac{1}{4} \left[\left(\frac{R}{r} \right)^2 - 1 \right] \qquad 6.$$

The solution of (6) is $\frac{r}{R} = .538$ 7.

Consider now that surface speed is not zero. Appendix II (a) shows that there will be no change in pressure distribution.

Hence the relation (7) holds for non zero speed also.

APPENDIX V

General Principle of Superposition

We start from the general equation 7.1 viz.

$$q = \text{div}\ \frac{\underline{U}\, h}{2} - \text{div}\left(\frac{h^3}{12\mu}\ \text{grad}\ p\right)$$

Let the particular values μ_a, U_a and the distributions q_a, h_a, p_a satisfy the equation. Thus:

$$q_a = \text{div}\ \frac{\underline{U}_a\, h_a}{2} - \text{div}\left(\frac{h_a^3}{12\mu_a}\ \text{grad}\ p_a\right) \qquad 7.2$$

It is required to show that U_a and the distributions q_a and p_a can be regarded as the sum of two component sets of values.

Consider the following component sets each of which is defined by a particular set of boundary conditions.

Component (i)

$U_i = U_a$, $p_i = O$ everywhere. Then from 7.1 the distribution is given by

$$q_i = \text{div}\ \frac{\underline{U}_a\, h_a}{2} \qquad 1.$$

or $$q_i = \frac{U_a}{2} \cdot \text{grad}\ h_a \qquad \text{since } U_a = \text{constant} \qquad 2.$$

The q_i distribution can be regarded as a fictitious oil flow diffusing through the pad face surface and proportional to the relative angle between the two faces.

$$q_i = \frac{U_a}{2}\frac{dh_a}{dx}$$

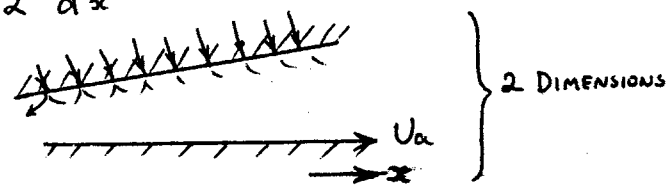

Step geometries may be treated by using Gausses theorem as applied to surfaces e. g.

$$\int_A \text{div } V \; dA = \int_\ell V \cdot \hat{n} \; d\ell$$

Hence since $q_i = \text{div } \frac{U_a h_a}{2}$

we have $q_i \, dA = \int_A \text{div } \frac{U_a h_a}{2} \, dA$

or $Q_i = \int_\ell \frac{U_a h_a}{2} \cdot \hat{n} \, d\ell = \frac{|U_a|}{2} \int_\ell h_a \hat{i} \cdot \hat{n} \, d\ell$ 3.

since U_a is a constant and where $\hat{i}$ is the unit vector in the $U(x)$ direction.

Hence the projection of a step in the x, y plane may be considered as surrounded by a line boundary ℓ enclosing area A which shrinks onto the line representing the projection of the step. The total flow component Q_i is therefore equal to $\frac{|U_a|}{2}$ times the projected area of the step looking in the $(-x)$ direction.

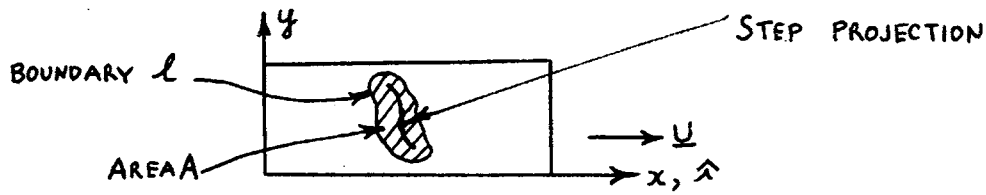

Component (ii)

$U_{ii} = O$, $q_{ii} = -q_i + q_a$. Then p_{ii} is given by

$$q_a - q_i = -\operatorname{div}\left(\frac{h_a^3}{12\mu_a}\operatorname{grad} p_{ii}\right) \qquad 4.$$

Adding (I) and (4)

$$q_a = \operatorname{div}\frac{U_a h_a}{2} - \operatorname{div}\left(\frac{h_a^3}{12\mu_a}\operatorname{grad} p_{ii}\right) \qquad 5.$$

Evidently then, comparing this with 7.2

$$p_i + p_{ii} = p_a \qquad 6.$$

Similarly it will be seen that

$$q_i + q_{ii} = q_a$$

$$U_i + U_{ii} = U_a$$

Hence in this sense the (i) and (ii) states are components of the actual state.

Pure Hydrodynamic Lubrication.

If μ is constant, 7.1 may be expanded to

$$q - \frac{U}{2}\cdot\operatorname{grad} h = -\operatorname{div}\left(\frac{h^3}{12\mu}\operatorname{grad} p\right)$$

$$= \frac{-1}{12\mu}\left[h^3\nabla^2 p + 3h^2\operatorname{grad} p\cdot\operatorname{grad} h\right] \qquad 7.$$

Pure hydrodynamic lubrication may be defined as occurring when $q = O$ everywhere.

In this case it is seen that $p = A_{(x,y,\mu)} U + p_o$ 8.

is a solution of (7) where A is defined by:

$$\hat{i} \cdot \text{grad } h = \frac{1}{12\mu} \left[h^3 \nabla^2 A + 3h^2 \text{grad} A \cdot \text{grad } h \right]$$

Invariably when (8) is integrated over an area to give the bearing load, the p_o integral is zero.

Hence the significant pressure component is $A U_a$ which everywhere is proportional to speed.

In the two dimensional case where $\underline{V}_y = 0$, 7.1 may be integrated ($q = 0$) giving

$$\frac{Uh}{2} - \frac{h^3}{12\mu} \frac{\partial p}{\partial x} = f(U, \mu)$$

where the R. H. S. is written to show that U and μ are the only allowable variables in this function.

We have already shown that grad p and hence all the L. H. S. is proportional to U. Hence $f(U,\mu)$ must be of the form $U\ell$ where ℓ is a fixed length to satisfy dimensional requirements.
The equation may therefore be written

$$\frac{h^3}{12\mu} \frac{\partial p}{\partial x} = \frac{U}{2} (h - h') \qquad 9.$$

The magnitude of h' may be gauged from the condition at maximum or minimum pressure. Here $\frac{\partial p}{\partial x} = 0$ and $h = h'$. Hence h' is between the limits of variation of h; corresponds to the h for maximum or minimum pressure, and is independent of speed.

Comparing V. 9 with II. 9 we see that

$$\frac{Uh'}{2} = \overline{\underline{V_x}}\, h \qquad 10.$$

i.e. $\frac{U h'}{2}$ is the flow per unit length under the hydrodynamic surface.

APPENDIX VI

Variation of h with β and U

It is not attempted here to present an exact treatment of this effect. A simplified model is presented to illustrate the mechanisms involved and to give an order of magnitude of the effect that might be expected.

Consider plane geometry and a rectangular pad whose x dimensions is a and y dimension b .

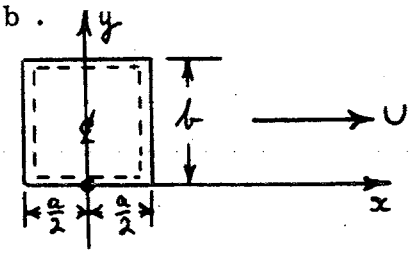

Fig. 1.

We consider tilting about the "parallel" axis, i. e. the centre line in the y direction. Let this axis be the y axis. The speed U of the moving surface is in the x direction.

Consider a pad with uniform narrow lands and under constant load. The plenum pressure may then be regarded as constant. The oil flow per unit width with U = O is then proportional to z^3 where z is the oil film thickness or clearance. The total oil flow $\overline{Q}_s$ in this case is:

$$\overline{Q}_s \propto \int_s z^3 \, ds$$ where the integral is taken around the perimeter.

For the two lands of length b we have

$$z = h\left(1 \pm \frac{\beta}{2}\right)$$

and for the two lands of length a we have

$$\mathcal{Y} = h\left(1 + \frac{\beta x}{a}\right)$$

It follows that

$$Q_s = \frac{K}{2}\left[bh^3\left\{\left(1-\frac{\beta}{2}\right)^3 + \left(1+\frac{\beta}{2}\right)^3\right\} + 2h^3\int_{-\frac{a}{2}}^{+\frac{a}{2}}\left(1+\frac{\beta x}{a}\right)^3 dx\right]$$

$$= Kh^3\left[a\left(1+\frac{\beta^2}{4}\right) + b\left(1+\frac{3\beta^2}{4}\right)\right]$$

If U is non zero, $\overline{Q_s}$ is augmented effectively (refer to Appendix V for principle of superposition) and becomes:

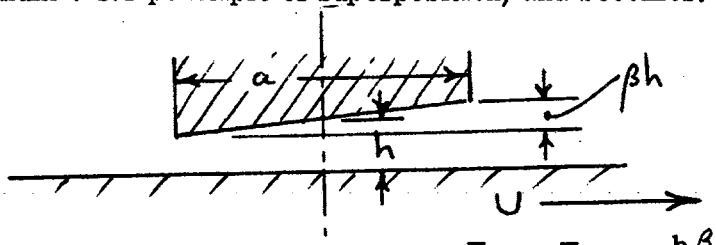

Fig. 2.

$$\bar{Q} = \bar{Q}_s - \frac{b\beta hU}{2}$$

Hence in this case

$$\bar{Q} = \overline{Q_s} - \frac{b\beta hU}{2} = Kh^3 f(\beta) \qquad 1.$$

where $$f(\beta) = a\left(1+\frac{\beta^2}{4}\right) + b\left(1+\frac{3\beta^2}{4}\right) \qquad 2.$$

It is convenient to define several new terms.

(a) When $\beta = 0$

$\overline{Q} = \overline{Q_s} = Kh^3 f(0)$ and therefore h is independent of speed. In this case define h as h_o.

(b) Define U_o such that

$$\overline{Q_s} = bh_o U_o$$

(c) h is normalized. Thus $h' = \frac{h}{h_o}$

(d) U is normalized. Thus $U' = \frac{U}{U_o}$

Substituting these new terms we have from (1)

$$bh_o U_o - \frac{b\beta hU}{2} = Kh^3 f(\beta)$$

i.e. $$bh_o U_o - \frac{b\beta U}{2h^2} = Kf(\beta)$$

i.e. $$\frac{b U_o}{h_o^2} \times \frac{1}{(h')^3} - \frac{bU\beta}{2h_o^2} \times \frac{1}{(h')^2} = Kf(\beta)$$

i.e. $$\frac{1}{(h')^3} - \frac{U'\beta}{2} \times \frac{1}{(h')^2} = \frac{K h_o^2}{b U_o} f(\beta) \qquad 3.$$

Also when $\beta = 0$, $h' = 1$, and

$$1 = \frac{Kh_o^2}{b U_o} f(0)$$

i.e. $$K = \frac{bU_o}{h_o^2} \times \frac{1}{f(0)}$$

Substituting for K in (3) then

$$\frac{1}{(h')^3} - \frac{U'\beta}{2} \times \frac{1}{(h')^2} = f'(\beta) \qquad 4.$$

where $f'(\beta)$ is the normalized $f(\beta)$ i.e. from 2

$$f'(\beta) = \frac{f(\beta)}{f(0)} = 1 + \frac{\beta^2}{4}\left(\frac{3 + \frac{a}{b}}{1 + \frac{a}{b}}\right)$$

$f'(\beta)$ depends on pad geometry. As an example $f'(\beta)$ is plotted for our model when $a = b$ (Fig. 3).

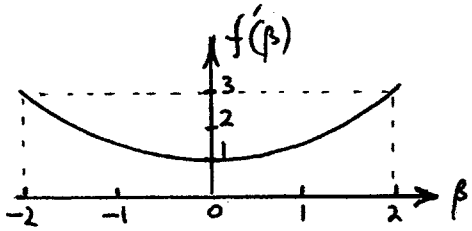

Fig. 3.

The solution of 4 can be obtained graphically.

Fig. 4 shows the results when $f'(\beta)$ is that shown in Fig. 3.

It is useful to express the ratio $\frac{P_h}{P}$ which is of importance in the text of this report, in terms of normalized speed and the aspect ratio $\frac{a}{b}$ of the pad. To this we must confine P_h to that value corresponding to $\beta = 0$. This special value is denoted by P_{h_o}

Then by definition

$$P_{h_o} = \mu \frac{UL}{h_o^2}$$

We also have from this appendix

$$\overline{Q_s} = K h_o^3 f(O)$$

and

$$f(O) = a + b$$

Also if we continue to adopt the simple model used in this appendix, $\overline{Q_s}$ may be expressed approximately as

$$\overline{Q_s} = \frac{h_o^3}{12\mu} \times \frac{dp}{dx} \times (\text{perimeter length})$$

$$= \frac{h_o^3}{6\mu} \times \frac{P}{L} (a + b)$$

Hence, comparing this with the other expression for $\overline{\underline{Q_s}}$ above we find

$$K = \frac{P}{6\mu L}$$

We have also by definition $\overline{\underline{Q_s}} = bh_o U_o$

and $U' = \frac{U}{U_o}$

Combining all these equations, the required ratio becomes

$$\frac{P_{h_o}}{P} \approx \frac{U'}{6}\left(\frac{a}{b} + 1\right) \qquad 5.$$

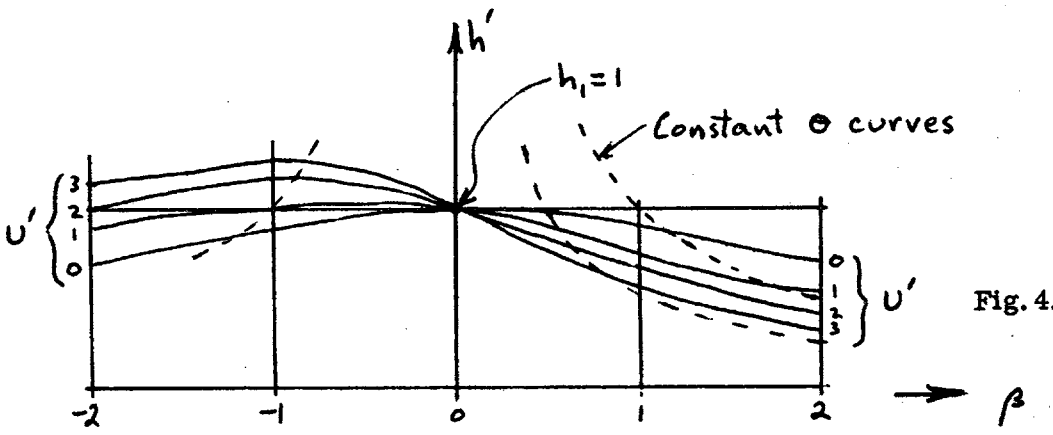

Fig. 4.

APPENDIX VII

Further Discussion on the Nature of the Boundary of the Cavitation Region

The left hand boundary (refer to Figs. 8.1, 2, 3 for co-ordinate system and conventions) is discussed in Section 8.

Equation 8.7 ($Q_r = \frac{\beta h^3}{12\mu} \frac{dp}{dx}$) will apply to either boundary in general. The R.H. boundary will differ from the L.H. in the allowable values of Q_v. For the R.H. boundary $Q_v \geq 0$ as with the L.H., and $\frac{dp}{d} > 0$ in the normal lubricant to satisfy $p > p_v$. It follows that Q_v and $\frac{dp}{dx}$ may have finite values in the normal lubricant and therefore that there may be a discontinuity in $\frac{dp}{dx}$ at the boundary.

This would be the case for example if a number of cylindrical surfaces such as shown in Fig. 8.3 were joined consecutively as shown at A in Fig. 8.4.

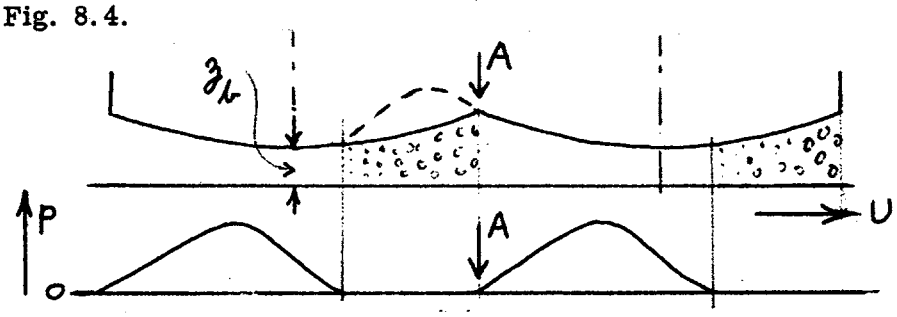

Fig. VII. 1

The discontinuity in $\frac{dp}{dx}$ is not necessarily associated with a discontinuity in $\frac{dh}{dx}$ as in Fig. VII. 1. For example any surface shape in the cavitation region (e.g. that shown dotted) would give the same pressure distribution, the only necessary condition being that $h \geq h_b$.

Otherwise the position of the R.H. boundary is governed by conditions to the right and the final defining pressure therein.

The distribution of V_x at the R. H. boundary, such as at A in Fig. 8.4. would also be discontinuous

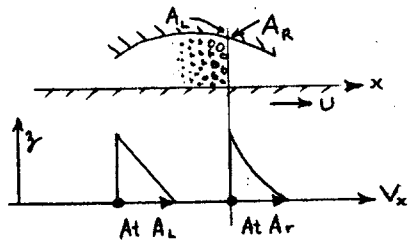

VII. 2

The liquid in the central regions of the film therefore suffers an impulsive deceleration on crossing the boundary as the mixture suddenly reverts to a single phase system. The impact would no doubt set up a succession of high pressure waves which would propogate in the normal lubricant in the immediate vicinity of the boundary. Such a mechanism is probably responsible for the damaging effect sometimes observed to be associated with cavitation.

The average pressure caused by the impacts may be estimated as follows. The average velocity of the liquid phase before the boundary is $\frac{U}{2}$ and after it is

$$(\frac{U}{2} - \frac{\gamma_c^2}{12\mu} \cdot \frac{dp}{dx}) \qquad (11.11)$$

where γ_c is the clearance at the R. H. cavitation boundary, or $\frac{U}{2}$ and $\frac{\gamma_b}{\gamma_c} \cdot \frac{U}{2}$, after V. 9 and V. 10 have been substituted. In this substitution γ_b, the γ at the L. H. boundary, is equivalent to h' in V. 9 because of the condition in both cases that $\frac{dp}{dx} = 0$.

The average step in pressures is therefore

$$\Delta p = \rho_L V_L \Delta V$$

$$= \rho_L \left(\frac{z_b}{z_c}\right)\left(1 - \frac{z_b}{z_c}\right) \frac{U^2}{4}$$

$$= \frac{\rho_L U^2}{4} (\gamma - \gamma^2)$$

where $\gamma = \frac{z_b}{z_c}$, ρ is density, and the subscript L refers to the liquid phase.

In our case

$\gamma \approx .3$
$\rho_L \approx 1$
$U \approx 75$

in units of:
foot
pound force (mass-slugs),
second

and $\Delta p \approx 2$ p.s.i.

This is not considered damaging to the small trailing edge strip exposed to impulses.

APPENDIX VIII

General equation for pressure between an infinitely long cylindrical surface and a moving plane surface

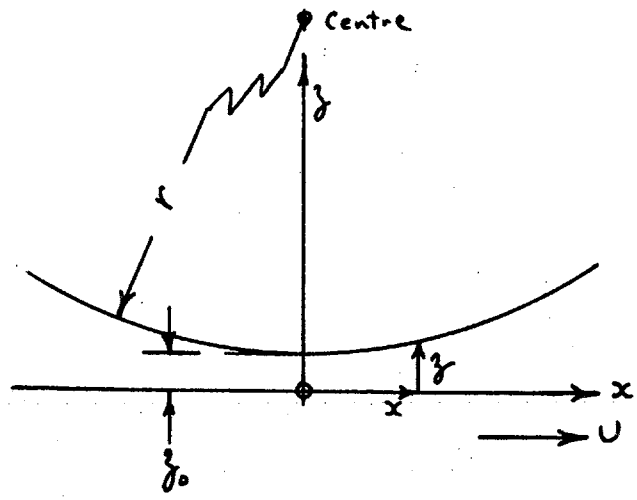

The equation for the cylindrical surface may be approximated by a parabola for small arc angles as discussed in Section 8.

Thus $$(z - z_0) = \frac{x^2}{2r}$$

or $$\frac{z}{z_0} = 1 + \xi^2 = z' \qquad 8.1$$

where $$\xi = \frac{x}{\sqrt{2r z_0}} \qquad 8.2.$$

Equation 9 in Appendix V is the general equation for two dimensional flow,

viz. $$\frac{h^3}{12\mu} \cdot \frac{dp}{dx} = \frac{U}{2}(h - h')$$

This may be written

$$\frac{h^2}{12\mu}\frac{dp}{dx} = \frac{U}{2}\left(1 - \frac{h'}{h}\right)$$

or in the present terminology

$$\frac{z^2}{12\mu}\frac{dp}{dx} = \frac{U}{2}\left(1 - \frac{\epsilon}{z'}\right) \qquad \text{VI. 1.}$$

where $z_0\epsilon = z_m$, the value where $\frac{dp}{dx} = 0$

Equation 8. 1 above may be substituted in V1. 1 to give

$$\frac{dp}{dx} = \frac{6\mu U}{z_0^2} \cdot \frac{\left(1 - \frac{\epsilon}{z'}\right)}{(1+\xi^2)^2}$$

or substituting 8. 2

$$p = 6\mu U\sqrt{\frac{2r}{z_0^3}}\int \frac{(1+\xi^2-\epsilon)}{(1+\xi^2)^3}\,d\xi + K \qquad \text{V1. 2.}$$

where K is an arbitrary constant.

The solution of the integral, which we have called $\mathcal{J}$, is

$$\mathcal{J} = \left(\frac{1}{2} - \frac{3\epsilon}{8}\right)\left(\tan^{-1}\xi + \frac{\xi}{1+\xi^2}\right) - \frac{\epsilon\,\xi}{4(1+\xi^2)^2} \qquad \text{V1. 3.}$$

Hence

$$p = 6\mu U\sqrt{\frac{2r}{z_0^3}} \times \mathcal{J}(\epsilon, \xi) + K \qquad \text{V1. 4.}$$

$\mathcal{J}$ is plotted against ξ for various values of ϵ in Fig. 8. 4.

Two views of the homopolar generator during construction. Rotors and bearings are in place and the outside shell is being built up around the rotors. The top half of the shell has been built and the bottom half commenced.

1. Two discs of lower rotor.
2. Busbar connections to outer jets.
3. Pipe connections to outer NaK jets.
4. Fibre-glass NaK deflecting baffle.
5. NaK collecting tray.
6. Hydraulically controlled NaK control valves.
7. NaK collecting tanks.
8. Magnet yoke.
9. Upper magnet field coil.
   (Lower coil under floor).
10. Upper pole.
11. Lower pole.
12. Rail for rotor assembly trolley.

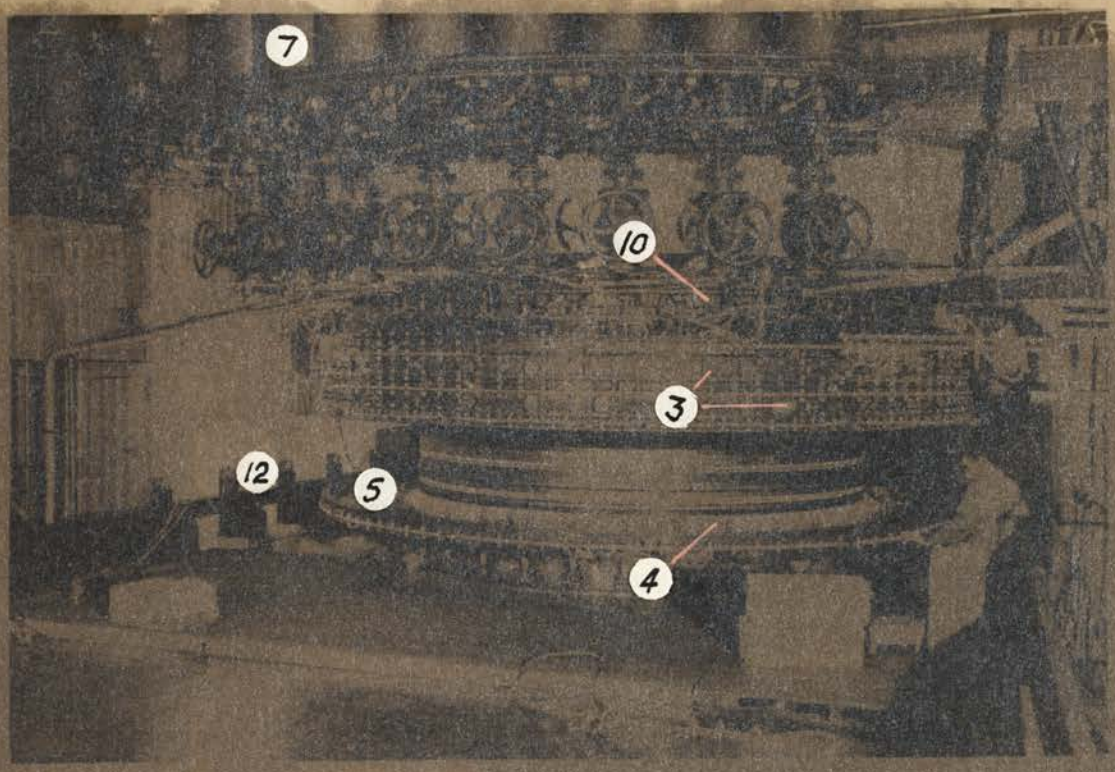
7
10
3
12
5
4

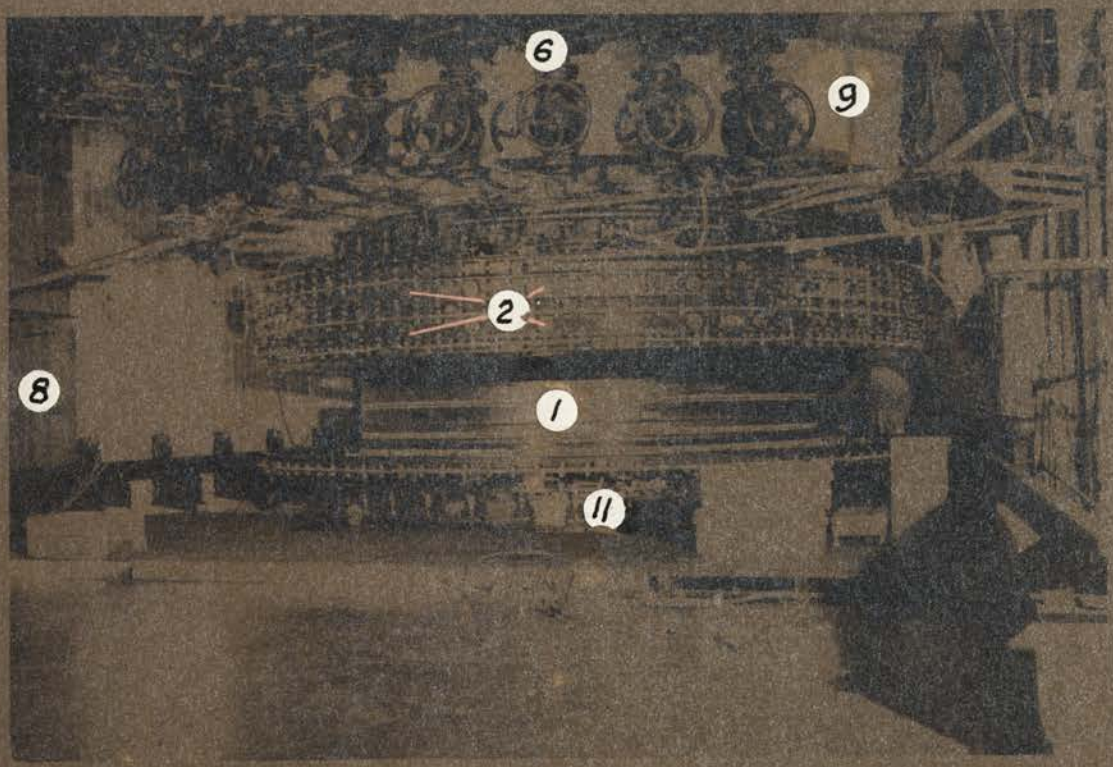
6
9
2
8
1
11

The small bearing complete with piping and instrument wires. Due to the bearing being on the bench in a horizontal position, a temporary support ring (labelled 1) is required.

View of large bearing from the rotor position.
The shaft, oil flinging ring and oil "tray" are removed.
This photo also shows the inner NaK jet of the Homopolar Generator.

1. Large pads.
2. Dynamic oil seal.
3. Static oil seal -pneumatically operated positive seal during shut down.
4. Oil lines to pad rams.
5. Lubricating oil drain pipes.
6. Inner NaK jet.

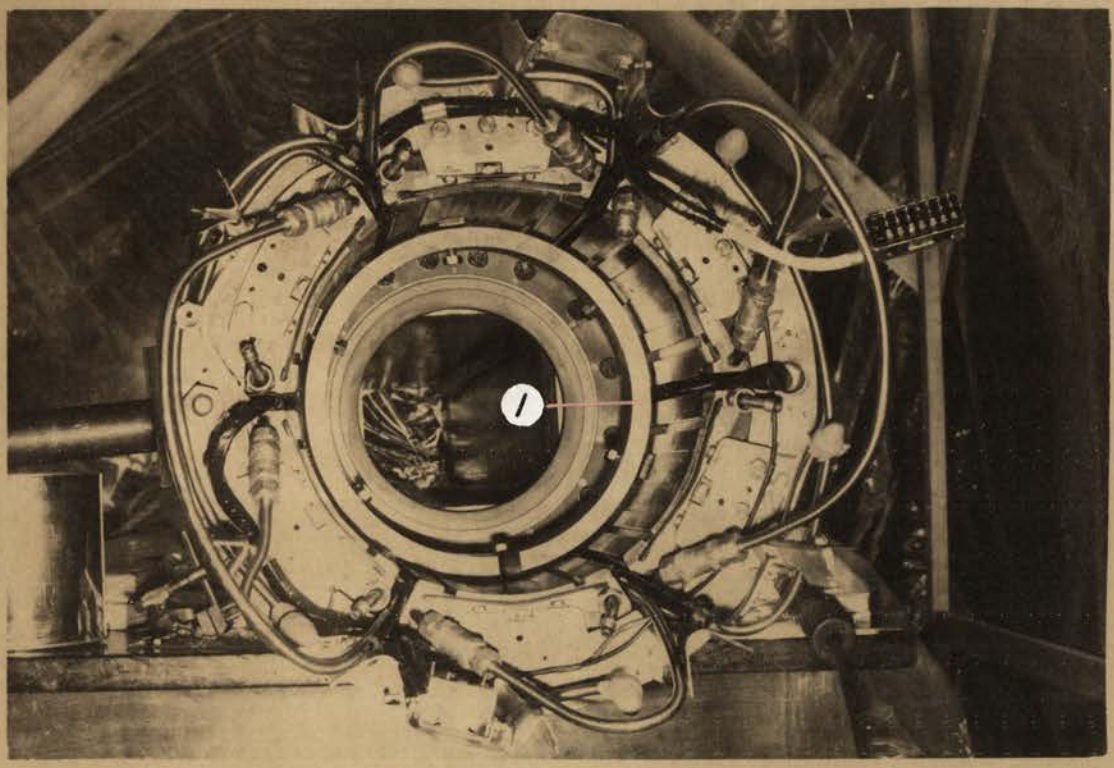
1

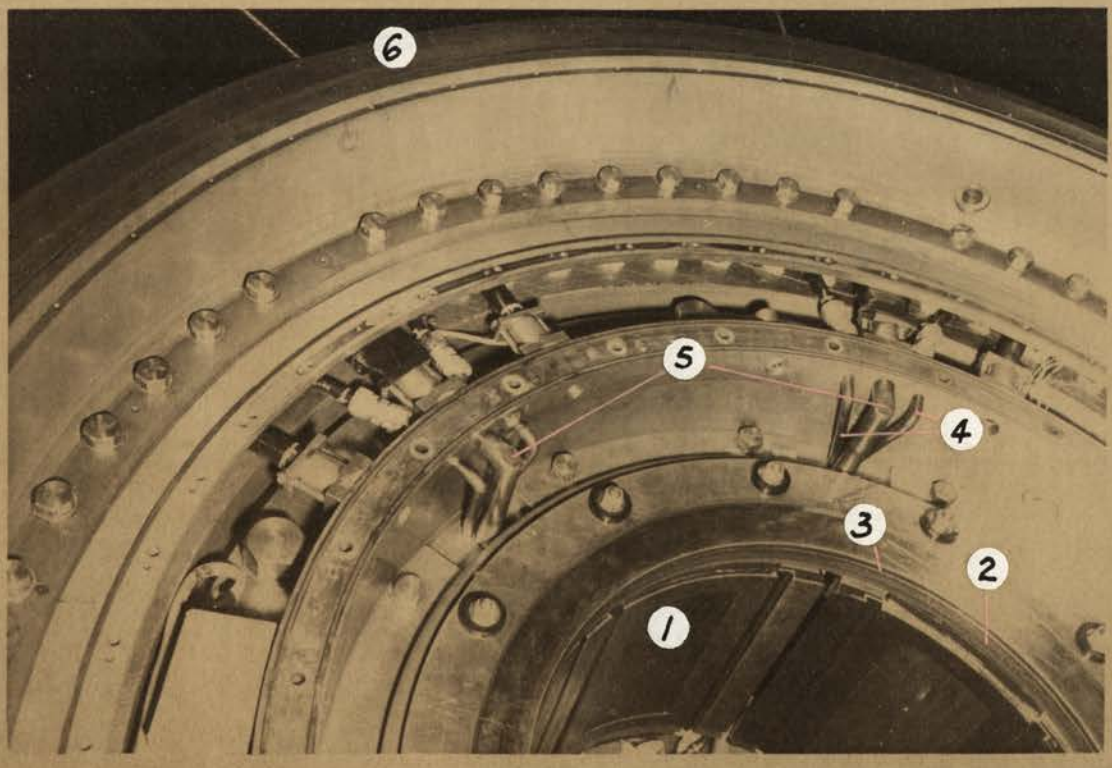
6
5
4
3
2
1

Large bearing. To the right is a large pad in place. In the centre and to the left can be seen parts of the rams after removal of their respective pads. The top of this photo is the large oil-seal end, the bottom is towards the small bearing. Between the two rams on the right are two ram oil lines which are fed from the oil-seal end. These pipes are not visible until they emerge near the bottom of the photo. The pipe feeding the large pad in the centre of the photo can be seen doubling back to an elbow screwed into the side of the ram. The second pipe supplies a small pad.

1. Large pad "cylinder".
2. Large pad.
3. Stabilizing surface.
4. Large ram oil supply line.
5. Retaining spring.

Large pad showing thermistors in pad face. These were included mainly as a safety precaution to give warning of any impending breakdown. They were also intended to throw light on the tilting behaviour of the pads.

1. Thermistors in "ferrobestos" pad facing material.
2. Thermistor leads.
3. Lubricating oil entry hole in plenum.
4. Insulating skirt over retaining springs.

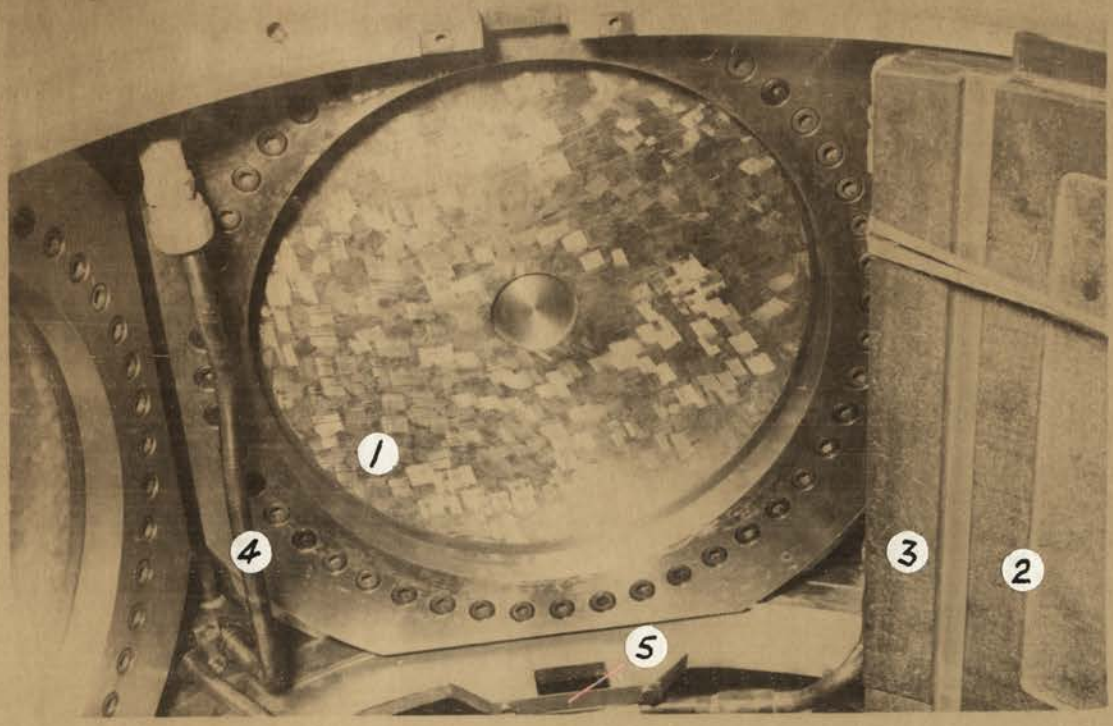
1
2
3
4
5

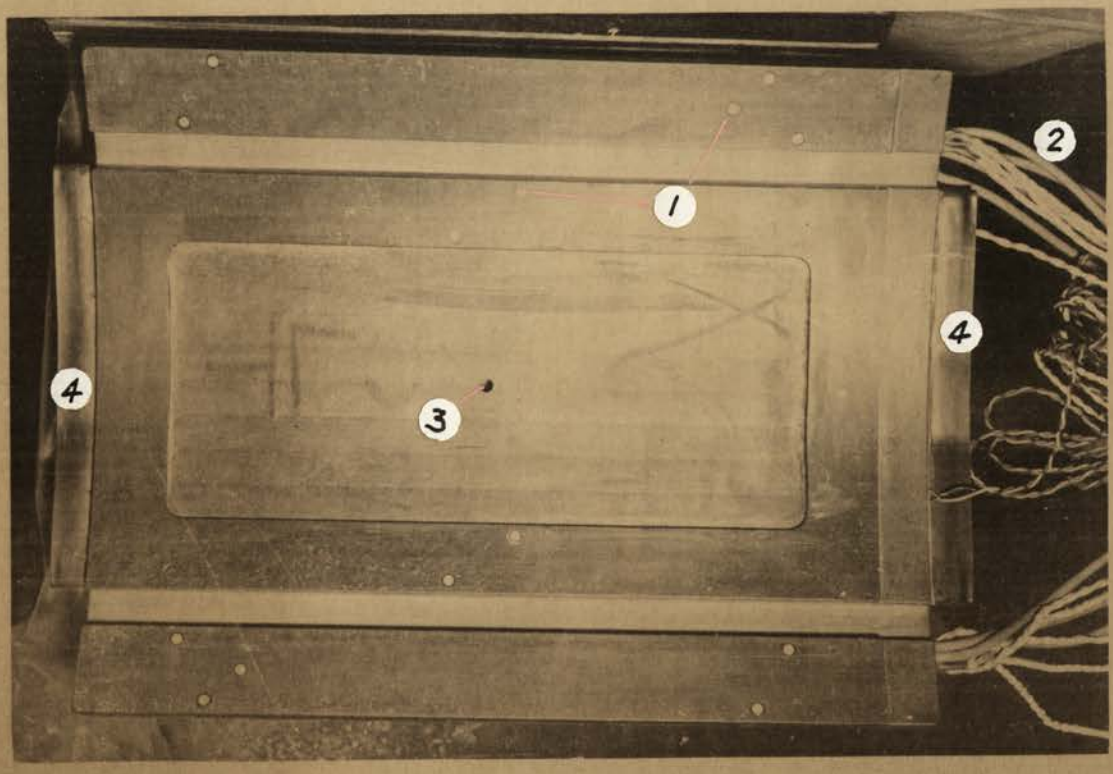
1
2
3
4
4

Small Bearing pads in housing but all removed from pole piece.

View from oil space between bearings.

1. Small pad.
2. Stabilizing surfaces.
3. Retaining springs.
4. Insulating guard over retaining springs.
5. Small ram "cylinder".
6. Make-up segments.
7. Inlet oil line to plenum with non-return valve in series.
8. Oil line to ram.

Small bearing pads in housing which in turn is in the pole piece. View from oil space between bearings.

1. Lubricating oil lines to large bearing. All lubricating lines entered from the vicinity of the thrust bearing, through the hole in the pole piece, and past the small bearing.
2. Oil lines to small rams. Supply lines to both small and large rams enter from across the pole face and pass through the large bearing.

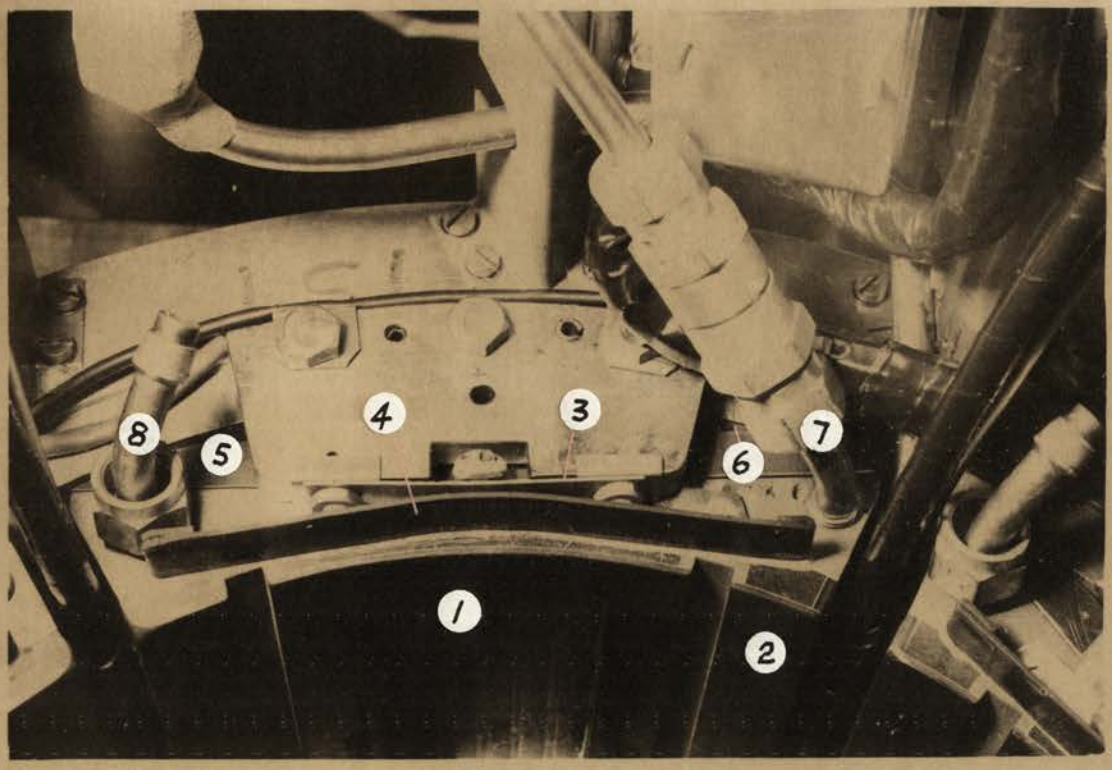
8
5
4
3
6
7
1
2

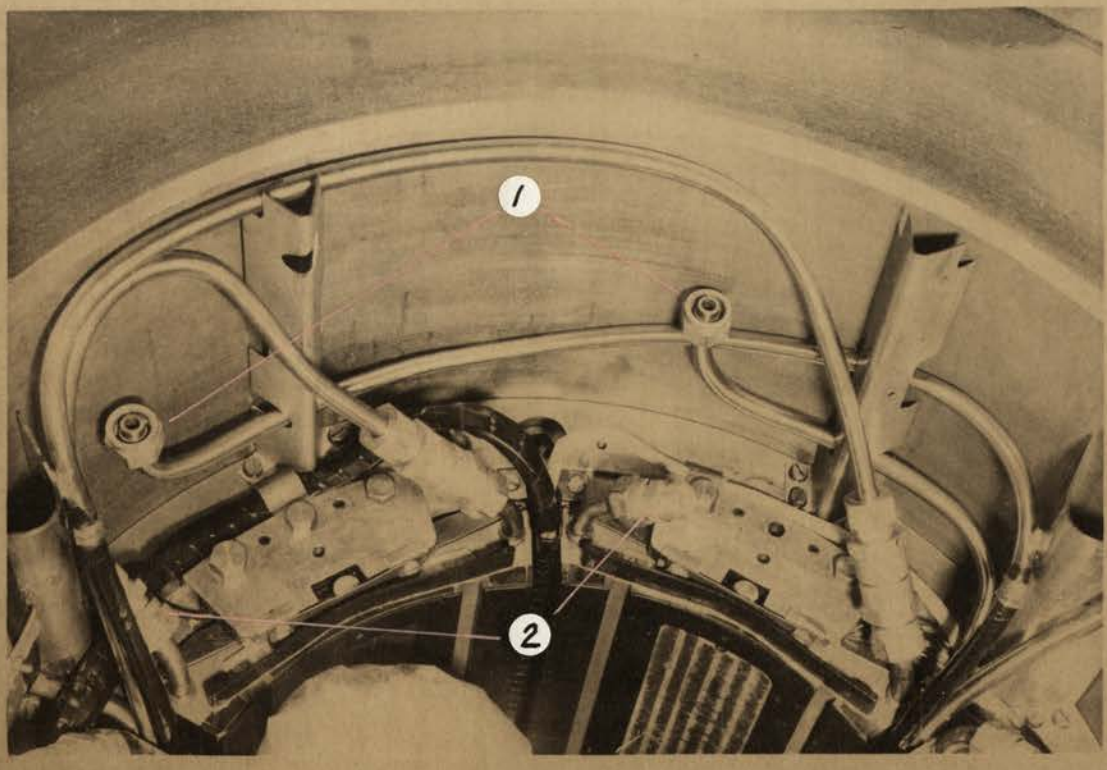
1
2

The guide bearing shaft being removed from lathe.

1. Bearing surfaces.

Connecting pipes between the two bearings with shaft in place.

1. Large bearing.
2. Small bearing.
3. Shaft.
4. Insulating pipe couplings.

   Note pipes are electrically insulated up to couplings.

Publications by Department of Engineering Physics

No.	Author	Title	First Published	Re-issued
EP-RR 1	Hibbard, L. U.	Cementing Rotors for the Canberra Homopolar Generator	May, 1959	April, 1967
EP-RR 2	Carden, P. O.	Limitations of Rate of Rise of Pulse Current Imposed by Skin Effect in Rotors	Sept., 1962	April, 1967
EP-RR.3	Marshall, R. A.	The Design of Brushes for the Canberra Homopolar Generator	Jan., 1964	April, 1967
EP-RR 4	Marshall, R. A.	The Electrolytic Variable Resistance Test Load/Switch for the Canberra Homopolar Generator	May, 1964	April, 1967
EP-RR 5	Inall, E. K.	The Mark II Coupling and Rotor Centering Registers for the Canberra Homopolar Generator	Oct., 1964	April, 1967
EP-RR 6	Inall, E. K.	A Review of the Specifications and Design of the Mark II Oil Lubricated Thrust and Centering Bearings of the Canberra Homopolar Generator	Nov., 1964	April, 1967
EP-RR 7	Inall, E. K.	Proving Tests on the Canberra Homopolar Generator with the Two Rotors Connected in Series	Feb., 1966	April, 1967
EP-RR 8	Brady, T. W.	Notes on Speed Balance Controls on the Canberra Homopolar Generator	Mar., 1966	April, 1967
EP-RR 9	Inall, E. K.	Tests on the Canberra Homopolar Generator Arranged to Supply the 5 Megawatt Magnet	May, 1966	April, 1967

No.	Author	Title	First Published	Re-issued
EP-RR 10	Brady, T.W.	A Study of the Performance of the 1000 kW Motor Generator Set Supplying the Canberra Homopolar Generator Field	June, 1966	April, 1967
EP-RR 11	Macleod, I.D.G.	Instrumentation and Control of the Canberra Homopolar Generator by On-Line Computer	Oct., 1966	April, 1967
EP-RR 12	Carden, P.O.	Mechanical Stresses in an Infinitely Long Homogeneous Bitter Solenoid with Finite External Field	Jan., 1967	
EP-RR 13	Macleod, I.D.G.	A Survey of Isolation Amplifier Circuits	Feb., 1967	
EP-RR 14	Inall, E.K.	The Mark III Coupling for the Rotors of the Canberra Homopolar Generator	Feb., 1967	
EP-RR 15	Bydder, E.L. Liley, B.S.	On the Integration of "Boltzmann-Like" Collision Integrals	Mar.,1967	
EP-RR 16	Vance, C.F.	Simple Thyristor Circuits to Pulse-Fire Ignitrons for Capacitor Discharge	Mar.,1967	
EP-RR 17	Bydder, E.L.	On the Evaluation of Elastic and Inelastic Collision Frequencies for Hydrogenic-Like Plasmas	Sept.,1967	
EP-RR 18	Stebbens, A. Ward, H.	The Design of Brushes for the Homopolar Generator at The Australian National University	Mar.,1964	Sept., 1967

No.	Author	Title	First Published	Re-issued
EP-RR 19	Carden, P.O.	Features of the High Field Magnet Laboratory at the Australian National University, Canberra	Jan., 1967	
EP-RR 20	Kaneff, S. Vladcoff, A.N.	Self-Organizing teaching Systems	Dec., 1968	
EP-RR 21	Vance, C.F.	Microwave Power transmission Ratio: Its Use in Estimating Electron Density	Feb., 1969	
EP-RR 22	Smith, B.D.	An Investigation of Arcing in the Electrolytic Switch/ Test Load Used with the Homopolar Generator	Oct., 1969	
EP-RR 23	Inall, E.K.	Use of the Homopolar Generator to Power Xenon Discharge Tubes and some Associated Switching Problems	Mar., 1969	
EP-RR 24	Carden, P.O.	Pivoted Hydrostatic Bearing Pads for the Canberra Homopolar Generator	Dec., 1969	
EP-RR 25	Carden, P.O. Whelan, R.E.	Instrumentation for the Australian National University 300 kilogauss Experimental Magnet	Dec., 1969	

Copies of this and other Publications (see list inside) of the Department of Engineering Physics may be obtained from:

The Australian National University Press,
P.O. Box 4, Canberra, A.C.T., 2600.
Australia.

Price: $A1.00

National Library of Australia Card Number and ISBN 0 85584 004 8